Tropical Water Quality Hub

National Environmental Science Programme

Final Report

Sediment tracing from the catchment to reef 2016 to 2018: Flood plume, marine sediment trap and logger data time series

Stephen Lewis, Zoe Bainbridge, Tom Stevens, Alex Garzon-Garcia, Chengrong Chen, Joanne Burton, Mohammad Bahadori, Mehran Rezaei Rashti, Jessica Gorman, Scott Smithers, Jon Olley, Phil Moody and Rob Dehayr

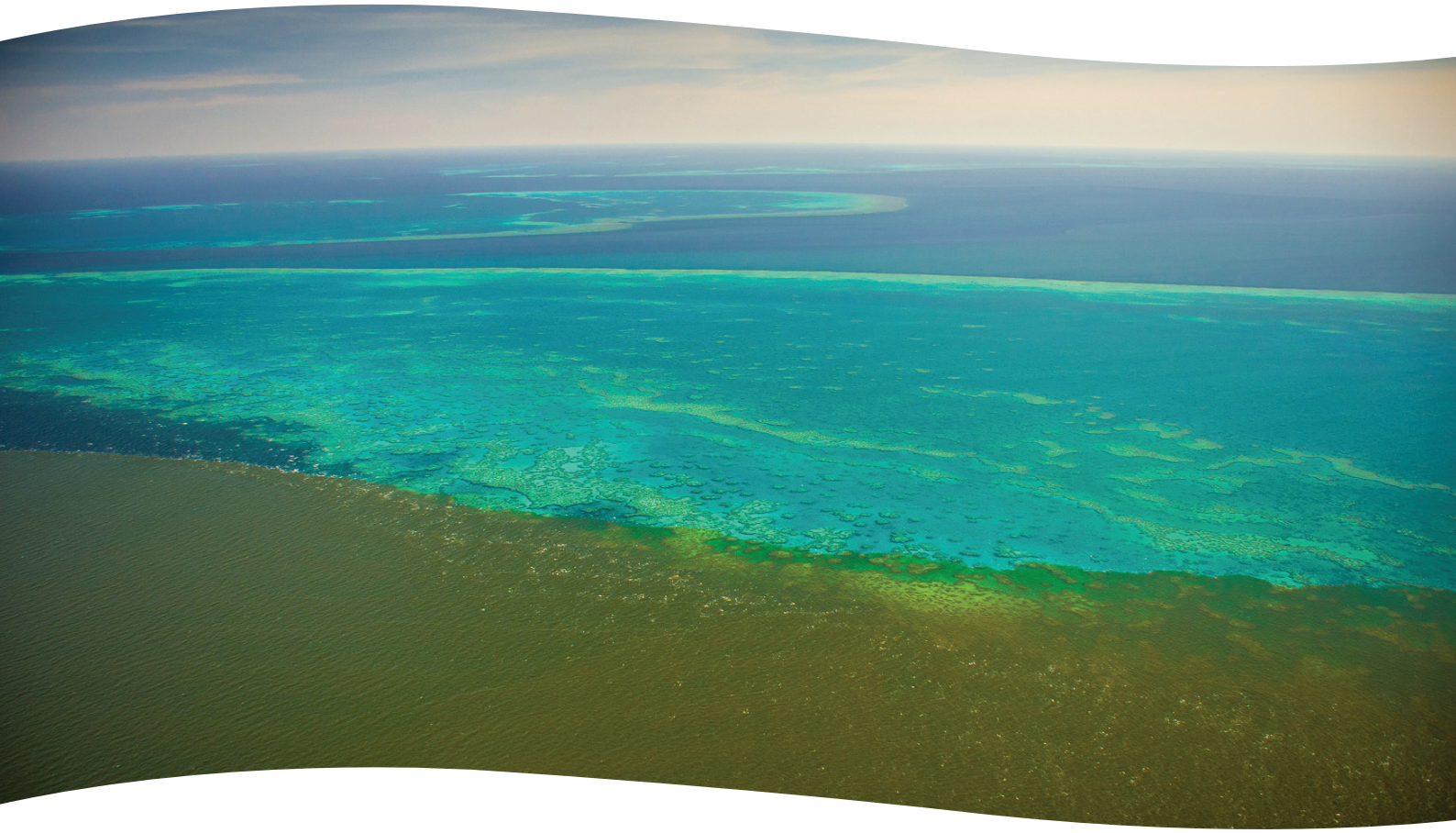

JAMES COOK UNIVERSITY AUSTRALIA

Sediment tracing from the catchment to reef 2016 to 2018: Flood plume, marine sediment trap and logger data time series

Stephen Lewis[1], Zoe Bainbridge[1], Tom Stevens[1], Alex Garzon-Garcia[2], Chengrong Chen[3], Joanne Burton[2], Mohammad Bahadori[3], Mehran Rezaei Rashti[3], Jessica Gorman[1], Scott Smithers[1], Jon Olley[3], Phil Moody[2], Rob Dehayr[2]

[1] Catchment to Reef Research Group, TropWATER, James Cook University
[2] Queensland Department of Environment and Science
[3] Australian Rivers Institute Griffith University

Supported by the Australian Government's
National Environmental Science Program
Project 2.1.5: What's really damaging the Reef? Tracing the origin and fate of the environmentally detrimental sediment

National Library of Australia Cataloguing-in-Publication entry:
978-1-925514-34-6

This report should be cited as:
Lewis, S., Bainbridge, Z. Stevens, T. Garzon-Garcia, A. Chen, C. Burton, J. Bahadori, M. Rezaei Rashti, M. Gorman, J. Smithers, S. Olley, J. Moody, P. Dehayr, R. (2018) *Sediment tracing from the catchment to reef 2016 to 2018: Flood plume, marine sediment trap and logger data time series.* Report to the National Environmental Science Program. Reef and Rainforest Research Centre Limited, Cairns (94pp.).

Published by the Reef and Rainforest Research Centre on behalf of the Australian Government's National Environmental Science Program (NESP) Tropical Water Quality (TWQ) Hub.

The Tropical Water Quality Hub is part of the Australian Government's National Environmental Science Program and is administered by the Reef and Rainforest Research Centre Limited (RRRC). The NESP TWQ Hub addresses water quality and coastal management in the World Heritage listed Great Barrier Reef, its catchments and other tropical waters, through the generation and transfer of world-class research and shared knowledge.

Cover photographs: (front) Burdekin flood plume over Old Reef in 2019; (back) Burdekin River mouth in 2019. Images by Matt Curnock.

This report is available for download from the NESP Tropical Water Quality Hub website:
http://www.nesptropical.edu.au

CONTENTS

LIST OF FIGURES

LIST OF TABLES

ACRONYMS

AIMS ..... Australian Institute of Marine Science
DES..... Department of Environment and Science
DIN..... Dissolved Inorganic Nitrogen
DoEE ..... Department of the Environment and Energy
DON..... Dissolved Organic Nitrogen
GBR..... Great Barrier Reef
GBRL..... Great Barrier Reef Lagoon
JCU..... James Cook University
MMP..... Marine Monitoring Program
NESP ..... National Environmental Science Program
POM……..Particulate Organic Matter
PON ..... Particulate Organic Nitrogen
PSU..... Practical Salinity Units
SCC ..... Suspended Sediment Concentration
SPM ..... Suspended Particulate Matter
TSS..... Total Suspended Solids
RRRC..... Reef and Rainforest Research Centre Limited
TWQ..... Tropical Water Quality
VSS..... Volatile Suspended Solids

ABBREVIATIONS

$mg.L^{-1}$ ..... milligram per litre
$g.d^{-1}$..... gram per day

ACKNOWLEDGEMENTS

We thank the laboratories at the Chemistry Centre, Department of Environment and Science and TropWATER, James Cook University for analysis of samples. We thank Simon Griffiths, Andreas Dietzel, Adam Wilkinson, Cassandra Thompson, Sofia Valero Fortunato, Blanche Danastas, Ian McLeod, Jane Waterhouse, Lauren Firby, Eridani Mulder and Glen Ewels for being part of the dive team who collected the resuspension sediment trap samples. The Marine Geophysics Laboratory is thanked for supplying and helping calibrate the nepholometers and current meters (in particular Simon Macdonald, Kallum Jones, James Whinney and Michael Santarossa) and help with data processing (Rachael Macdonald and James Whinney). Cassandra James expertly constructed the plots of the logger time series of our 7 sites. We thank Jason and Bec from Mission Beach Charters and Andrew Mead from Aussie Barra Charters for assisting in the flood plume sampling. Additional flood plume samples (as well as the historical dataset) were collected and analysed as part of the Great Barrier Reef Marine Park Authority's Marine Monitoring Program (MMP). Jane Mellors sampled the Burdekin plume on the 5th March 2018. Zoe Bainbridge's Advance Queensland research fellowship is acknowledged for laboratory-based marine sediment preparation method development. Emily Lazarus investigated the particle size analytical method as part of this Advance Queensland fellowship. We thank Michele Skuka (AIMS) for discussions on the TSS methods. We also thank Barbara Robson for her assistance with calculating plume travel times used in the calculation of dissolved inorganic nitrogen generation rates in the plume. We thank A&O Engineering for general help with frame manufacture and modification. This project is funded by the Australian Government's National Environmental Science Program (NESP) through the Tropical Water Quality (TWQ) Hub managed by the Reef and Rainforest Research Centre (RRRC) with additional funding from the Queensland Department of Environment and Science's Reef Water Quality Science Program and in-kind support from the Chemistry Centre, Landscape Sciences, Department of Environment and Science (DES). Professor Jon Brodie is thanked for providing a constructive review which improved the report.

EXECUTIVE SUMMARY

A synthesis of recent research has refined our conceptual understanding of the transport, fate and impacts of fine suspended sediment delivered to the Great Barrier Reef (GBR) lagoon (Bartley et al., 2014; Lewis et al., 2015; Bainbridge et al., 2018). Specifically it is recognised that only a portion of the fine sediment delivered from rivers draining into the Great Barrier Reef Lagoon (GBRL) reaches coral reefs and seagrass meadows. The specific sources of this sediment, which reduce photic depth and water clarity and affects the health of corals and seagrasses, are as yet unresolved. NESP TWQ Hub Project 2.1.5, *What's really damaging the Reef? Tracing the origin and fate of the environmentally detrimental sediment*, was developed to address this research gap and attempts for the first time to characterise and trace the origin(s) and fate of this environmentally detrimental sediment using samples collected in flood plumes and during resuspension events. This includes characterising and determining the origin of the particulate organic matter in the floc aggregates.

Field logistics, technological, analytical and knowledge constraints have previously hampered the characterisation and tracing of sediments transported in resuspension events and in flood plumes within the Great Barrier Reef lagoon. As such a core part of this project was to develop equipment to collect samples in the quantity required for a thorough sediment characterisation, and the protocols for sample collection and treatment required to undertake the diverse array of analysis and laboratory experiments conducted. The project team successfully sampled two minor river discharge and associated plumes from the Burdekin catchment, two moderate to large events from the Tully River and one plume from the Johnstone River. In addition, the team studied the spatial and temporal variability of resuspension events and sediment dynamics at seven GBRL inshore locations using continuous logger data (10 min sampling intervals) over 2 ½ years and analysed the quantity of sediment collected in newly designed sediment traps along with a thorough characterisation of these sediments. The time invested in development of these new sampling protocols and refinement with each event was significant and will benefit future GBRL projects and contribute to the international literature in this field.

This project has utilised the patented SediSampler® and the SediPump® to collect suspended sediment samples in resuspension events and flood plumes, respectively. Experimental studies have been carried out to highlight the influence of sediment trap spacing and tilt on the capture of plume and resuspended sediment in the traps. Specifically, the influence of trap spacing can be variable across sites with some sites showing little variation between a 3D (i.e. 3 diameter widths) and 9D spacing, although on occasion the 3D spacing collected less sediment than the 9D. Traps with a high tilt (i.e. 20° or more) generally collect a greater mass of sediment accumulated in the trap. A number of other innovative processes have been developed including analysis of suspended particulate matter in the SediSamplers® so the samples remain wet, analysing sediment colour and procedures to treat the sample for particle size (i.e. organic-removal step) to directly analyse the mineral component. In addition, we have investigated the most optimal procedures to analyse total suspended solids (TSS) across the catchment to marine continuum as well as examined the trends in suspended particulate matter over flood plumes from the Burdekin, Tully and Fitzroy Rivers. Relationships have been established between turbidity and TSS for all seven inshore marine sites containing continuous turbidity loggers where the linear relationship at the Dunk Island site showed high variability

between benthic sediment from the dry season and that associated with wet season runoff of suspended particulare matter (SPM). Relatively new analytical techniques have also been applied to characterise the particulate organic matter in the catchment and marine suspended sediments in the Great Barrier Reef including the analysis of ^{13}C NMR and bacterial/fungal communities. In addition, new experimental designs have been implemented to measure Dissolved Inorganic Nitrogen (DIN) generation in flood plumes.

Flood plumes from the Tully River were sampled over the 2016/17 and 2017/18 wet seasons. The plumes represented moderate to large flood events from the Tully River and satellite images highlighted plumes regularly impinging on our Dunk Island monitoring sites. In all Tully plumes, suspended particulate matter (SPM) concentrations were <40 $mg.L^{-1}$ at the end of river and reduced to <20 $mg.L^{-1}$ by the 15 salinity zone. The size of the sediment flocs in the Tully plumes generally increased with increasing salinity, although interestingly the general floc sizes were smaller in the 2018 plumes compared to 2017. Particle size (organic removed) at the end-of-river site showed that ~70% of particles were <16 µm and this increased to ~90% by the 20 salinity zone.

We sampled two plumes from minor events in the Burdekin. We note that due to a lack of a moderate to major flood event from the Burdekin River to influence our sites over the 2016-2018 period our interpretations can only be based on what we have observed thus far, and may be subject to change in the coming seasons. The first plume was as a result of Tropical Cyclone Debbie and was sourced from the Bowen-Broken-Bogie area of the Burdekin while the second plume in 2018 was sourced from the Upper Burdekin sub-catchment. Satellite images showed that the 2017 plume initially moved south-eastward before moving northwards during the waning flow. As a result, the influence of this plume at our logger sites in both Cleveland and Halifax Bays was fairly negligible. In comparison, the 2018 Burdekin River plume moved northward up the coast and impinged on all our logger sites. Over both plumes, SPM concentrations rapidly decreased from >600 $mg.L^{-1}$ at 0 salinity to <30 $mg.L^{-1}$ by ~ 12 salinity as has been observed in previous studies while the proportion of organic matter in the Burdekin plume increased from 12% to >25% by 25 PSU. Sediment flocs were observed in all samples collected in the Burdekin plume. Sediment particle size (organic-removed) showed that ~ 80% of the particles at the end-of-river were <16 µm which increased to >90% by the ~ 5 salinity zone and this either remains similar over the salinity gradient or in some cases, we observed a small increase in the coarser particles (under investigation but likely siliceous plankton).

The generation of dissolved inorganic nitrogen from suspended sediment in plume events was measured using laboratory extraction and incubation techniques. DIN generation from plume sediment was measured in the two sampled Burdekin River plumes. DIN generation was significant, accounting for 38% and 12% of the whole of catchment DIN loads measured at Inkerman for the Bowen-Broken-Bogie (2017) and Upper Burdekin (2018) events, respectively. Given that both events were minor we could expect larger DIN generation from sediment in larger events. Particulate inorganic nitrogen (PIN) conversion to DIN (i.e. ammonium desorption) was an important process accounting for between 23% and 60% of the generated DIN load. The technique developed for this project is valuable as it provides us with information on the cycling rates of N in the plume that cannot be obtained from direct DIN measurements. In comparison, there was little DIN generation in the Tully plume. These results indicate that

an additional benefit of the management of soils to reduce erosion from grazing lands is the reduction of DIN produced from the eroded sediments in the marine environment.

The organic matter in samples from the Burdekin, Tully and Johnstone flood plumes were more similar to soil samples collected from the Johnstone catchment than marine sediment trap samples confirming a terrestrial source of organic material in the plumes. In addition when compared with samples from the Tully and Johnstone plume, the organic matter in the Burdekin plume had been decomposed to a greater extent and the carbon components measured by ^{13}C NMR in the Burdekin plumes were less labile than the organic matter in the plumes from the Johnstone and Tully Rivers. Finer scale detail of erosion process and spatial sources during these events is currently being developed using the geochemical, radionuclide and organic matter datasets collected.

Preliminary results from the tracing of the river bed and suspended sediment in the Johnstone catchment, using the novel approach of combined isotopic and geochemical fingerprints, suggested that the rainforest land use contributed a significant proportion of sediment (33.1 ± 14.5%) and particulate nitrogen (53.5 ± 7.3%) at the end of catchment; however, when the proportional area of rainforest is considered (i.e. 52% of the catchment area), the relative sediment contribution from this land use is much lower compared to the agricultural land uses examined (grazing, sugarcane, bananas). In particular, the banana land use (~4% of the catchment area) seemingly contributed a much higher contribution. However, as only one snapshot sampling was carried out in this preliminary study, multiple samples from the Johnstone River catchment and plume over a season is recommended in the extension component of this project to further improve reliability of the model prediction.

Our preliminary findings suggest that the sediment dynamics at marine sites in the inshore GBRL region likely fall into three separate categories including sites where: 1. input of new terrigenous sediments have by far the greatest influence on sediment exposure and subsequent resuspension (e.g. Dunk Island, Orpheus Island, Havannah Island, Cleveland Bay?); 2. input of new terrigenous sediments are at least equivalent to resuspension events which likely increases upon larger river discharge events (e.g. Cleveland Bay?, Orchard Rocks) and; 3. input of new terrigenous sediments are less than or equal to common resuspension events (e.g. Middle Reef, Geoffrey Bay). Hence because of these differences in sediment dynamics, the study reveals which sites are most influenced by newly delivered riverine sediment and hence where management in the catchment for sediment erosion would improve water quality and likely ecosystem health at those coral reef and seagrass meadow sites. In particular, Dunk Island experienced several moderate to large flood events from the Tully River between 2016 and 2018 and the logger and sediment trap data highlighted the elevated influence of suspended sediment around Dunk Island both during the flood and in the 4 to 5 months thereafter. This provides some of the first empirical data to support the findings of the satellite photic depth modelling of Fabricius et al. (2014, 2016) where the delivery of new terrigenous sediment considerably influences water clarity on the inshore Great Barrier Reef.

1.0 INTRODUCTION

A synthesis of recent research has refined our conceptual understanding of the transport, fate and impacts of fine suspended sediment delivered to the Great Barrier Reef lagoon (Bartley et al., 2014; Lewis et al., 2015; Bainbridge et al., 2018). Specifically it is recognised that only a portion of the fine organic-rich sediment fraction delivered from rivers draining into the Great Barrier Reef Lagoon (GBRL) reaches coral reefs and seagrass meadows. The specific sources of this sediment, which affects the health of corals and seagrasses, are as yet unresolved. NESP Project 2.1.5, *What's really damaging the Reef? Tracing the origin and fate of the environmentally detrimental sediment*, was developed to address this research gap and attempts for the first time to characterise and trace the origin(s) and fate of this environmentally detrimental sediment using samples collected in flood plumes and during resuspension events.

The key objectives of this project include:

- Trace the environmentally detrimental sediment that reduces photic depth and water clarity during both flood plume and resuspension events at key locations in the GBRL (i.e. coral reefs and seagrass meadows) back to a specific catchment source (core objective).
- Characterise and determine the origin of the particulate organic matter in the floc aggregates.
- Determine the spatial and temporal variability of sediments in resuspension events in Cleveland, Halifax and Rockingham Bays.

This final report will provide all data collected and analysed from 2016 and 2018 in the NESP 2.1.5 project. We highlight the extensive development of methods undertaken to measure and trace suspended particulate matter across the catchment to reef continuum (Section 2). Specifically we show the importance of accuracy in the measurement of suspended particulate matter (SPM) through both total susupended solids (TSS) and particle size methodologies and the influence of sediment trap spacing and tilt on trap sediment accumulation. We present the flood plume data over the 2016/17 and 2017/18 wet seasons showing the trends in SPM concentrations and sediment particle size over the estuarine mixing zone for different rivers and present a detailed characterization of sediment as it moves from the catchment to reef (Section 3). We present the potential for bioavailable nutrient (BAN) production within the two considerable flood plumes from the Burdekin River in 2016/17 and 2017/18 which were derived from two different catchment sources (Bowen-Broken-Bogie and Upper Burdekin, respectively) (Section 4). A novel method of quantifying the contribution of sediment and particulate nitrogen from different land use sources and a thorough characterization of organic matter in flood plumes and sediment traps are presented in Section 5. Finally, Section 6 presents the continuous sediment trap accumulation and logger data over 2 ½ years and shows the influence of recent elevated river discharge events on these continuous records.

2.0 MEASURING SUSPENDED PARTICULATE MATTER IN THE ENVIRONMENT

Study design and sample processing

Field logistics, technological, analytical and knowledge constraints have previously hampered the tracing of sediments transported in resuspension events and in flood plumes within the Great Barrier Reef lagoon. The development of the patented SediSampler® (Stevens T. 2013) and SediPump® (Stevens T. 2018) have been critical in allowing the collection of the required mass of sediment in resuspension events and flood plumes, respectively so that detailed physical, chemical and biological analysis can be conducted. This development has allowed a sufficient amount of material to be collected (that was unobtainable in previous research) for detailed tracing to be performed for the first time. However, additional development of analytical protocols were needed to ensure minimal sample contamination in the collection and processing of sediment samples prior to analysis. In that regard, the NESP project in conjunction with Zoe Bainbridge's Advance Queensland research fellowship has now produced a detailed sample processing protocol for both the resuspension and flood plume samples (Figures 2.1 & 2.2). We note that an assessment of potential contamination using the SediSampler® and the SediPump® has also been carried out using a bentonite standard. The developments of the laboratory sample processing has included the capture of the sediment colour, the measurement of sediment mass (mineral and organic) without needing to dry the sample, microphotographs of the sediment particles within each sample, the removal of salts in the sample prior to drying (without contamination) and determining the most optimal method of sample treatment for particle size analysis (Figure 2.3). We have examined the influence of different treatment options on particle size which ensures that the integrity of the individual particles is captured. The different treatments included salt removal, organics removal, carbonate removal and sediment dispersion with calgon and sonication. Our results suggest that treatment to remove the organics (with hydrogen peroxide) provides the most reliable estimates of the original "mineral" particle size of the sample (i.e. closest to the terrestrial source) (Bainbridge et al., In prep). These findings were implemented in our particle size analysis conducted throughout the project, with results presented in Section 3 all having had organic removal prior to analysis. Tables 3.1 and 3.2 also present particle size results with salt removal pre-treatment only as a comparison, as this provides a measure of how the particles will behave in the marine setting. Refer to Bainbridge et al. (2012) for detailed description of the particle size ranges presented in this report.

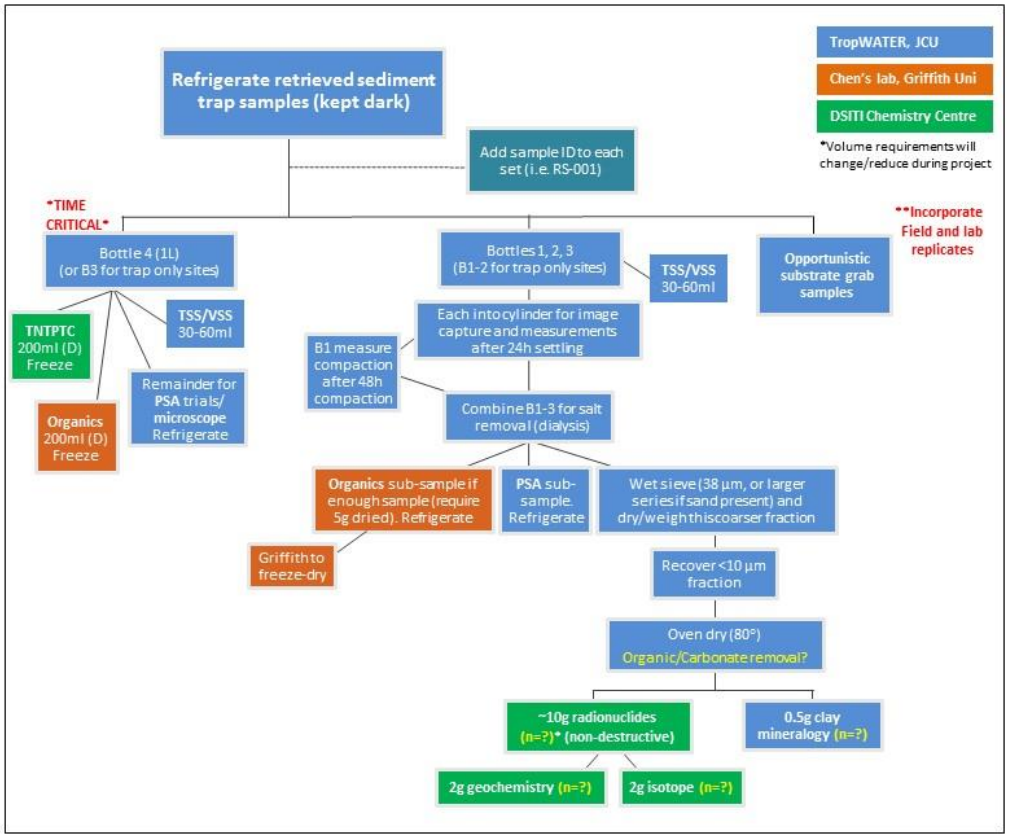

Figure 2.1. Flow chart of the sampling processing procedure for the resuspension samples collected in the sediment traps.

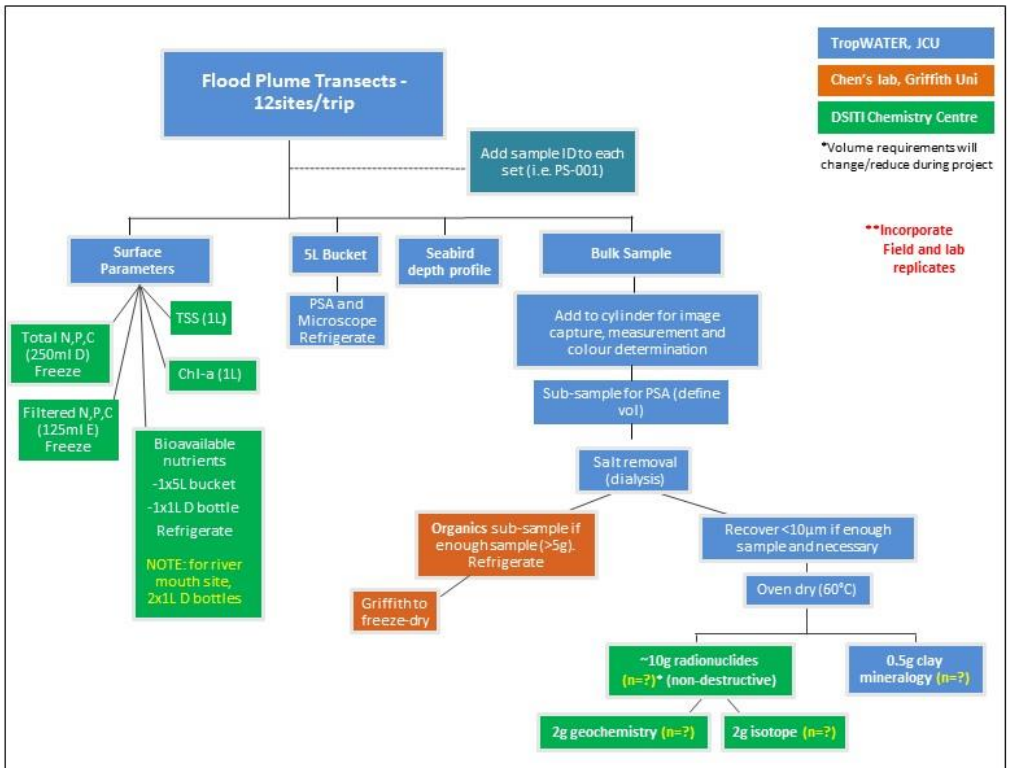

Figure 2.2. Flow chart of the sampling processing procedure for the flood plume samples.

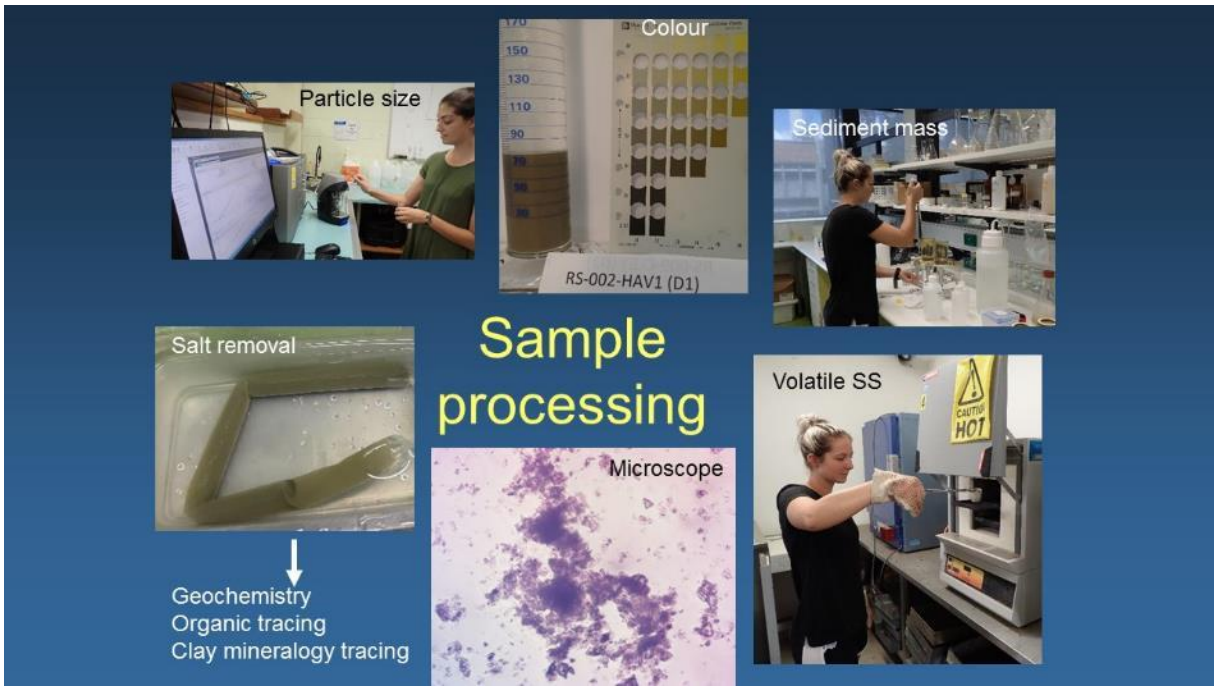

Figure 2.3. A visualisation of some of the different sediment processing steps.

A total of seven sites have been established across a longitudinal gradient from the Burdekin River mouth including an inshore-offshore gradient as well as at Dunk Island in the path of the Tully River (Figure 2.4). All seven sites contain four sediment traps surrounding a nephelometer which measures turbidity, sea pressure, light and a current meter which measures current speed and direction (Figure 2.5). Additional configurations of three sediment traps have been deployed at Pelorus Island, the reef toe (i.e. deeper location) of the Havannah Island site as well as on the opposite sides of Havannah Island and Dunk Island. Deployments of the sediment traps have occurred at these sites continuously since June 2016 with changeovers typically occurring every 2-3 months.

Flood plumes were sampled along a salinity gradient transect using the SediPump® to collect the mass required for organic and inorganic tracing. Additional samples were collected for suspended particulate matter, dissolved and particulate nutrients (nitrogen, phosphorus and carbon), bioavailable particulate nutrients, particle size and microscope analysis. Some modifications (i.e. filter cartridge, intake hoses) were made to the SediPump® configuration to better optimise the amount of sediment collected in the plumes.

Figure 2.4. The seven locations where the SediSampler® have been deployed with a nephelometer and current meter.

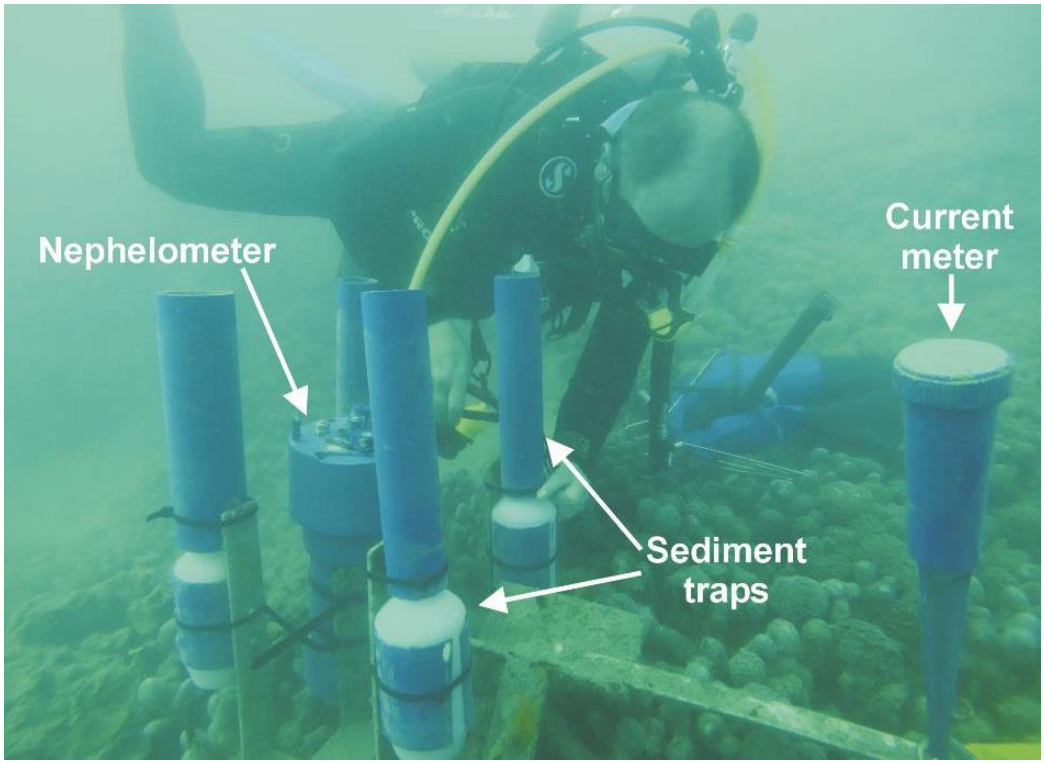

Figure 2.5. The SediSampler® (Sediment traps), surrounded by the nephelometer and current meter (Image: Ian McLeod).

Suspended particulate matter sampling method comparison

Measurements of suspended sediment in freshwaters are conducted using two common methods including total suspended solids (TSS) and suspended sediment concentration (SSC). Briefly, the TSS method involves the filtering of a known volume of water (generally 1L) through a preweighed filter paper. The filter paper is then dried for ~ 24 hours at 105° C and reweighed to obtain a concentration in $mg.L^{-1}$. The SSC method involves the evaporation of a known volume of water where the dried material is weighed to provide a concentration in $mg.L^{-1}$. Both techniques have pros and cons. Some researchers argue when coarser (i.e. sand sized) particles are present the TSS method likely underestimates the concentration and hence the SSC method is considered a more 'true' representation (see Gray et al., 2000). However, the SSC method also measures the dissolved solids and therefore requires the measurement of total dissolved solids to separate the dissolved and particulate fractions. In most cases, either method is likely suitable but in special scenarios where particle size is particularly fine (or coarse) or dissolved salts are elevated, one method would be preferred over the other. Indeed in marine settings the SSC method is not possible due to the dissolved salts in seawater and the TSS method is used exclusively.

TSS measurement of suspended sediments across the GBR catchments have historically used GF/C filter papers (1.2 µm nominal pore size) according to the APHA (2005) Standard Method 2540-D (e.g. Wallace et al., 2016). Other agencies such as the EPA recommend GF/F filter papers (0.7 µm nominal pore size) as a standard method in freshwaters. In the marine environment, a different mix of filter papers have historically been used, here in the GBR the Australian Institute of Marine Science (AIMS) use the 0.4 µm polycarbonate filter papers (as well as in their historical catchment monitoring program, M. Skuza, personal communication 2018) and the James Cook University (JCU) flood plume program used the 1.2 µm GF/C filter papers up to the 2017/18 season before transitioning to 0.4 µm polycarbonate filters for the 2018/19 season. While the TSS method does appear to be fairly straight forward, there are many issues that can be encountered including choice of filter paper, the volume of freshwater used to flush the sample of dissolved salts, the volume of sample to filter to achieve acceptable precision and the experience of the technician (see Neukermans et al., 2012). As reliable measurements of SPM are critical in our project, we conducted a study to quantify the differences of each TSS method (and SSC in freshwater) so we could gain a better appreciation on the quality control of our results as well as for historical datasets. We chose 8 different samples to perform our analysis on where we collected 20 L of sample from each site. Each sample was well mixed before being subsampled into 1 L bottles for triplicate analysis (i.e. each filter paper was analysed 3 times) using 1.2 µm GF/C, 0.4 µm polycarbonate and 0.2 µm pore size filter papers. The samples taken in the freshwater reaches of streams were also analysed using the SSC method along with total dissolved solids analysis. The sites included: the Burdekin Falls Dam (BFD) in the dry season which is characterised by year-round persistent turbidity of very fine colloids typically <1 µm in size (see Cooper et al., 2017); two samples from the Burdekin River at Inkerman Bridge in elevated flow characterised by high sediment concentrations; 1 sample each from the Tully and Johnstone end-of-river (freshwater) sites during elevated flow characterised by lower sediment concentrations; 3 samples from the higher salinity (>20 PSU) sections of flood plumes from the Burdekin and Tully Rivers, including both surface and near the bottom water column sampling of the Tully plume site. A summary of the particle size results for these samples are provided in Table 2.1.

Table 2.1. Particle size distribution results from the samples analysed for TSS and SSC. The numbers reflect the percentage where particle size is below a certain fraction or within a fraction range. Note end-of-river and plume samples have had organic removal treatment prior to analysis.

Sample	% organic	Focal size fractions (µm)		Particle size distribution (µm)			
		<0.5	<20	<3.9	3.9-15.6	15.6-63	>63
Burdekin Falls Dam	20	50	89	70	17	11	2.5
Burdekin (end-of-river) #1	12	0.5	90	38	47	15	0.1
Burdekin (end-of-river) #2	12	0.8	89	40	45	14	1
Burdekin plume (23 salinity)	26	15	85	57	26	10	6
Johnstone (end-of-river)	29	0	64	13	44	37	7
Tully (end-of-river)	18	0	88	26	57	16	1
Tully plume – surface (31 salinity)	33	6	84	39	41	17	3
Tully plume – depth (34 salinity)	22	-		-			

For the BFD sample, there was a large difference in the TSS concentration measured via the 1.2 µm filter paper (5.5 ± 0.3 $mg.L^{-1}$) compared with the 0.4 and 0.2 µm filter papers (82 ± 4 $mg.L^{-1}$ and 78 ± 5 $mg.L^{-1}$, respectively; Figure 2.6). The SSC was much higher (197 ± 12 $mg.L^{-1}$), however when the total dissolved solids were subtracted, the result (99 ± 10 $mg.L^{-1}$) was closer in line with the 0.4 and 0.2 µm finer filter papers. As previously mentioned, the BFD sample represents a 'special case' scenario where most of the particles are colloidal (<1 µm) in size throughout dry season ambient conditions (Table 2.1). These results make a case that if sampling should occur to evaluate water quality guidelines for suspended sediment in lakes/dams under low flow conditions, then either the 0.4 and 0.2 µm filter papers (or SSC subtracting the total dissolved solids) should be used.

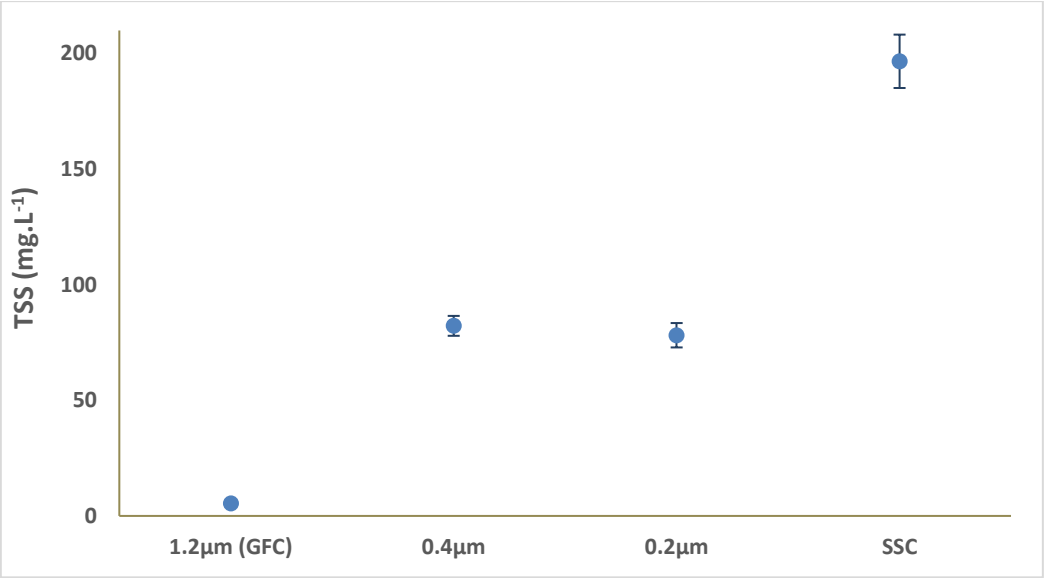

Figure 2.6. Burdekin Falls Dam suspended sediment results using the different filter papers. Note these wide variations only likely apply for low flow conditions when the bulk of particles suspended are colloidal (<1 µm).

The suspended sediment results using the different filter papers and SSC methods on Burdekin end-of-river water samples were comparable with the largest difference between the 1.2 µm filter paper (906 ± 5 $mg.L^{-1}$) and the 0.2 µm filter paper (1040 ± 19 $mg.L^{-1}$) for the end-of-river #1 sample (Figure 2.7). This difference (~14%) for this high TSS concentration is quite reasonable given other uncertainties in field and lab sampling (i.e. largely related to subsampling to ensure all particles remain in suspension). In fact, a split sample run in a separate laboratory using a 1.2 µm filter paper reported a TSS concentration of 998 $mg.L^{-1}$. Indeed, the precision of the triplicate samples (generally within 5 to 10%) highlights the reproducibility of the filter papers. Interestingly, the suspended sediment results from the Burdekin plume sample were markedly different between the 0.2 µm (300 ± 4 $mg.L^{-1}$), 1.2 µm (21 ± 0.4 $mg.L^{-1}$) and 0.4 µm (16 ± 1.6 $mg.L^{-1}$) filter papers (Figure 2.7). We cannot fully explain this result as the particle size on this sample was mostly >1 µm (Table 2.1) so we would expect little difference between the filter papers (or similar to the difference between the 1.2 and 0.4 µm filter papers). Incidentally, the TSS concentration reported by a different laboratory (1.2 µm filter paper) from a split sample from the same flood plume site reported a concentration of 19 $mg.L^{-1}$.

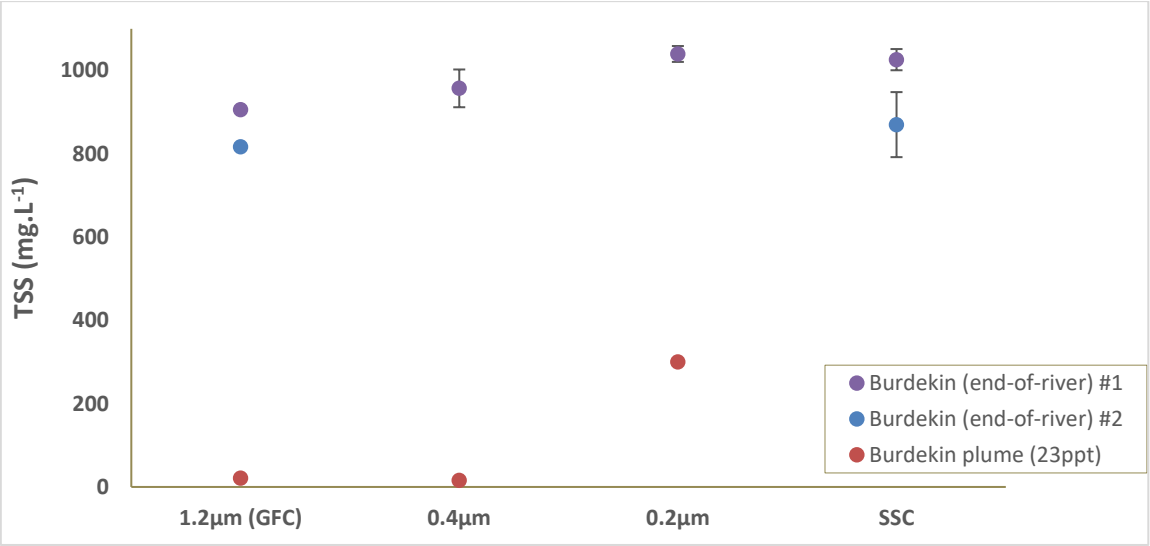

Figure 2.7. Suspended sediment results from samples from the Burdekin end-of-river site and the flood plume. Note that SSC was not performed on the flood plume sample because of the high total dissolved solids.

Suspended sediment results from samples from the Johnstone and Tully Rivers and Tully flood plume show quite variable results and do not always display a systematic change with the use of finer filter papers (Figure 2.8). For example, the Tully plume – depth sample had a TSS concentration of 8.8 ± 0.8 mg.L^{-1} with the 1.2 µm filter paper, 4.8 ± 0.5 mg.L^{-1} with the 0.4 µm filter paper and 16.7 ± 2.1 mg.L^{-1} with the 0.2 µm filter paper (Figure 2.8). In contrast, for the Johnstone end-of-river site the 0.4 µm filter paper yielded the highest result (15 ± 5 mg.L^{-1}) compared to the 1.2 µm (7.1 ± 0.3 mg.L^{-1}) and 0.2 µm (8.7 ± 3.1 mg.L^{-1}) filter papers. Samples from the Tully end-of-river site were within error margins across the three filter papers used (Figure 2.8). The difference between the TSS and the SSC results for the end-of-river sites likely highlight the amount of total dissolved solids (i.e. particles <0.2 µm) in the sample. In addition, for the flood plume samples (i.e. higher salinity), the higher TSS concentrations for the 1.2 µm filter papers (compared to the 0.4 µm polycarbonate) likely reflect the retention of salts in the glass filter papers (M. Skuka, personal communication 2018).

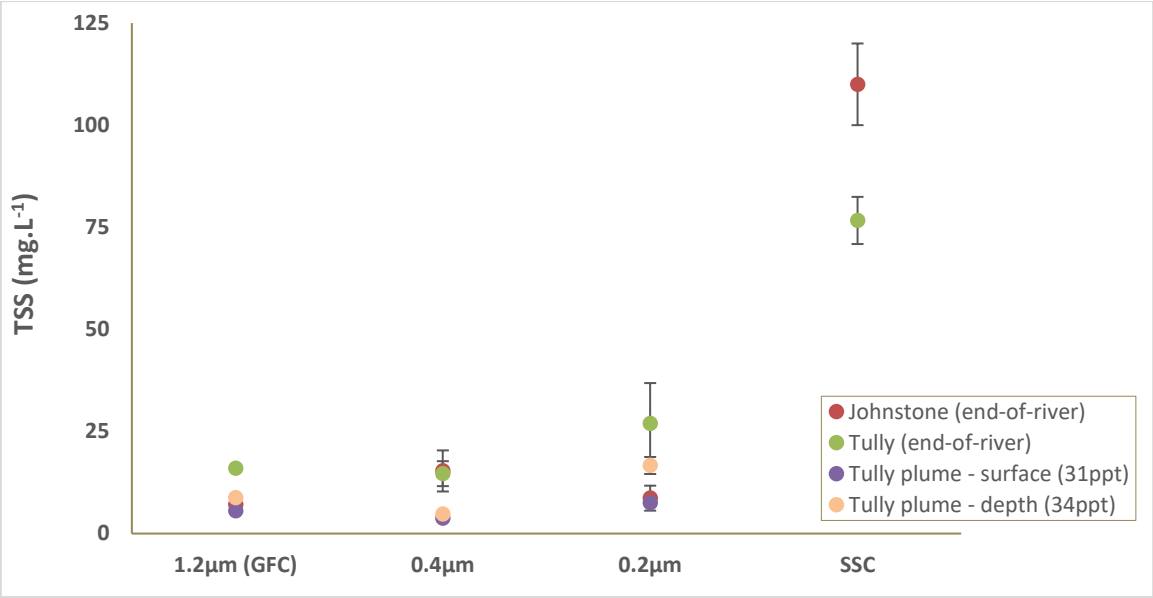

Figure 2.8. Suspended sediment results from samples from the Johnstone and Tully Rivers and Tully flood plume.

Overall, we consider that while there are some discrepancies in the TSS results across different filter papers in our analysis, there was no clear systematic difference between the results and in particular between the 1.2 µm and 0.4 µm filter papers currently used in GBR catchment and lagoon monitoring programs. Logically it could be thought that for the same water sample, the 0.4 µm filter papers would consistently yield higher TSS results than the 1.2 µm filter papers due simply to the finer pore size and ability to capture the finer particles. However, there are several considerations for the quality of these data including the flushing of salts from the sample with freshwater (for marine samples) where under flushing could leave behind precipitated salts upon drying leading to a higher TSS result while over flushing could potentially break apart the pore spaces and cause an underestimation of TSS (particularly for the GF papers see Neukermans et al., 2012). Indeed, blank samples using filtered (0.2 µm) water (either freshwater or seawater depending on the samples being analysed) should be performed with the analysis to examine the potential of salt retention on the filter papers (M. Skuza personal communication, 2018). In addition, the sediment concentration potentially could also be taken into account prior to analysis as the volume of water filtered in the analysis would greatly help the precision of the samples (see Neukermans et al., 2012). For samples > 100 $mg.L^{-1}$ the 1.2 µm filter papers likely provide a more reproducible result with greater precision, although for samples < 10 $mg.L^{-1}$ the 0.4 µm filter papers likely provide a more robust result. Our preliminary results suggest that the accuracy of data where TSS is reported to be <20 $mg.L^{-1}$ (i.e. common for GBRL flood plume sampling where salinities are typically >10 PSU), that the error is likely to be in the order of ± 3 $mg.L^{-1}$ between the 1.2 µm and 0.4 µm filter papers. This provides some confidence in interpreting historical TSS datasets.

Suspended particulate matter trends over the estuarine mixing zone

As we now have an appreciation of the reliability of the TSS (SPM) results, we can evaluate historical flood plume datasets to examine how SPM concentrations vary over the estuarine mixing zone for different rivers and over multiple flood years. For this analysis we chose datasets from the Burdekin (145 samples; data over 8 years: Figure 2.9), Fitzroy (101 samples; data over 3 years: Figure 2.10) and Tully (378 samples; data over 8 years: Figure 2.11) Rivers. We present the data into three separate panels, (1) full dataset over the estuarine mixing zone; (2) the 0 – 10 salinity zone and; (3) the 10 – 36 salinity zone (Figures 2.9-2.11). This allows a better visualisation of the dataset particularly for the rivers where the initial (i.e. at 0 salinity) SPM concentration is generally much higher (e.g. Burdekin and Fitzroy Rivers). The results highlight that most SPM in the Burdekin and Fitzroy Rivers is deposited between the 0 and 5 salinity zone with the vast majority of samples falling from >150 $mg.L^{-1}$ at 0 salinity (freshwater) to < 20 $mg.L^{-1}$ by 5 salinity, and remaining below 20 $mg.L^{-1}$ thereafter (Figures 2.9 and 2.10). In contrast, the Tully River initial concentrations at 0 salinity are in the order of 20 to 40 $mg.L^{-1}$ and most samples generally fall below 20 $mg.L^{-1}$ by the 5 salinity zone (Figure 2.11). Indeed, samples showing concentrations >20 $mg.L^{-1}$ where salinities are >5 in the Tully estuarine mixing zone likely indicate an additional contribution from resuspension of benthic sediments.

As most sediment in the larger rivers is deposited in the 0 to 10 salinity zone and the deposited sediment in this zone is largely retained near the river mouth (see Lewis et al., 2014), it is the behaviour of SPM in the 10 to 36 estuarine mixing zone that travels furthest and is likely the most ecologically important. Hence it is critical to examine the variability of TSS/SPM concentrations for this part of the salinity zone for the different rivers to appreciate their effect on the GBR. Conceptually, the sediment exported from a river with much lower sediment loads (e.g. Tully River) may be just as important as a river with much higher sediment loads (e.g. Burdekin River) if most of the sediment in the larger river is deposited in the 0 to 10 salinity zone and the concentrations in both rivers beyond the 10 salinity zone are similar. In fact, when the SPM data for the Burdekin, Fitzroy and Tully Rivers are examined over systematic salinity increments, the Burdekin and Fitzroy Rivers generally have higher concentrations over the estuarine mixing zone up to at least the 25 salinity zone (Figure 2.12). For example, SPM across the estuary of the Burdekin River falls from 42 (± 64) $mg.L^{-1}$ in the 5 – 10 salinity zone to 19 (± 21) $mg.L^{-1}$ in the 10 – 15 salinity zone. Mean SPM concentrations remain in this range (~ 20 $mg.L^{-1}$) until falling to 4.8 (± 6.3) $mg.L^{-1}$ in the 25 – 30 salinity zone. In contrast, SPM concentrations across the estuarine mixing zone for the Tully River fall from 23 (± 21) $mg.L^{-1}$ in the 5 – 10 salinity zone to 8.3 (± 5.3) $mg.L^{-1}$ in the 10 – 15 salinity zone and then fall to 3.9 (± 2.8) $mg.L^{-1}$ in the 25 – 30 salinity zone (Figure 2.12). Hence it appears that after the 25 salinity zone, SPM in the Burdekin and Tully River plumes have similar concentrations, although further research is required to examine the composition of the SPM. Our preliminary observations indicate that there appears to be more terrigenous (mineral) sediment in the SPM remaining in the Burdekin plume while the Tully appears to have higher organics/floc material. In that regard, the SPM in one river could be more predominantly composed of phytoplankton and the other could still contain more terrigenous (mineral) sediment which, in turn, could have a greater influence on light attenuation. Interestingly, SPM concentrations across the Fitzroy River estuarine mixing zone are higher than both the Burdekin and Tully River with mean SPM of 23 (± 3) $mg.L^{-1}$ in the 25 – 30 salinity zone (Figure 2.12).

While the mean SPM concentrations in the 20 – 25 salinity zone of the Burdekin estuarine mixing zone (20 ± 20 $mg.L^{-1}$) is ~3 times higher than the Tully (6.5 ± 6.4 $mg.L^{-1}$), the difference is much less compared to when the total sediment exported from both rivers is taken into account (i.e. >40 times difference: 92 kt for Tully versus 4000 kt for Burdekin, Kroon et al., 2012). Again, this highlights the importance of sediment deposition in the 0 – 10 salinity zone and indeed, this relationship could also explain why Fabricius et al. (2014, 2016) found much stronger correlations between satellite photic depth and river discharge as opposed to sediment load. However, the Burdekin mean annual discharge is also ~ 3 times higher than the Tully and so when this factor is applied the relative load (i.e. flow by concentration) of the most ecologically important sediment would be ~ 9 times greater from the Burdekin. Clearly, it is not just the volume of river discharge (i.e. more water discharged = greater plume extent) that is important but also the delivery of flow to the GBR. For example, the Tully River can have multiple discharge events over the year while the Burdekin commonly will only have one flow event where the vast majority of flow will be delivered to the GBR and produce a much larger offshore plume. Other important factors to consider are differences in the SPM that is exported from the river and the additional SPM (i.e. marine organic material) formed and transported within the plume. Hence it is critical to not only document the changes in TSS concentration across the salinity gradient of the different rivers but also to characterise SPM composition over this gradient.

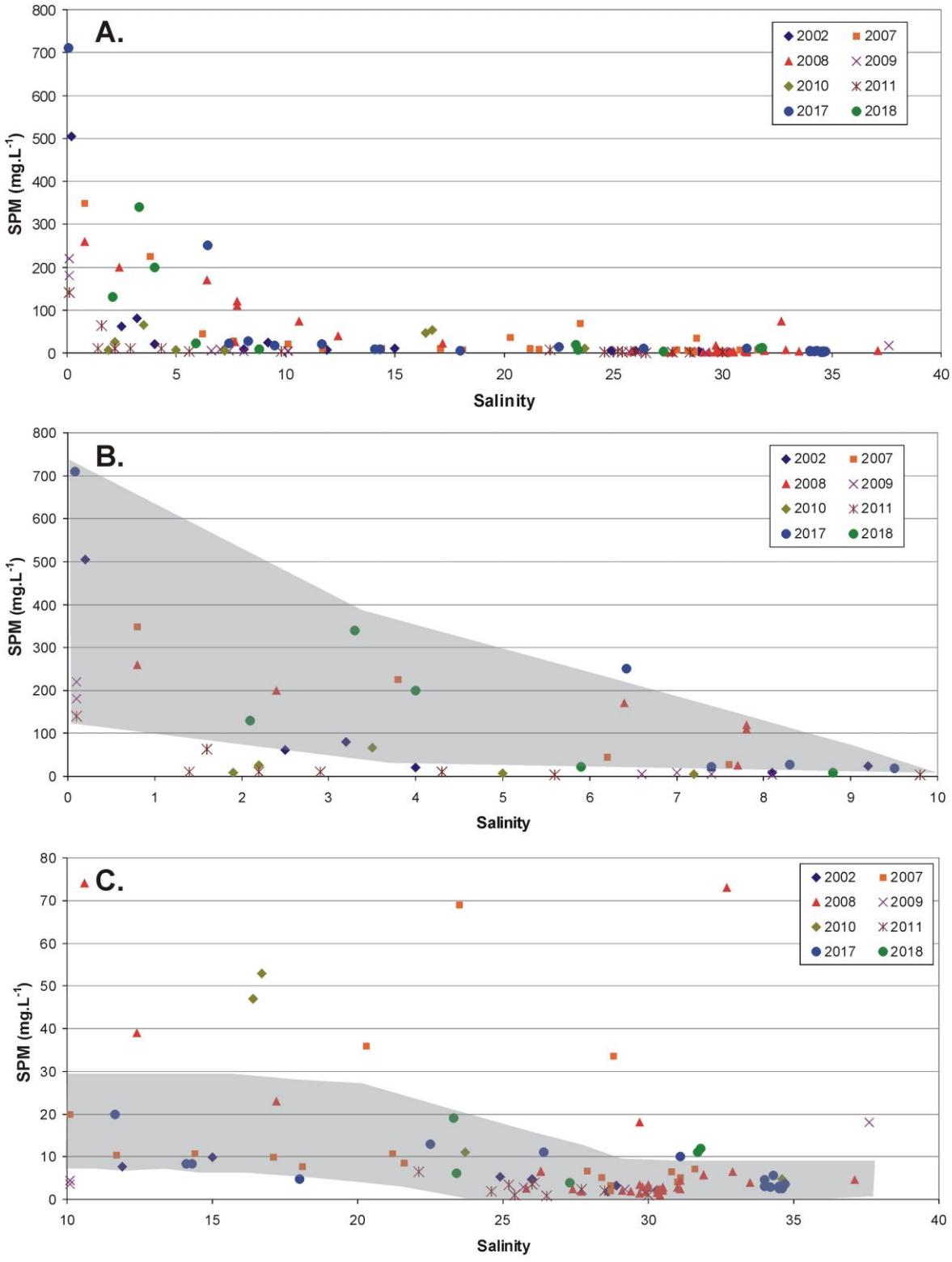

Figure 2.9. Plots of SPM data over the estuarine mixing zone for the Burdekin River plume over different years including the full dataset (A), between 0 to 10 salinity (B) and 10 to 36 salinity (C).

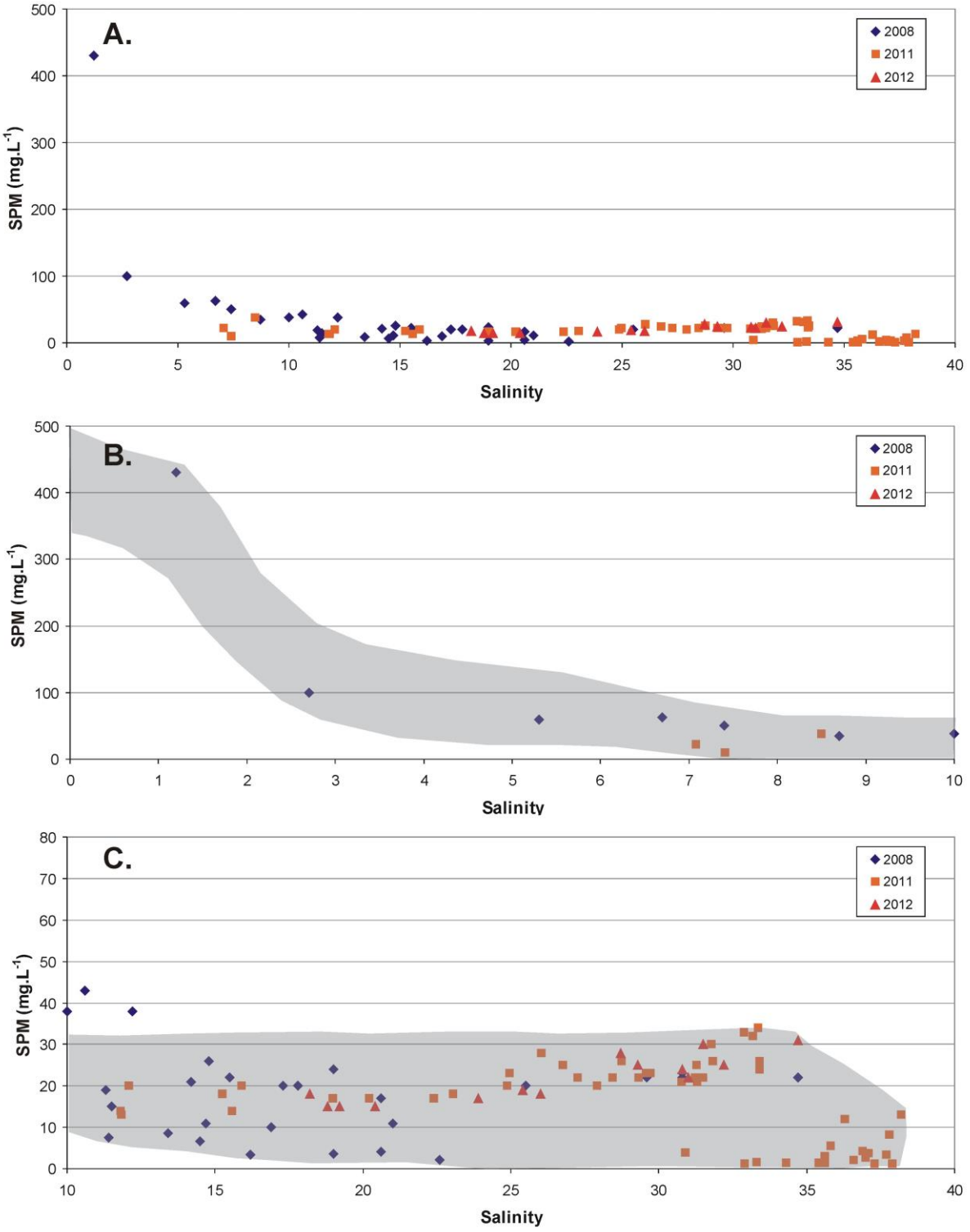

Figure 2.10. Plots of SPM data over the estuarine mixing zone for the Fitzroy River plume over different years including the full dataset (A), between 0 to 10 salinity (B) and 10 to 36 salinity (C).

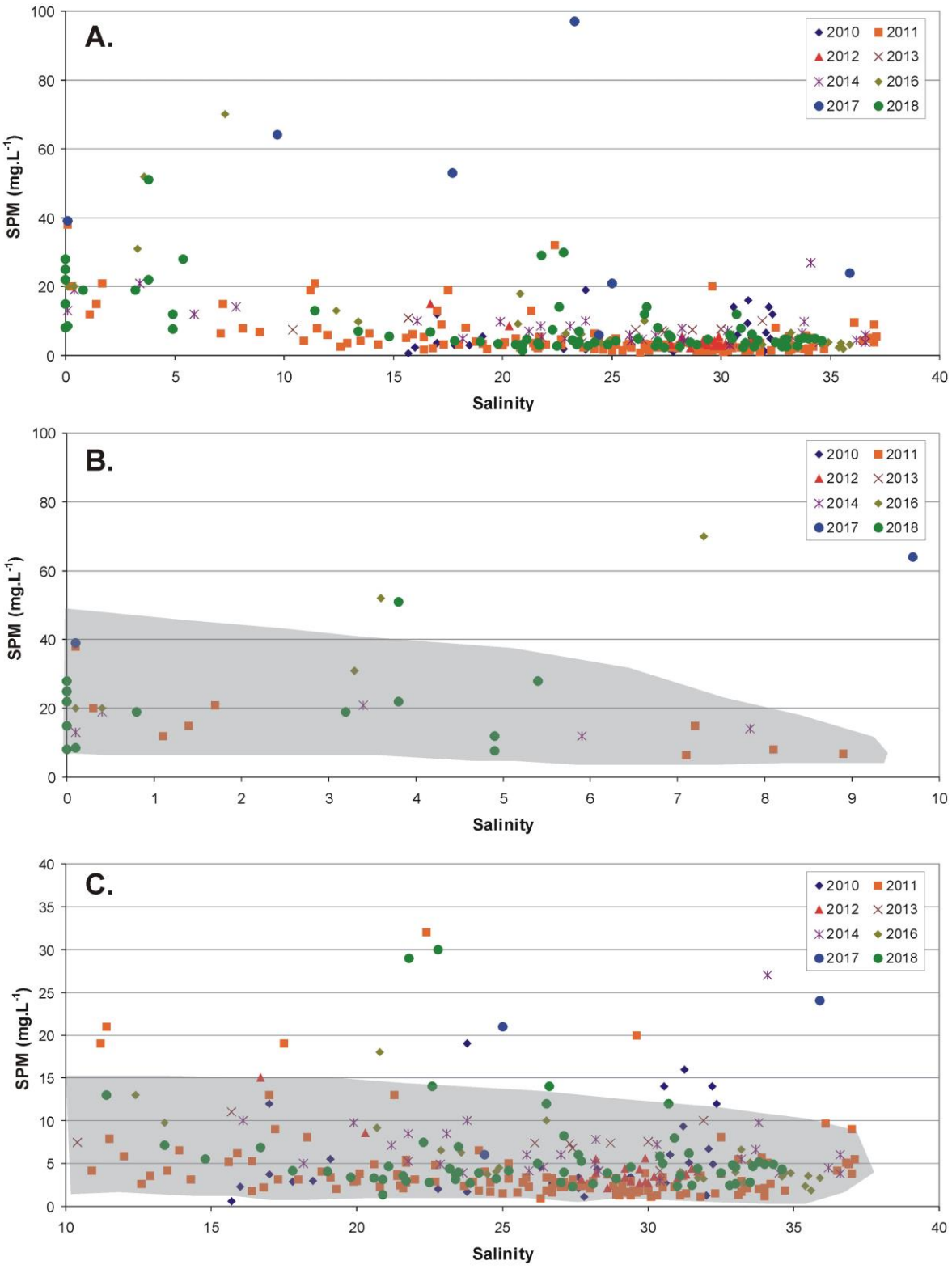

Figure 2.11. Plots of SPM data over the estuarine mixing zone for the Tully River plume over different years including the full dataset (A), between 0 to 10 salinity (B) and 10 to 36 salinity (C).

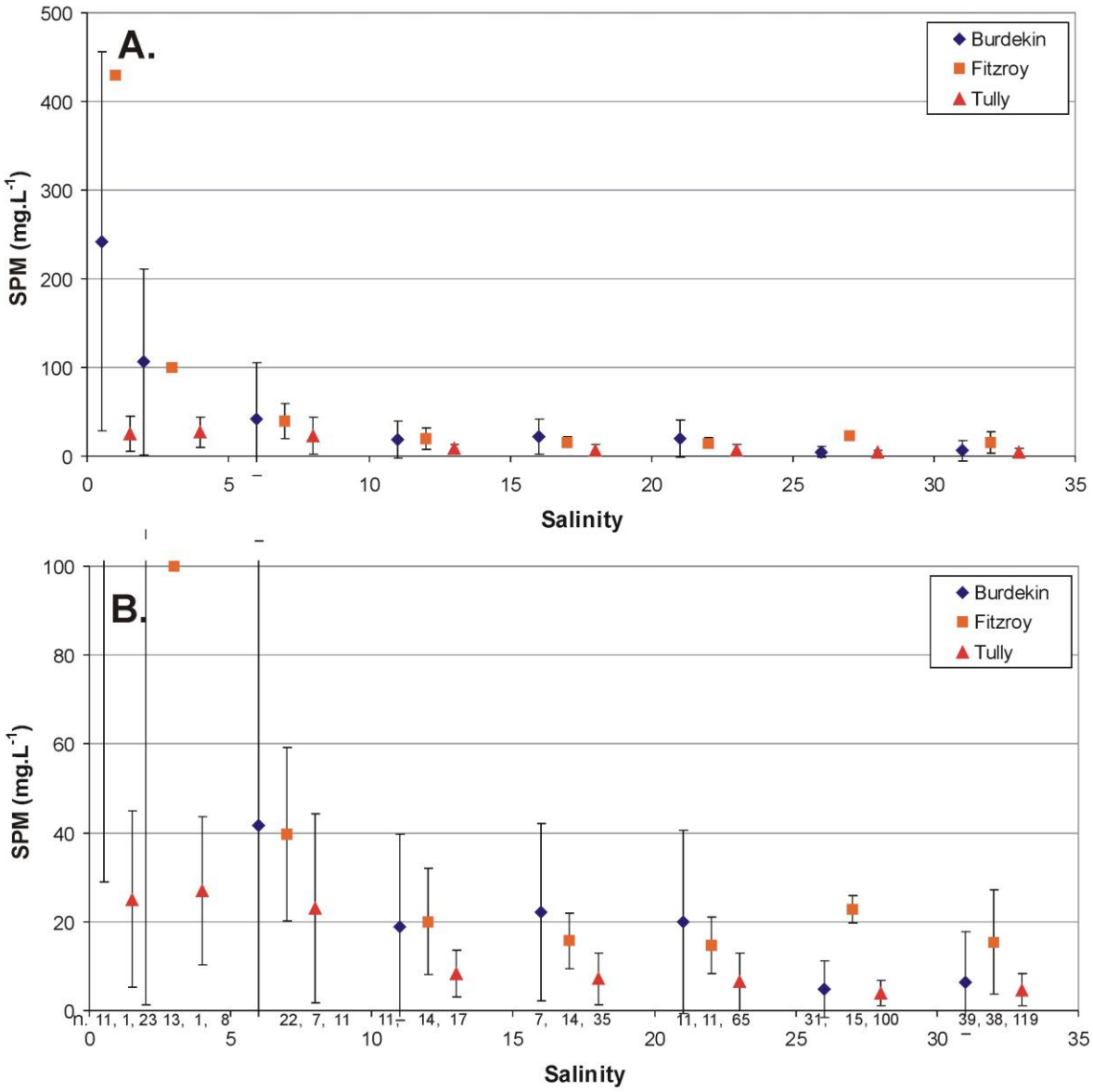

Figure 2.12. Summary statistics of SPM data (including 1θ standard deviation) over the estuarine mixing zone for the Burdekin, Fitzroy and Tully River plumes over different salinity ranges. Note panel B reduces the scale on the y axis so the higher salinity zones can be more easily viewed. Number of samples (n) are provided along the x axis of panel B.

Turbidity calibrations with suspended particulate matter at the logger sites

The nephelometers used at our marine sites continuously measure turbidity at 10 min intervals which is related to the suspended sediment concentration. However, the relationship between turbidity and suspended sediment concentration will vary from site to site and potentially over time due to variability in sediment properties such as particle size and colour. Hence we conducted site-specific turbidity-suspended sediment calibrations using benthic sediments collected from our 7 sampling sites. The standard procedure is to add sediment collected from our site (in our case sieved to represent the < 75 µm fraction) in filtered water with dissolved pool salt (to represent ~ 5 PSU salinity) to systematically increase the raw nephelometric turbidity unit (NTU) counts of 0, 1, 3, 6, 18, 35 and 100 NTU. At each of these raw NTU counts a sample for TSS analysis was collected. The raw NTU counts on the nephelometer were calibrated to normalise/standardise NTU readings and these were directly plotted against the measured TSS concentration to establish a linear relationship. We used 0.4 µm polycarbonate filter papers for our TSS analysis (based on our findings from the previous section), although for some sites we collected duplicate TSS samples to analyse using 1.2 µm GF/C papers to examine the difference in the relationship that this method adjustment may cause. Furthermore we also conducted additional calibrations of the same sediment ~ 14 days apart to ensure the relationship was consistent and replicable over time (i.e. nephelometer drift) and for our logger sites where the normalised turbidity readings were much higher (e.g. Middle Reef, Cleveland Bay, Orchard Rocks) we measured a further point > 250 normalised NTU. As the properties of the sediment at our Dunk Island site changed over the ~ 2 ½ years of monitoring, we also examined the turbidity-suspended sediment relationship with sediments collected from the sediment trap and the benthic sediment from the same deployment period (April 2017 following considerable flooding in the Tully River) as well as benthic sediment collected during the dry season (July 2017). We note that as the turbidity-suspended sediment calibration was not strictly linear, and particularly so for the higher concentrations, in most cases we only used the calibrations up to the ~ 80 normalised NTU readings to construct the linear relationship (i.e. excluding the higher concentrations). In that regard, the c value typically became < -3 when these outer points were considered for the linear relationship, highlighting that the linear relationship fails to cross near the origin which is not desirable (i.e. as ~0 NTU should be very close to 0 TSS). In comparison, the linear relationship crosses close to the origin where the values up to ~ 80 normalised NTU were used which also accounts for the vast majority of our field logger data readings. We note on the rare occasions where the logger recorded > 80 normalised NTUs, the suspended sediment concentration would be underestimated using these linear relationships. We have extended the linear trendline out as a dotted line to the outer datapoint to highlight this general underestimation.

The turbidity-suspended sediment calibrations for the Dunk Island site showed very similar linear relationships for the sediment collected in the SediSampler® (February to April 2017 deployment, Dunk3, red dots) and benthic sediment collected in April 2017 (Dunk1, blue diamonds: Figure 2.13). In comparison, the benthic sediment sample collected in July 2017 showed a different linear relationship between the turbidity-suspended sediment concentration points (Dunk2, blue squares). Hence for the Dunk Island logger site we applied a wet season calibration for periods where considerable flooding from the Tully River had occurred using the benthic sediment calibration (suspended sediment = 1.481 × normalised NTU) and a dry season calibration where there was no considerable new terrigenous sediment input during the logger period (suspended sediment = 1.105 × normalised NTU). This is an important finding

as it suggests that for every 1 normalised NTU increase, under wet season conditions the suspended sediment concentrations in the water column are in the order of 1.5 times greater compared to dry season conditions (e.g. in this time series a normalised NTU reading of 10 is equivalent to a suspended sediment concentration of 11.1 $mg.L^{-1}$ in the dry season and 14.8 $mg.L^{-1}$ in the wet season while a reading of 30 NTU is equal to 33 $mg.L^{-1}$ in the dry season and 44 $mg.L^{-1}$ in the wet season). Interestingly, there was little difference in the linear relationship between the measurement of TSS using the 0.4 µm and 1.2 µm filter papers for the SediSampler® sample (suspended sediment = 1.5996 × normalised NTU versus suspended sediment = 1.4456 × normalised NTU, respectively). However, a larger difference in the linear relationship using the different TSS filter papers was evident for the benthic sediment sample from April (suspended sediment = 1.481 × normalised NTU versus suspended sediment = 0.9577 × normalised NTU, respectively).

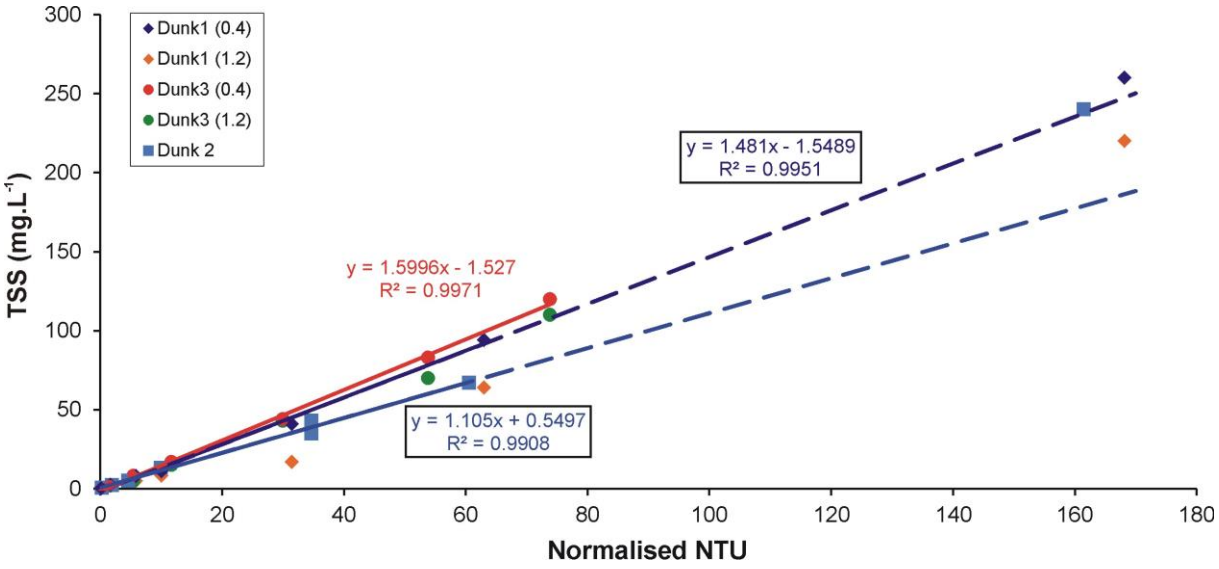

Figure 2.13. Dunk Island site calibration between normalised NTU and suspended sediment concentration.

There was less temporal variability in the benthic sediments at the sites in Halifax Bay (Havannah Island and Orpheus Island) and so only one normalised NTU – suspended sediment calibration was performed for each site. The calibration was similar between both sites (suspended sediment = 1.5496 × normalised NTU versus suspended sediment = 1.4628 × normalised NTU for the Havannah Island and Orpheus Island sites, respectively) and these relationships were also used to calibrate the normalised NTU readings to suspended sediment concentrations for our logger data at these sites (Figure 2.14). We note there was a considerable difference in the linear relationship calculated for Havannah Island site on the repeated samples (suspended sediment = 1.5496 × normalised NTU versus suspended sediment = 1.1713 × normalised NTU, respectively), although this is likely due to either a raw NTU misreading or an outlier in the TSS analysis (Figure 2.14a). This result will be investigated at a later date to ensure the most accurate relationship is used to convert normalised NTU to suspended sediment concentration at this site. In comparison, we note the repeated measurements (orange squares) showed strong agreement for samples taken from Orpheus Island (Figure 2.14b) and Geoffrey Bay (Figure 2.16a)

Similarly only one sediment calibration was performed for each of the four Cleveland Bay sites with normalised NTU – suspended sediment calibrations ranging from suspended sediment = 1.3163 × normalised NTU at the Geoffrey Bay site to suspended sediment = 1.7444 × normalised NTU at the Cleveland Bay site (Figures 2.15 and 2.16). These relationships were applied to the respective logger sites to convert normalised NTU to suspended sediment concentrations. We note that there was some difference in the linear relationship using the different TSS filter papers for the Orchard Rocks site (suspended sediment = 1.5628 × normalised NTU for the 0.4 µm filter paper versus suspended sediment = 1.3321 × normalised NTU for the 1.2 µm filter paper). Given this variability observed across measurements from our different sites, we would recommend that future calibrations of the normalised NTU and suspended sediment concentration relationship apply the 0.4 µm polycarbonate filters. In our findings, measurements using the 1.2 µm GF/C papers generally underestimated suspended sediment concentration.

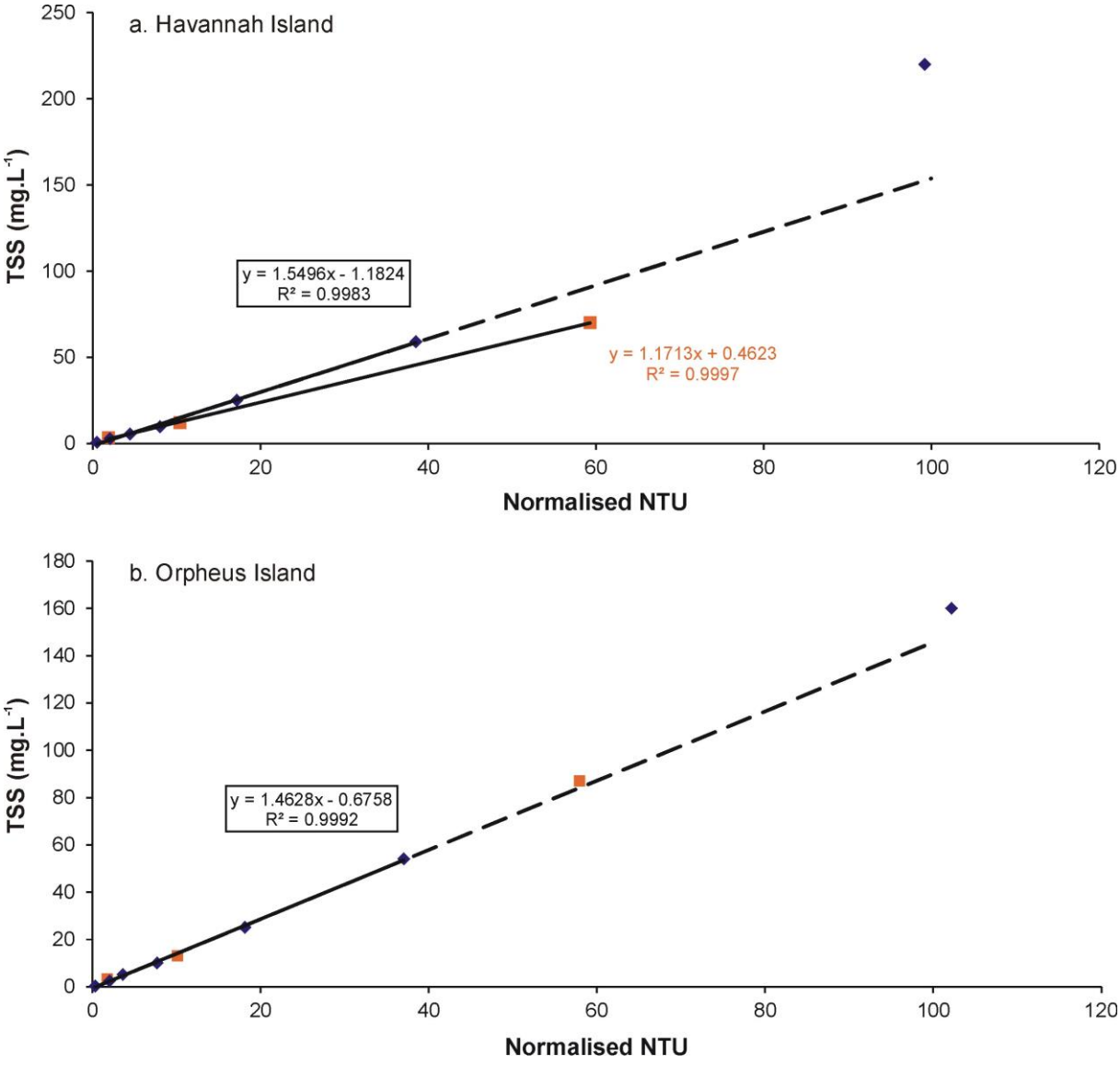

Figure 2.14. Halifax Bay sediment calibrations between normalised NTU and suspended sediment concentration for the Havannah Island site (a) and the Orpheus Island site (b).

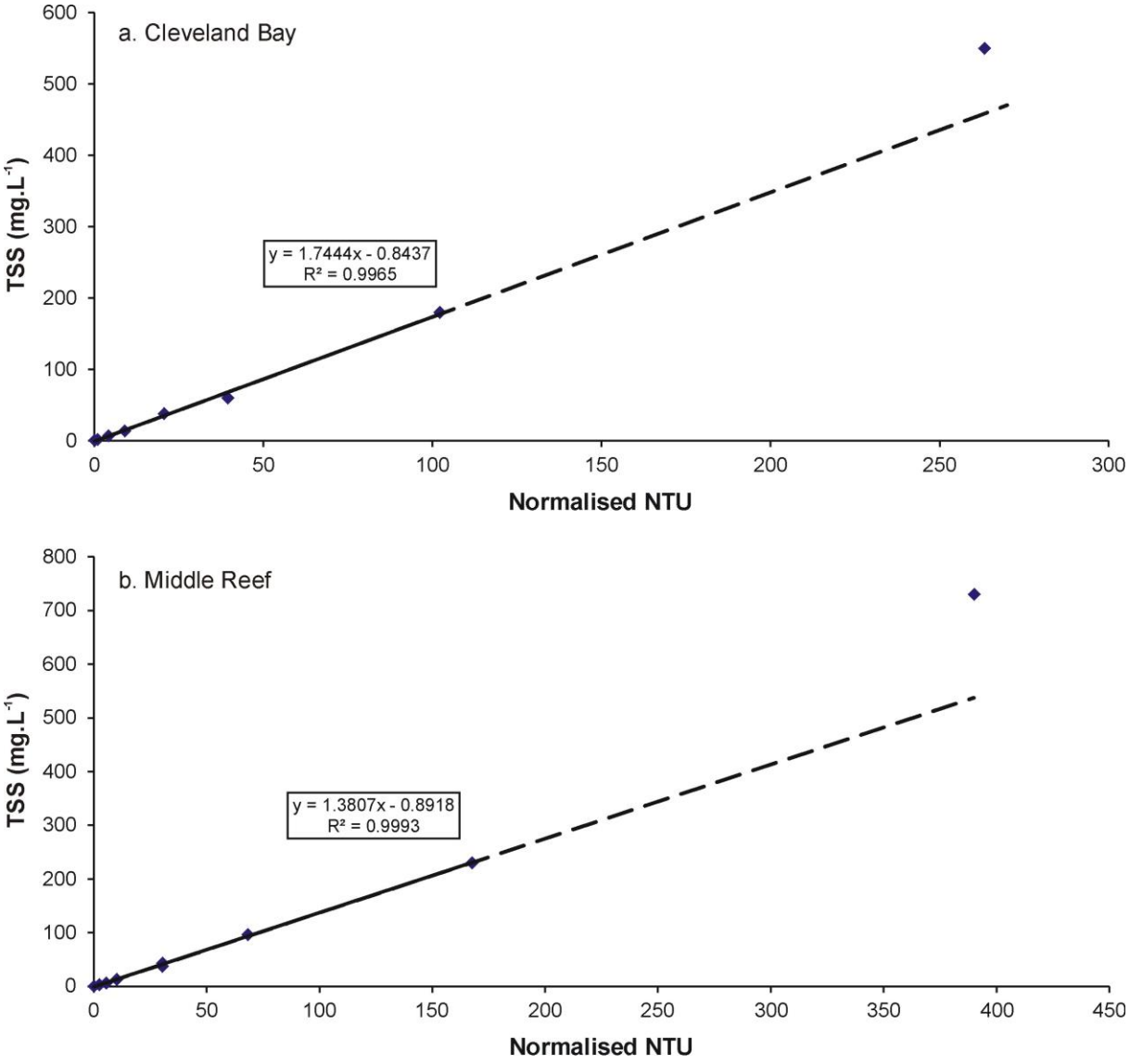

Figure 2.15. Inner Cleveland Bay sediment calibrations between normalised NTU and suspended sediment concentration for the Cleveland Bay site (a) and the Middle Reef site (b).

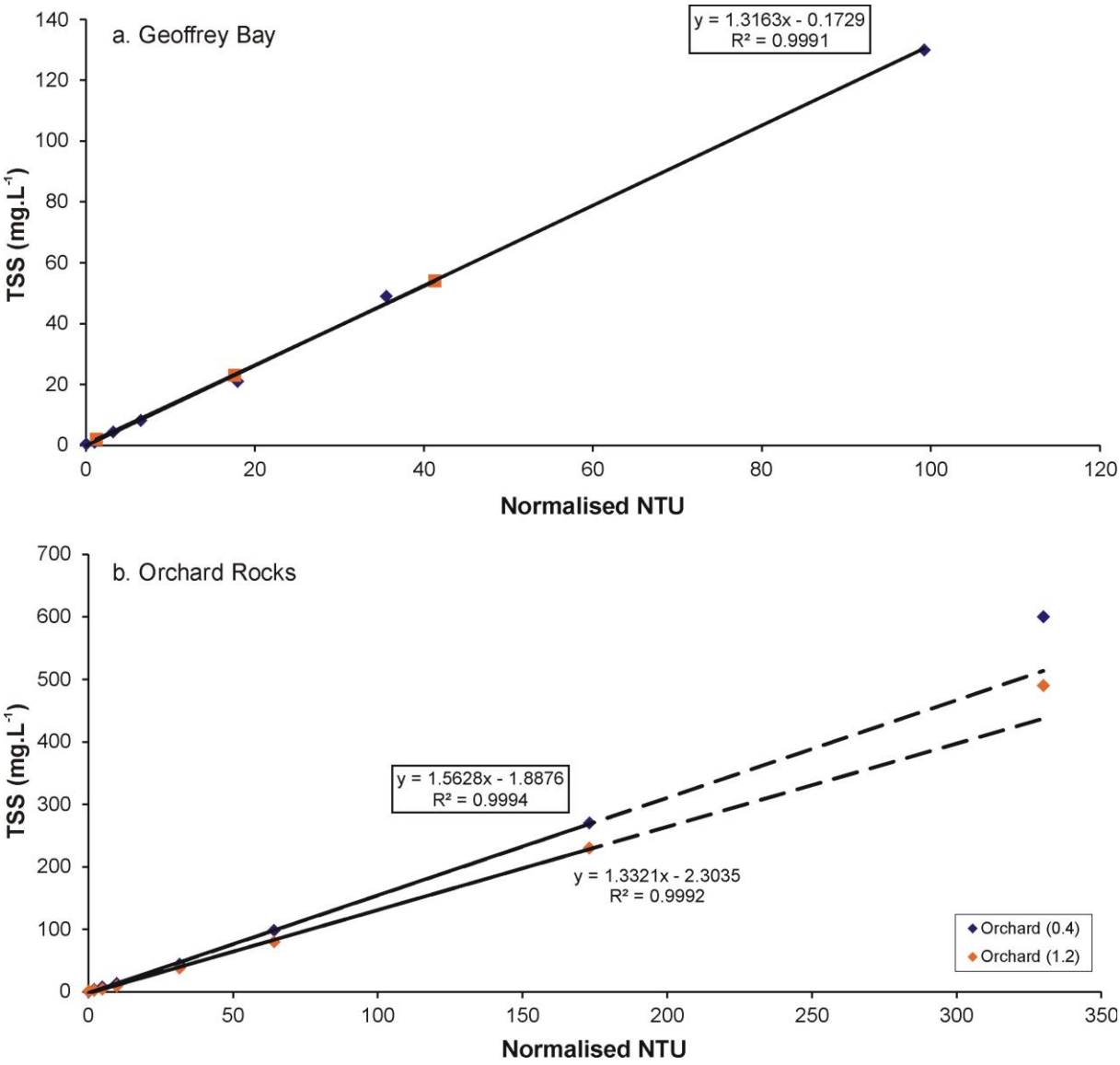

Figure 2.16. Outer Cleveland Bay sediment calibrations between normalised NTU and suspended sediment concentration for the Geoffrey Bay site (a) and the Orchard Rocks site (b).

Results from sediment traps: collection efficiency with variable spacing and tilt

Experiments on trap spacing

This NESP project includes a sampling design of four sediment traps separated by 180 mm, mounted on frames (Figure 2.5). Our aim was to determine to what extent our trap spacing could be considered independent and representative for collections of suspended sediment accumulation rates. Experiments to date have been limited to short durations using small straight channeled flumes, with no adequate field studies testing trap spacing in shallow coastal waters adjacent to coral reefs or subtidal seagrass fields (Gardner, 1980; Noder, 1999). To investigate the role of spacing we included spacing frames at the Havannah Island and Geoffery Bay sites for three consecutive deployments, and one flume experiment.

Field Experiments - Spacing

The set up entailed having an array of 8 evenly spaced SediSampler® 55s sediment traps positioned 540mm (9 diameter widths: 9D) apart from adjacent traps. This frame was positioned around the existing standard NESP frame trap set up such that the distance between the 9D spacing traps and the 3D NESP traps was also 540mm (Figure 2.17). These traps were also paired and positioned to be parallel to the corresponding NESP frame traps (Figure 2.17). The Havannah site was 9 metres deep and located on a relatively sheltered reef slope, whereas the Geoffery Bay site was at 5 metres depth and experienced higher exposure to south-easterly winds and swell.

Figure 2.17. The sampling design set up for investigating the role of spacing on collection efficiency for sediment traps. In the centre is the standard NESP trap frame which is surrounded by the 9D spaced traps (Photo: Cassandra Thompson).

The trap collection rates throughout the Havannah spacing study show excellent precision for both the NESP frame and the spacing frame traps (Figure 2.18). While there were significant differences in the rates of collection between the treatments on the second and third deployments, the collection rates differed by less than 9%. These differences showed no trend.

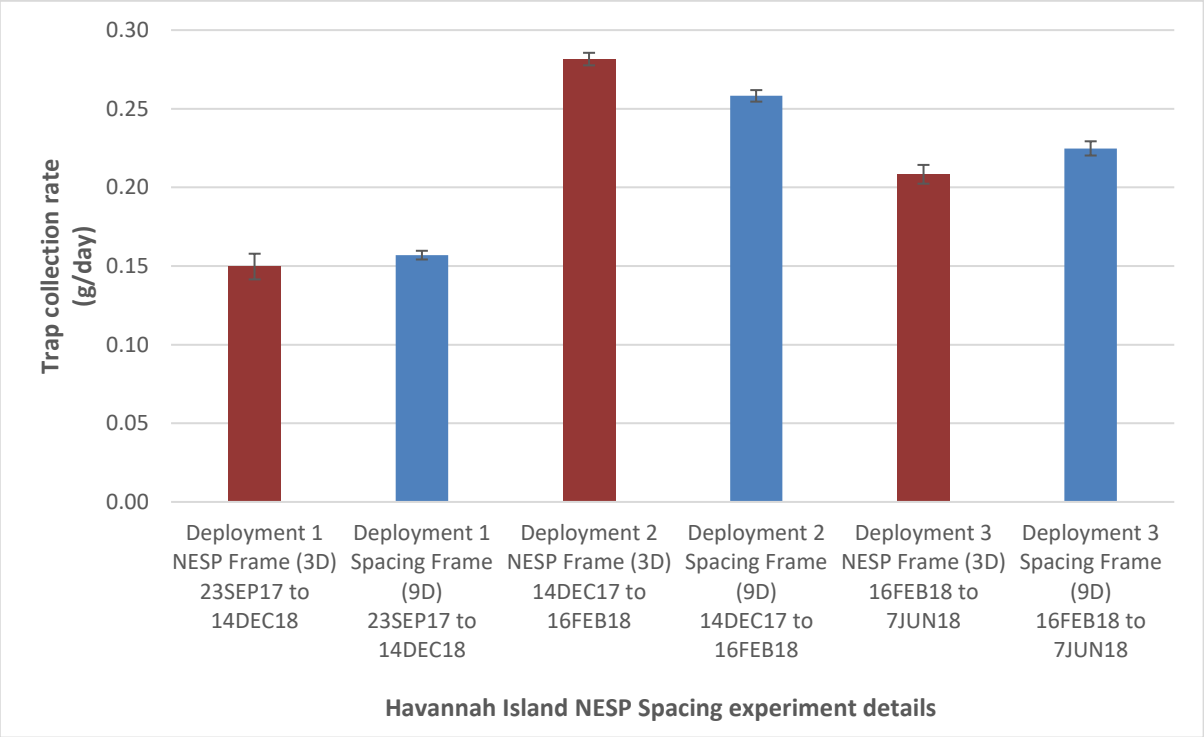

Figure 2.18. Sediment Trap spacing experiment at Havannah Island, Halifax Bay, NESP site showing large differences in trap accumulation rates between deployments, high precision in trap collection rates for both the NESP and Spacing frames and no obvious trend between spacing treatments.

The results from the Geoffrey Bay spacing deployments also show excellent precision for both the NESP frame and the spacing frame traps (Figure 2.19). There were significant differences in the rates of collection between all of the treatments. The NESP frame traps (3D) consistently showed trends of collecting less sediment than the spacing frame traps (9D). These collection rates differed by as much as 53% for the highest rate of collection. Further analysis will look at how these sites and deployments compared regarding differences in composition and particle size of the samples, and other data such as trap orientation and flow velocity, suspended sediment concentration and small differences in tilt.

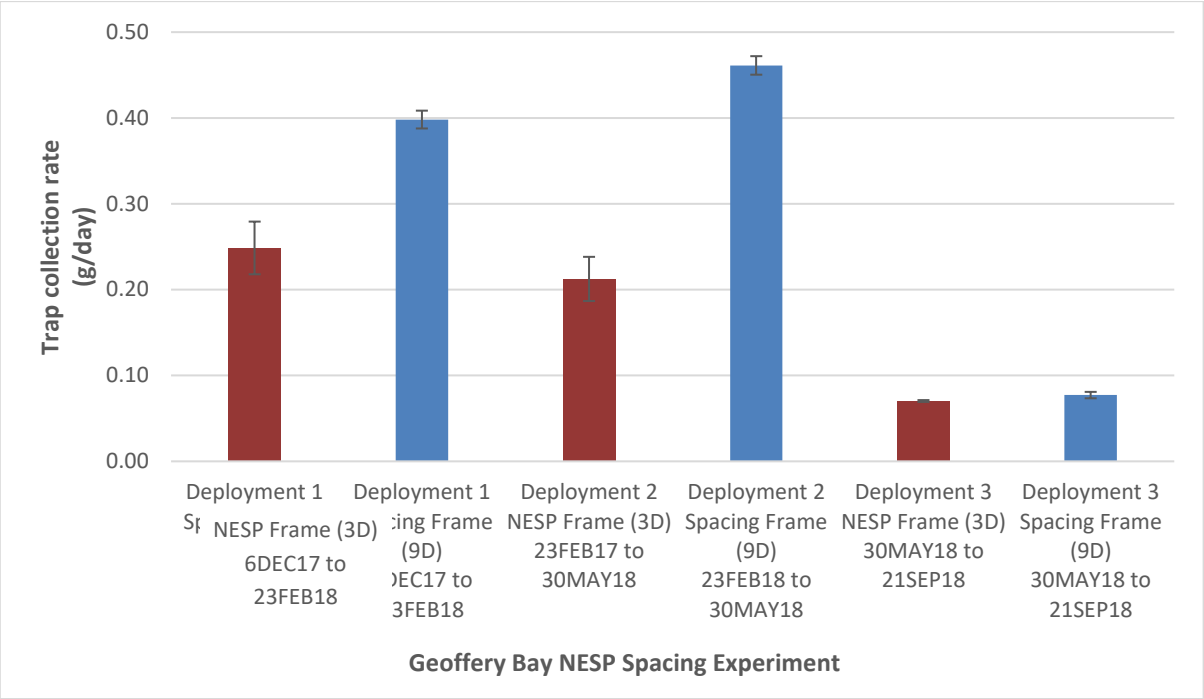

Figure 2.19. Sediment trap spacing experiment at Geoffrey Bay, Magnetic Island NESP site showing differences in trap accumulation rates between deployments, high precision in trap collection efficiencies and a trend of less material collected in the NESP 3D spaced traps.

Flume experiments –Spacing

Given the difficulty of environmental control in field experiments, we also undertook a flume spacing experiment. Three treatments were tested using the same spacing as the field experiment (3D and 9D) and a 0.65D (39mm) spacing (Figure 2.20). Three replicate traps were used for each treatment with an additional head and tail trap with the same spacing. The flume was filled with saline water (30 PSU) and dosed with sediment already collected from traps used in Cleveland Bay, Townsville. The water was circulated in the flume using a pump system which drew water from the middle of the floor of the flume and discharged from 6 evenly spaced outlet jets located at the circumference. All the traps were positioned 300 mm from the wall of the flume and at the same depth. The sediment was re-suspended every 8 to 12 hrs using a broom with a small rapid pumping motion around the circumference of the flume. The turbidity would reach ~ 30 NTU after resuspension and drop to ~ 15 NTU after 12 hrs. The mean flow speed at the mid-point between the 9D spaced traps was 3.6 cm.s^{-1}.

The flume spacing experiment showed no significant difference between the traps at 3D (180 mm) and 9D (540 mm) spacing. There was however a 2% difference between traps with 0.65D (39 mm) spacing compared to the 3D spaced traps (Figure 2.21). The reduction in the collection rates relative to the reduced trap spacing may support the trend seen at the Geoffrey Bay deployments. We intend to replicate this experiment and hope to also look at the role of different flow velocities on sediment accumulation in traps with different spacing.

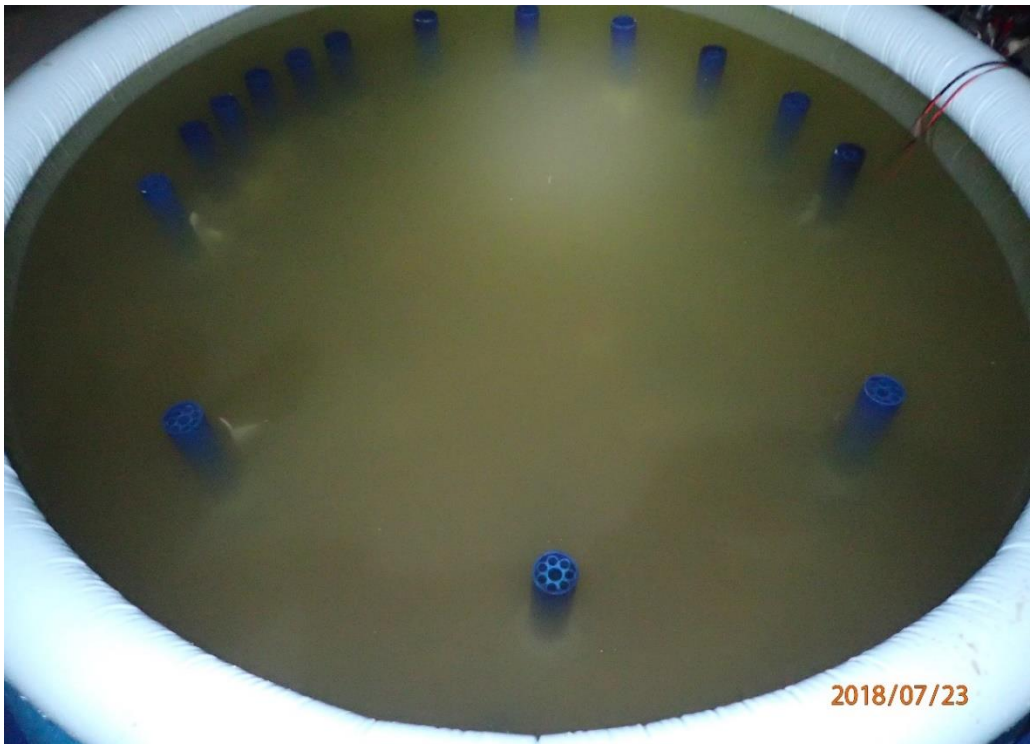

Figure 2.20. Circular flume experiment with 3 replicate traps and a head and tail trap at each 0.65D, 3D and 9D spacing.

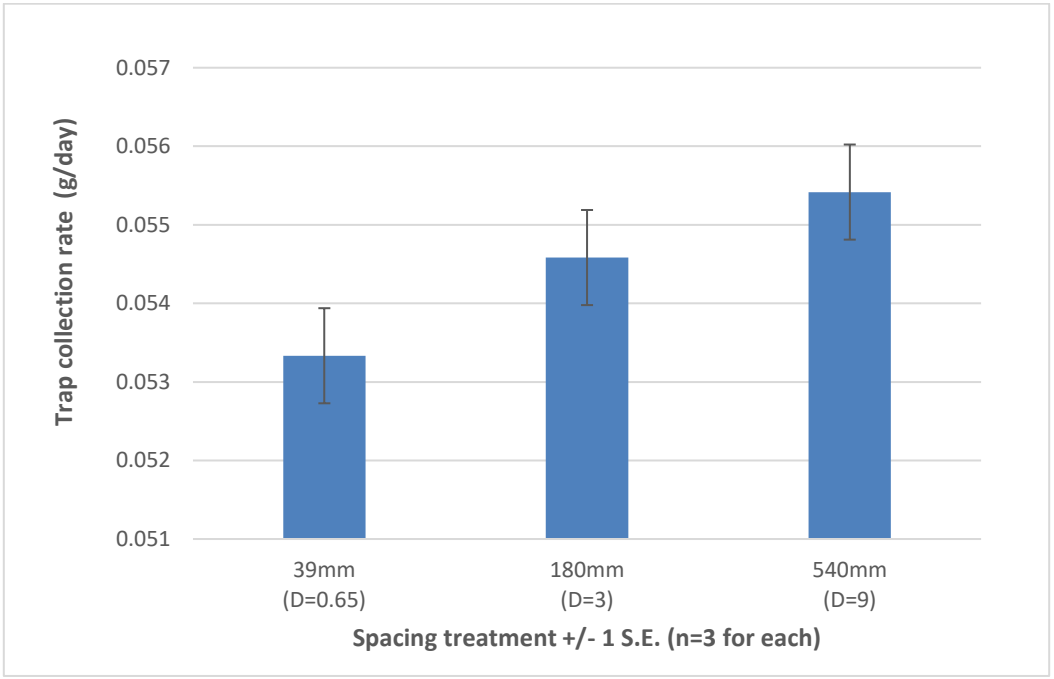

Figure 2.21. Sediment trap collection rates from a circular flume experiment with trap spacing of 0.65D, 3D and 9D.

Experiments on trap tilt

Tilt is an important factor that needs to be accounted for when reporting sediment trap collection rates and explaining trap function. Only a couple of papers to date have effectively looked at the effect of tilt (Gardiner 1985, Chiswell et al 2015). Results from existing tilt experiments on cylindrical traps show a rapid increase in the rate of collection due to trap tilt and the extent of this effect may be different for the Sedisampler® 55s. The mechanism for this increase in collection rate has not been explained and the rate of increase is far greater than the theoretical geometric, or secant increase associated with the cross sectional area, commonly reported as being important when reporting collection rates.

We set up an experiment at the Geoffrey Bay site looking at the effect of tilt on the SediSampler® 55s sediment traps. Two additional frames, similar to the spacing frame, were installed in the vicinity of the NESP standard frame. Each frame had 8 traps with 2 intended alternating treatments of 5 and 20°, and 10 and 30° tilts. The central spacing frame was considered the zero tilt treatment. The frames however deformed such that the tilts were effectively random ranging from 0° to 43° degrees.

Three deployments were undertaken with the SediSampler® 55s. On retrieval of the first deployment we observed that many of the traps had a tilt greater than 15 degrees, and there were blockages in the trap heads. This material was lost and these traps were dropped from the tilt analysis. Subsequent deployments collected and recorded the material remaining in the trap heads. Collection rates were standardised to the mean value calculated from the central zero tilt treatment frame and plotted against their respective tilt (Figure 2.22). It is important to note that there still may have been a spatial environmental gradient between these frames across this study.

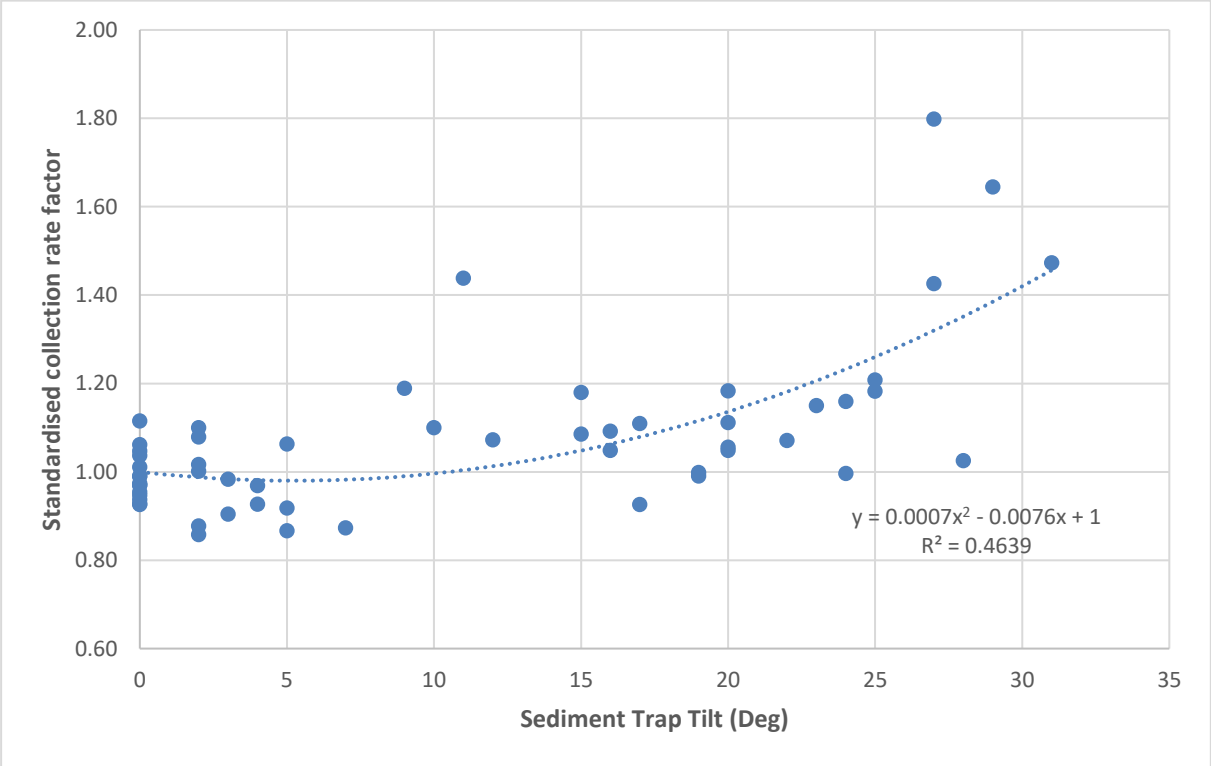

Figure 2.22. Standardized SediSampler® 55s trap collection rates for respective tilt treatments showing an increasing rate of collection with increasing tilt.

We also undertook three tilt experiments for the SediSampler® 55s traps in a circular flume. Eight traps were spaced evenly with the center of each trap head 300 mm from the wall of the flume and at the same depth from the surface. All trap tilts were orientated perpendicular to the radial flow direction. The 8 trap tilts per experiment were intended to be: 0, 0, 5, 10, 15, 20, 25 and 30 degrees, although the actual recorded tilts were a little different in practice. The standardised collection factors were calculated by dividing each trap's collected mass by the mass from the trap with the least tilt. Whilst there were a few outliers, our results show that there is a strong increase in the collection rate with tilt (Figure 2.23).

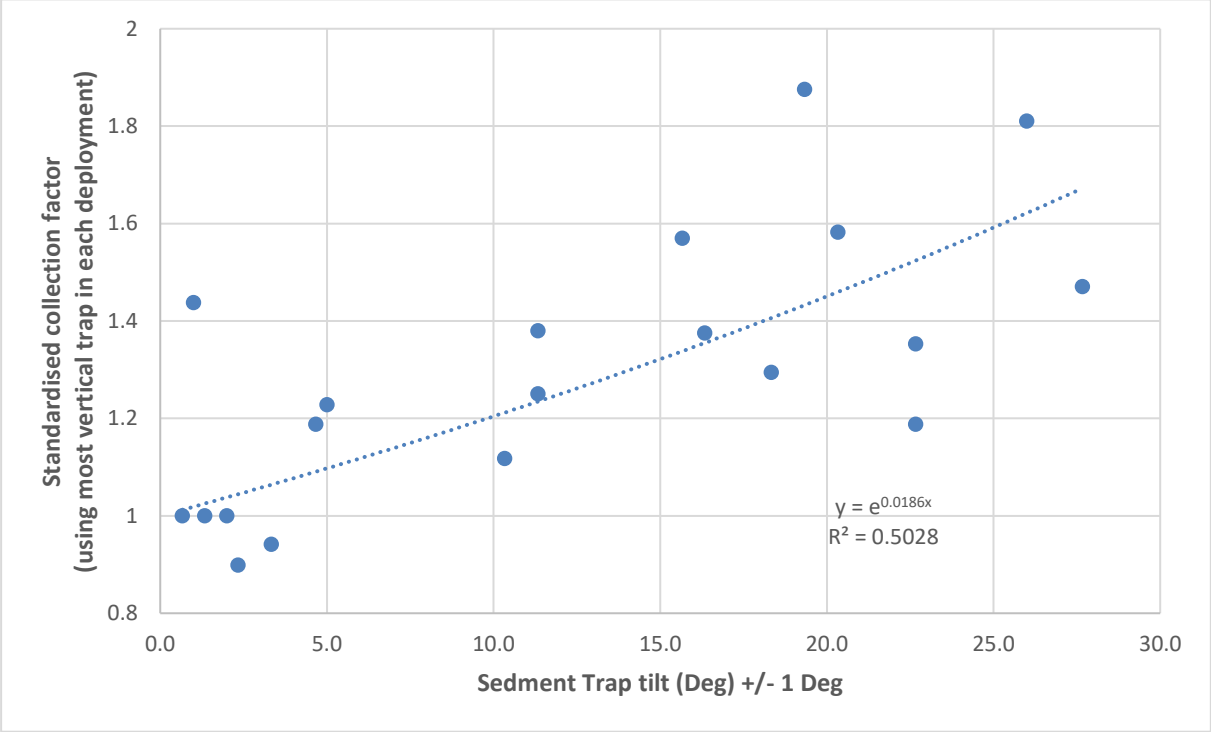

Figure 2.23. Standardised SediSampler® 55s trap tilt collection rate factors measured from circular flume experiments.

3.0 FLOOD PLUME PART 1: OVERVIEW AND SUSPENDED PARTICULATE MATTER CHARACTERISATION

Wet Tropics – Tully River

2017 plume event

Heavy rainfall occurred in the catchments of the Wet Tropics from the 7th to 10th January 2017 which triggered a moderate flow event in the Tully River (Figure 3.1) and a sizable flood plume offshore. Cloud cover prevented obtaining a clear satellite image of the flood plumes from the Tully and Johnstone Rivers until the 12th January which showed a sizable influence along the inner and mid shelf (Figure 3.2). Sampling within the freshwater reaches of the Tully River yielded a suspended particulate matter (SPM) concentration of 39 $mg.L^{-1}$ consisting of 18% organic material (i.e. volatile suspended solids of 7 $mg.L^{-1}$). SPM concentrations were higher in the initial mixing stages of the plume (64 and 97 $mg.L^{-1}$ in the <1 practical salinity units (PSU) reach). It is likely these higher concentrations may be due to the influence of sediment resuspension as these samples were taken directly offshore from the Tully mouth in relatively shallow water (<3 m) within choppy seas (Figure 3.3a). The outer reaches of the plume near Bedarra Island had a SPM concentration of 18 ± 5 $mg.L^{-1}$ at 22 PSU while outside the visible plume boundary yielded a SPM concentration of 6 $mg.L^{-1}$ at 35 PSU; hence even though it appeared that sampling was undertaken outside of the plume there was still a clear freshwater influence in the measured data (Figure 3.3A).

The sediment collected using the SediPump® showed a clear change in sediment colour (and presumably composition) between the sample collected near the Tully River mouth (<1 PSU) and the sample collected near Bedarra Island (22 PSU) (Figure 3.4). Interestingly, sediment flocculation was observed throughout the estuarine mixing gradient and flocs were even present in the freshwater reaches of the Tully River, although the size of the flocs generally increased with higher salinity (Figure 3.3C). Particle size along the estuarine mixing zone generally became finer with increasing salinity with 67% of the sediment in the <16 µm size in the freshwater compared to 95% <16 µm at salinity 22 from the sample taken from plume waters at Bedarra Island (Figure 3.3B).

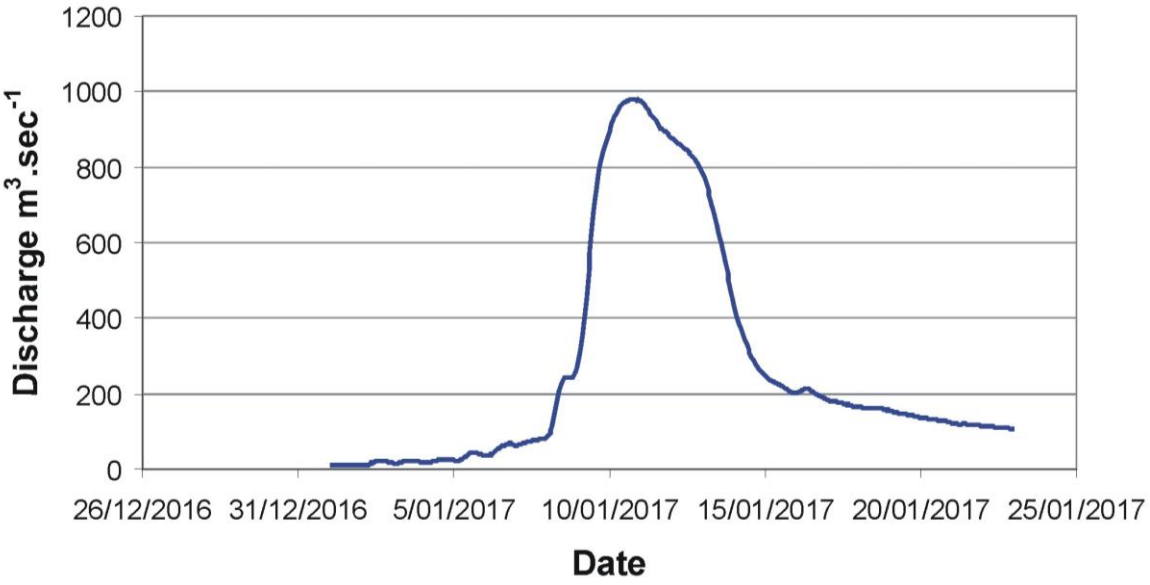

Figure 3.1. River discharge (hourly cumec) at Tully River (Euramo gauge) for January 2017.

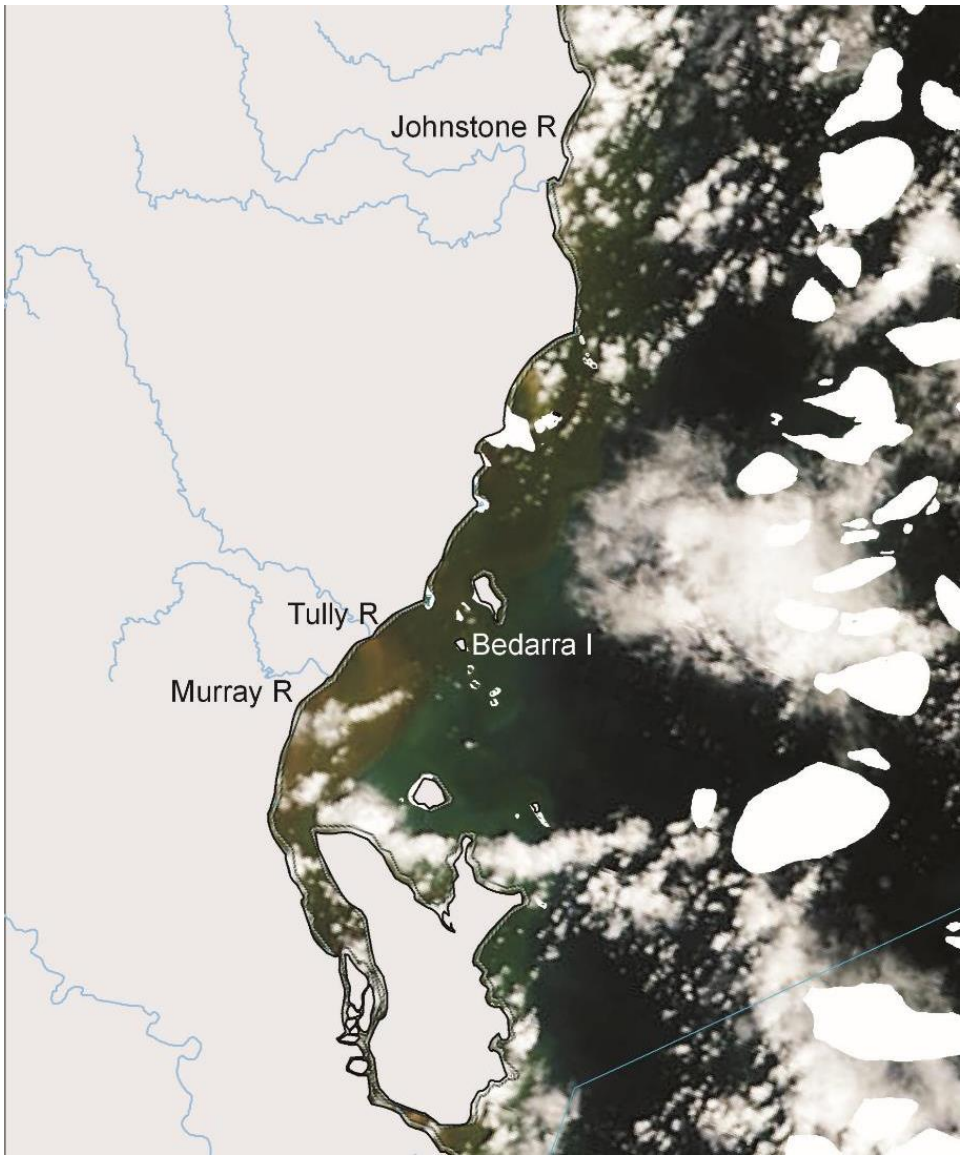

Figure 3.2. True colour satellite image showing the Tully and Johnstone River plumes taken on the 12/1/2017. A transect of samples across the salinity gradient were collected on the 11th January from the Tully River mouth to Bedarra Island with additional samples collected from Dunk Island and Sisters Island on the 19th January. Sampling of the Johnstone plume occurred on the 15th January (Image: MODIS satellite image modified by Caroline Petus).

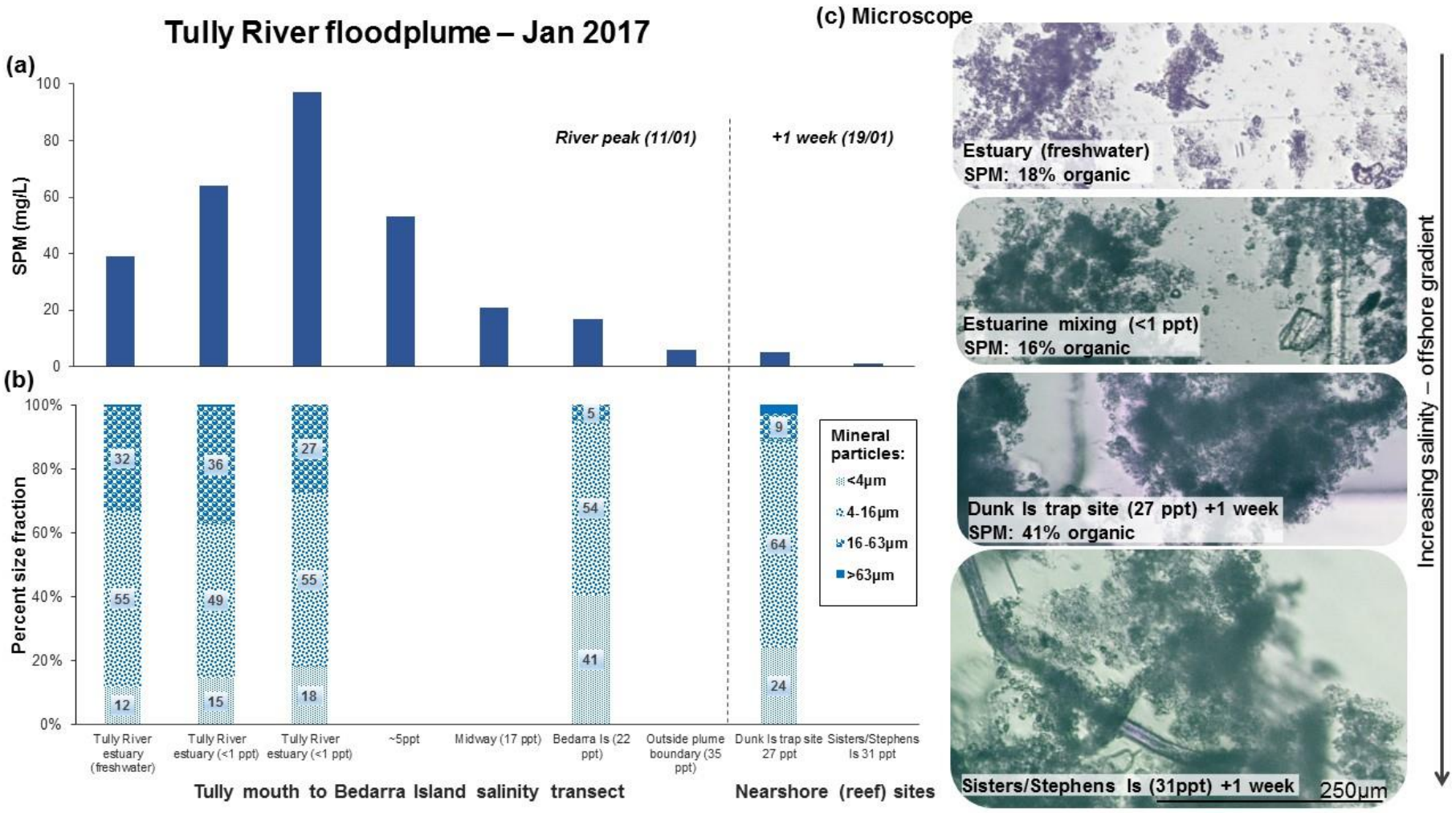

Figure 3.3. Suspended particulate matter, mineral particle size and floc microscope images for the 2017 Tully River mouth and adjacent floodplume transect.

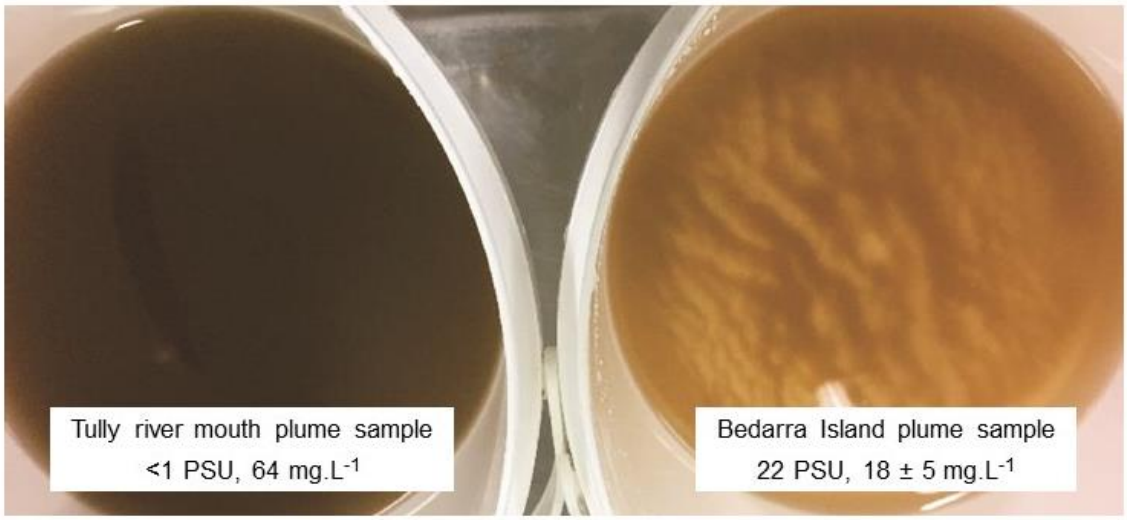

Figure 3.4. An example of the colour change of the suspended particulate matter from the sediment collected in the SediPump® between the Tully River mouth (left) and Bedarra Island (right) plume samples collected on January 11, 2017.

2018 plume event

The Wet Tropics region experienced a sizable wet season in 2017/18 with major flooding occurring in many rivers including the Herbert and Tully Rivers. In fact, the Tully River had two major flow events (peaked on the 10th March and 28th March, respectively) as well as two moderate level flow events (peaked on 19th January and 7th February, repectively) and one minor event (peaked on 27th Janurary), while the Herbert had a very large flow causing major flooding around the Ingham township which peaked on the 9th March (Figure 3.5). The total discharge for the water year (1st October to 30th September) is 6.4 TL for the Herbert River and 4.2 TL for the Tully River. Figure 3.5 shows the daily ML discharge for the Tully and Herbert Rivers and the red diamonds show when sampling of the flood plumes occurred offshore.

Satellite images, when not obstructed by cloud cover, clearly distinguish the extent of the flood plumes from the Tully and Herbert Rivers over March 2018 (Figure 3.6). The flood plumes generated by major flows from the Tully and Herbert Rivers are shown in satellite imagery to be mainly confined on the inner shelf with perhaps some influence on parts of the mid shelf (Figure 3.6). Importantly, these images highlight the influence of the plumes on Dunk Island, where we have our sediment traps and logger deployed. Indeed, the image from the 29th March show a particularly turbid area in the vicinity of our sampling site (Figure 3.6D).

Sampling of the Tully flood plume in 2018 was restricted on a number of occasions to shorter times on the water or until a few days after peak river flow due to poor weather. However, extensive sampling of the Tully plume waters across the estuarine mixing zone over January to March 2018 was conducted (see Figure 3.5). SPM concentrations of samples collected along the salinity gradient from the Tully River estuary (freshwater) to the Dunk Island trap site following the early February flood event were low across the entire transect, decreasing from 20 $mg.L^{-1}$ in freshwater (Figure 3.7A). Flocs were much smaller in this event compared to that of 2017 (refer Figure 3.3), again with small flocs present in the freshwater reaches of the Tully River (Figure 3.7C). Particle size along the entire transect was dominated by the <16 µm

fraction (71-95%), with an increase in the finest clay fraction (<3.9 µm) in plume waters at the Dunk Island trap site (observed on both 9th and 14th February; Figure 3.7B).

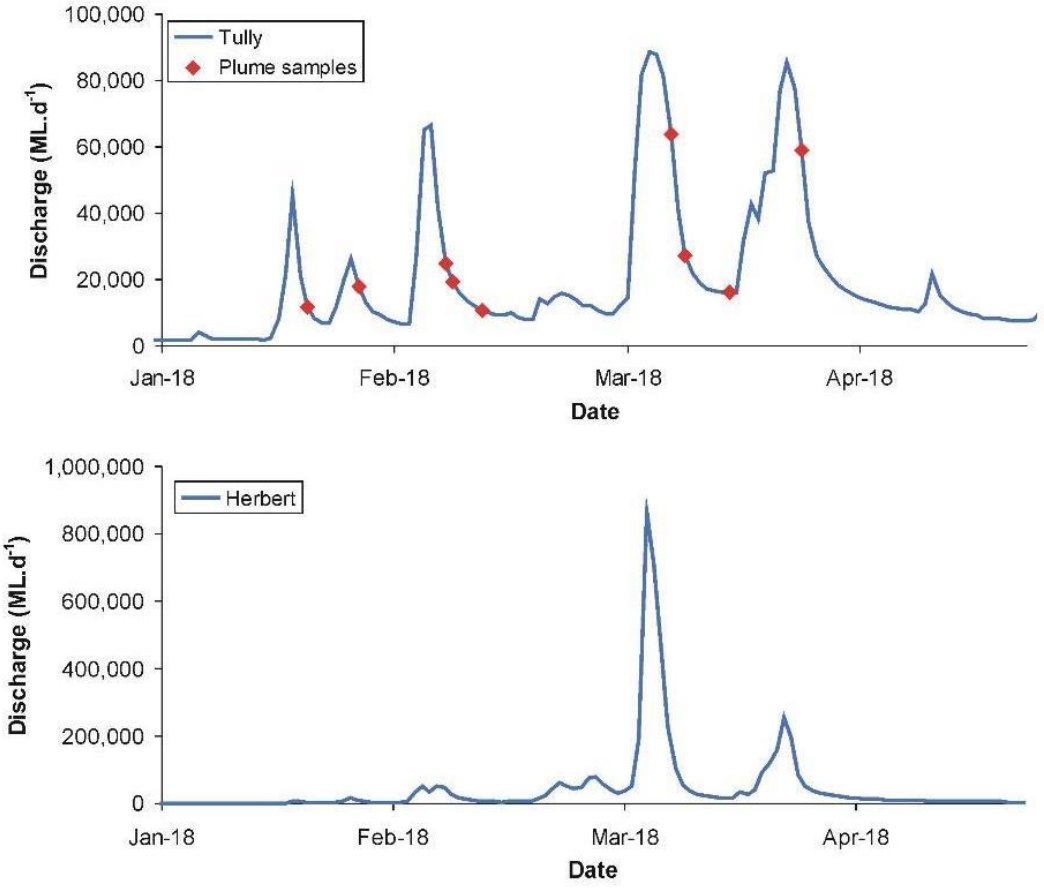

Figure 3.5. River discharge (in ML per day) from January 1 to April 30 2018 for the Tully (top, Euramo gauge) and Herbert (bottom, Ingham gauge) Rivers. Red diamonds show when plume sampling occurred offshore from the Tully River mouth.

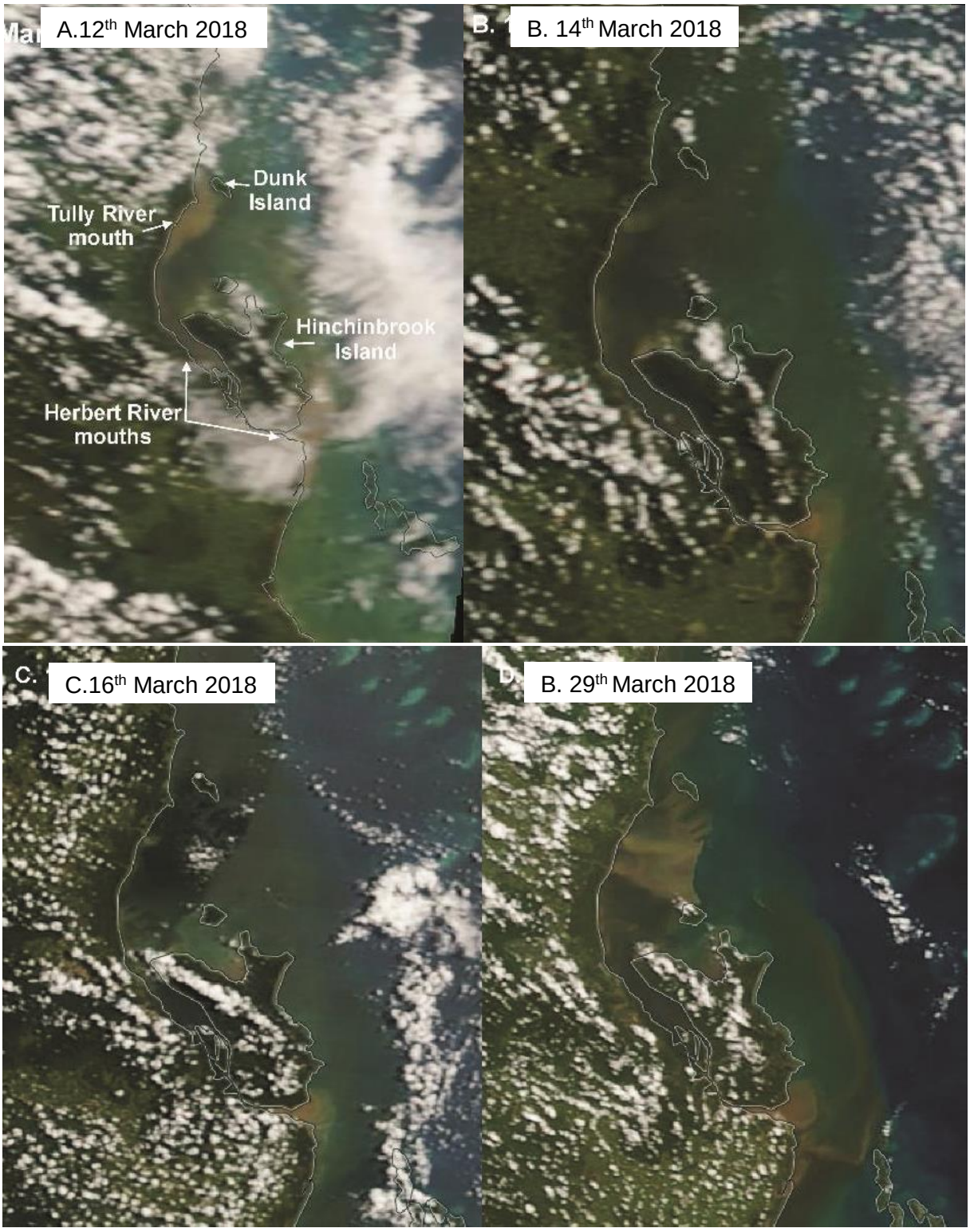

Figure 3.6. Satellite images of the flood plume from the Tully (+Murray) and Herbert Rivers on the 12th (A), 14th (B), 16th (C) and 29th (D) March 2018.

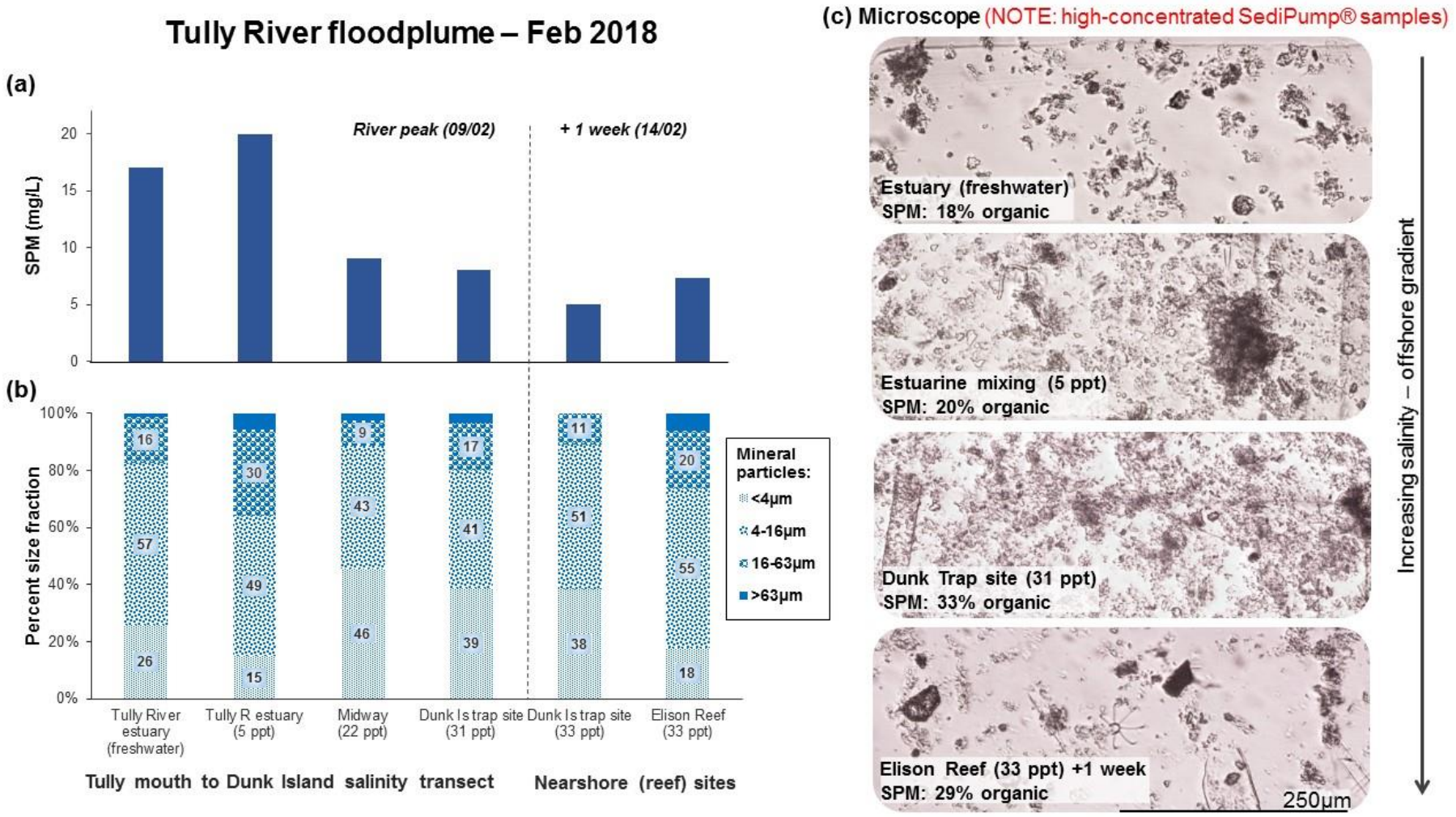

Figure 3.7. Suspended particulate matter, mineral particle size and floc microscope images for the 2018 Tully River mouth and adjacent floodplume transect sampled on the 9th and 14th February, 2018.

Burdekin

2017 plume event

Heavy rainfall associated with the crossing of Tropical Cyclone Debbie occurred in the Bowen-Broken-Bogie River sub-catchments of the Burdekin catchment in March 2017 and triggered very fast stream rises across these sub-catchments. The Burdekin River at Home Hill (Inkerman Bridge) peaked at a moderate flood level at ~ 2 am on 30th March 2017 (Figure 3.8) with discharge almost exclusively from the Bowen-Broken-Bogie River sub-catchments below the Burdekin Falls Dam; such an event from only this "below dam" source area is rare for the Burdekin. Seven samples were collected over the Burdekin flow hydrograph at the Inkerman Bridge with TSS concentrations reaching ~1800 mg.L^{-1} near the peak flow (Figure 3.8). Using this data a sediment load of 1.5 million tonnes was calculated over this six day flow event. Particle size was relatively consistent over this discharge event, with 82±3% of mineral particles <16µm (Figure 3.10B). Bulk samples were collected near the peak flow for tracing purposes (currently being analysed).

The Burdekin River flood plume was sampled on the 31st March 2017 over the salinity gradient with satellite images showing the plume moving in an easterly/south-easterly direction coinciding with the northerly winds at this time (Figure 3.9). SPM concentrations rapidly decreased in the plume from 580 mg.L^{-1} at <1 PSU to 235 mg.L^{-1} at 6 PSU, 27 mg.L^{-1} at 12 PSU and <15 mg.L^{-1} by 14 PSU and thereafter (Figure 3.10A). These measurements are consistent with earlier studies of the Burdekin flood plume in previous years (Devlin and Brodie, 2005; Bainbridge et al., 2012). A wide range of sediment particles (quartz, silt and finer) and some organic flocs were observed in the end-of-river Inkerman site (Figure 3.10C). Sediments became sparser along the salinity gradient as SPM concentrations rapidly decreased, with a greater number of flocs observed in the higher salinities of Upstart Bay (Figure 3.10C). With this increase in the presence of flocs, the proportion of organic matter (measured as volatile suspended solids) in the Burdekin plume increased from 11% at <1 PSU to 25% at 26 PSU (Figure 3.10C). Plume water sampled outside the initial turbulent mixing zone at the river mouth (i.e. >1 PSU) was dominated (89-94%) by the <16µm sediment fraction (salinity range 6-26 PSU; Figure 3.10B).

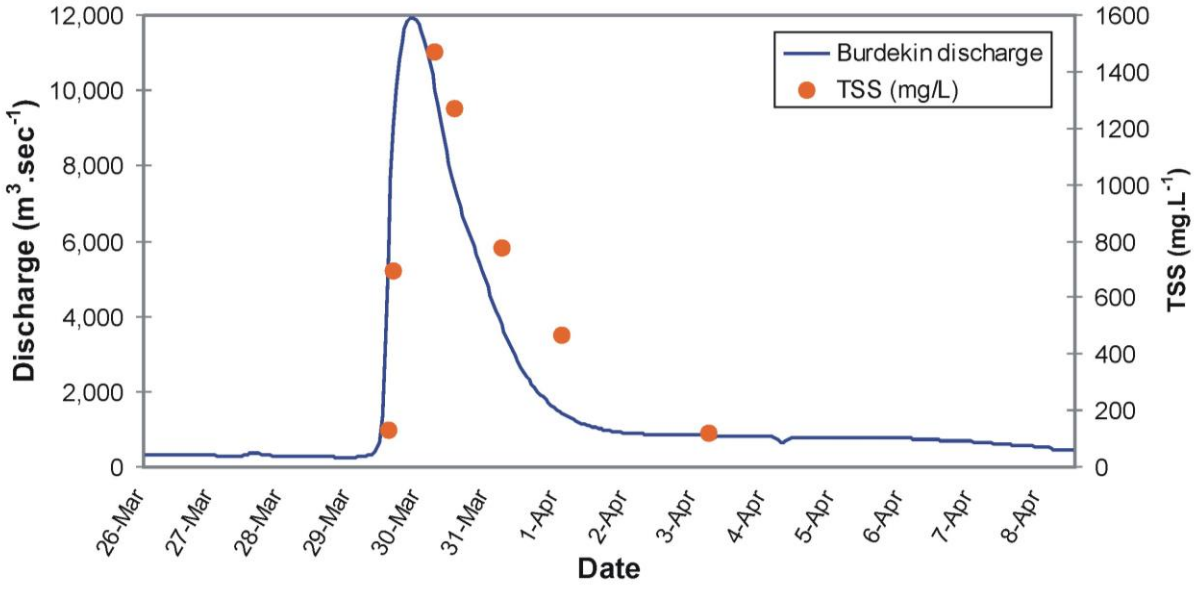

Figure 3.8. River discharge (in ML per day) from March 26 to April 10 2017 for the Burdekin River (Clare gauge). TSS concentration (red circles) collected at Inkerman Bridge (d/s Clare gauge) also displayed along this discharge event associated with Tropical Cyclone Debbie. Note, plume sampling offshore from the Burdekin River mouth (31st March) was conducted on the morning following end-of-river peak discharge.

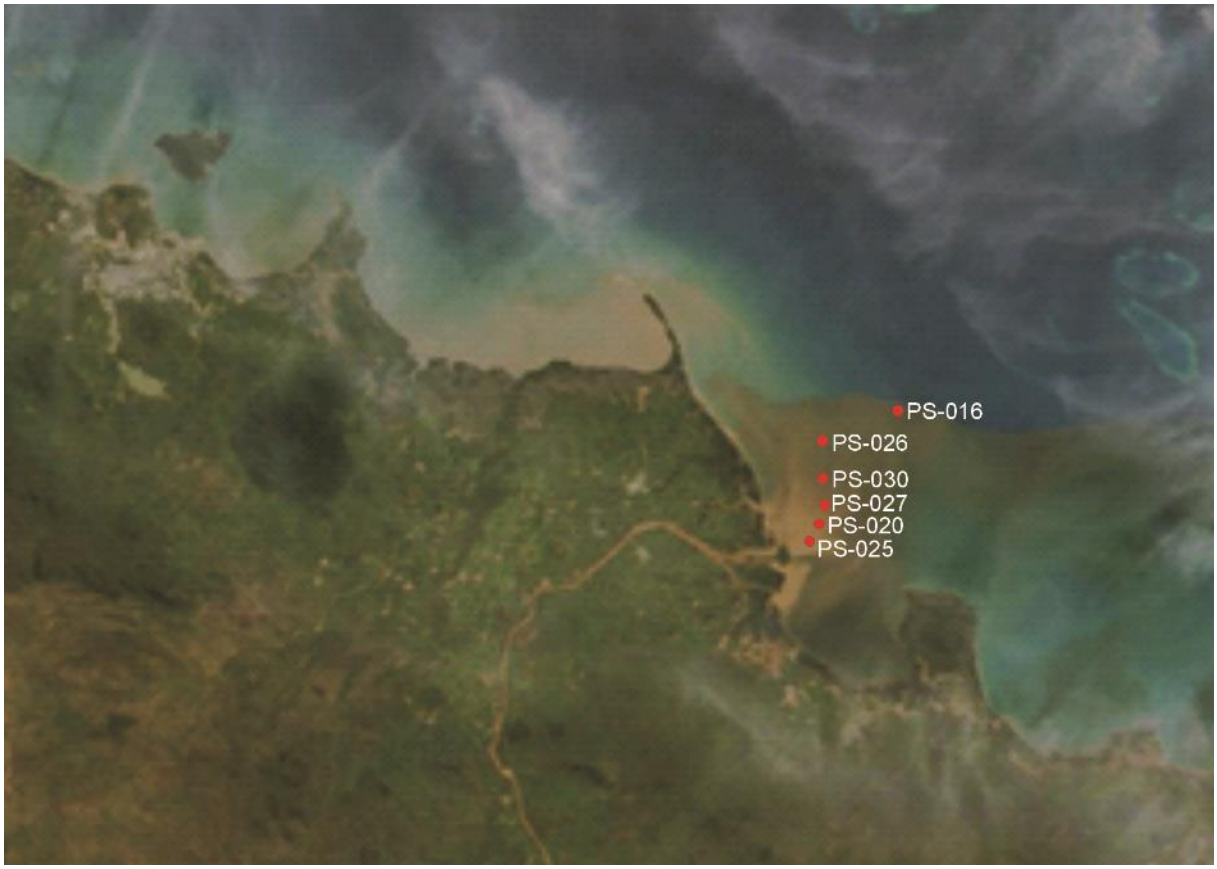

Figure 3.9. Satellite image of the Burdekin River flood plume from 31st March 2017 showing the sampling sites (Image: MODIS satellite image modified by Caroline Petus).

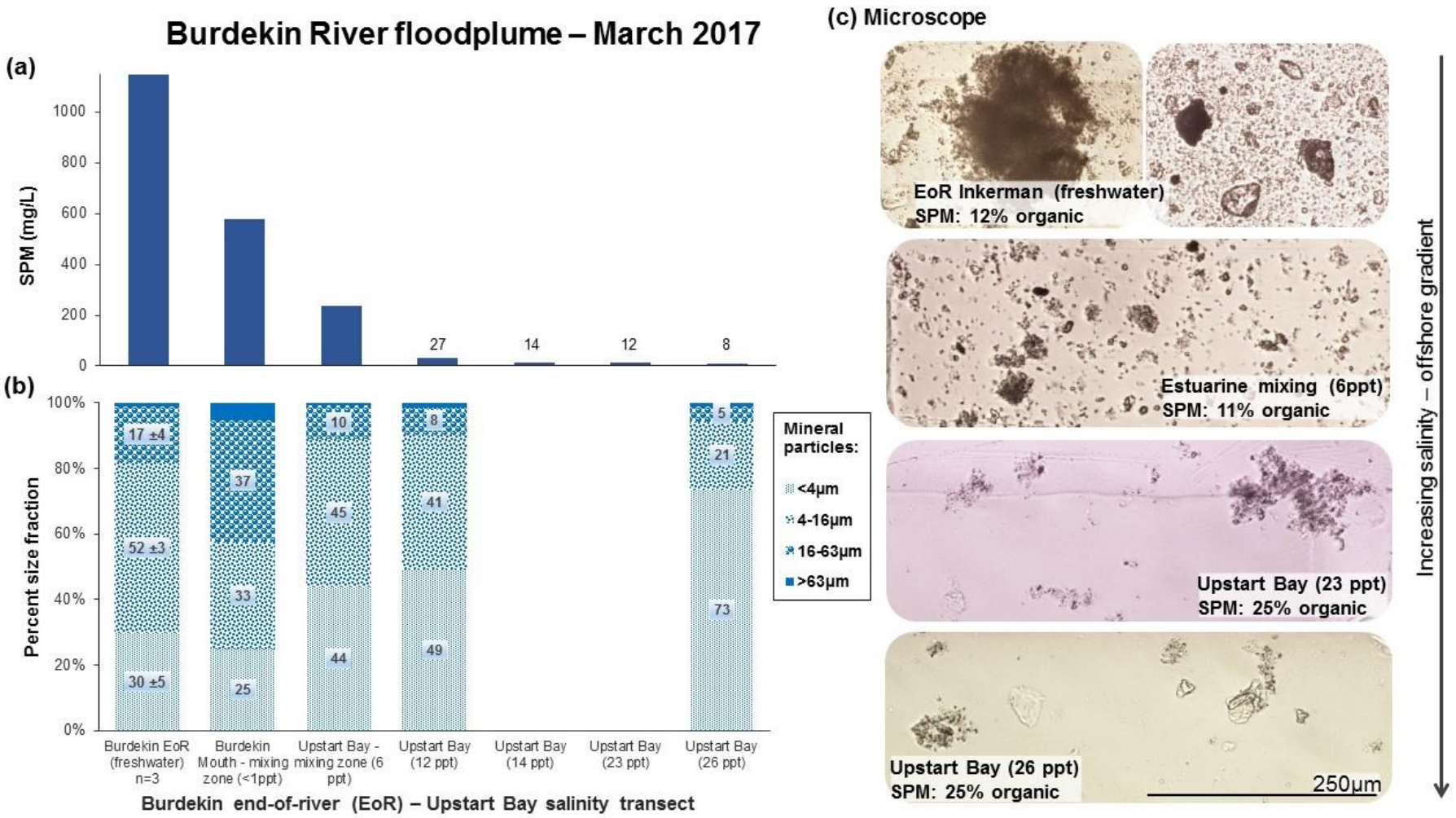

Figure 3.10. Suspended particulate matter, mineral particle size and floc microscope images for the 2017 Burdekin River estuarine mixing zone and offshore gradient within Upstart Bay, 31 March 2017.

2018 plume event

Heavy rainfall occurred in the upper Burdekin River catchment in late February/early March 2018 which triggered minor flood levels in the downstream river reaches to the Burdekin Falls Dam. While the end-of-river water level for the Burdekin River peaked just below minor flood level on the 5th March, the flow event was the largest in the catchment area above the dam since 2012 and total Burdekin River discharge in 2017/18 (5.5 TL; Figure 3.11) was slightly below the long-term median (6.2 TL). Five samples were collected over the Burdekin flow hydrograph at the Inkerman Bridge with TSS concentrations reaching ~1000 $mg.L^{-1}$ near the peak flow. Particle size was relatively consistent over this discharge event, with 85±3.5% of mineral particles <16µm (Figure 3.12B). Bulk samples were collected near the peak flow for tracing purposes (currently being analysed).

The available satellite image of the Burdekin plume on the 6th March (i.e. 1 day after peak discharge) shows the extent of the plume largely confined within Upstart Bay and beginning to extend into Bowling Green Bay (Figure 3.12). The next available image from the 10th March shows the plume now extending well northwards past Magnetic Island and into the Palm Island Group (Figure 3.12B). Clear images also available from the 13th and 29th March (Figures 3.12C and 3.12D, respectively) show the influence of the plume continuing in the region around the Palm Island Group, including our sediment trap site at Havannah Island. Importantly the images show the extent of the Burdekin plume was largely confined to the inner shelf of the Great Barrier Reef and did not impinge on the mid shelf.

Sampling of the Burdekin flood plume was restricted to short trips in Upstart Bay on the 5th and 6th March and off Magnetic Island on the 13th March due to poor weather. However, the limited sampling still captured the 0 to 10 salinity zone as well as some samples from the 25 to 30 salinity zone. Similarly to the 2017 plume event, SPM concentrations rapidly decreased from 644 $mg.L^{-1}$ at the end-of-river Inkerman freshwater site (at flood peak), to 200 $mg.L^{-1}$ at 4 PSU, 19 $mg.L^{-1}$ at 23 PSU, and <15 $mg.L^{-1}$ (32 PSU) at the Orchard Rocks, Magnetic Island sediment trap site (Figure 3.13A). An example of the change in SPM across the estuarine mixing zone of the Burdekin River can be seen in Figure 3.14A where concentrations fall quickly over the salinity gradient; however pumping with our SediPump® shows SPM of similar colour can still be recovered in the higher salinity zones/northern extent of the plume (e.g. 32 salinity). Similarly to the 2017 event, organic matter in the 2018 plume increased from 12% at Inkerman to ~25% in salinities >23 PSU within Upstart Bay and the northern plume waters sampled at Orchard Rocks (Figure 3.13C). Mineral particles in the plume water sampled at these two higher salinity sites comprised 83% of the <16µm sediment fraction (Figure 3.13B).

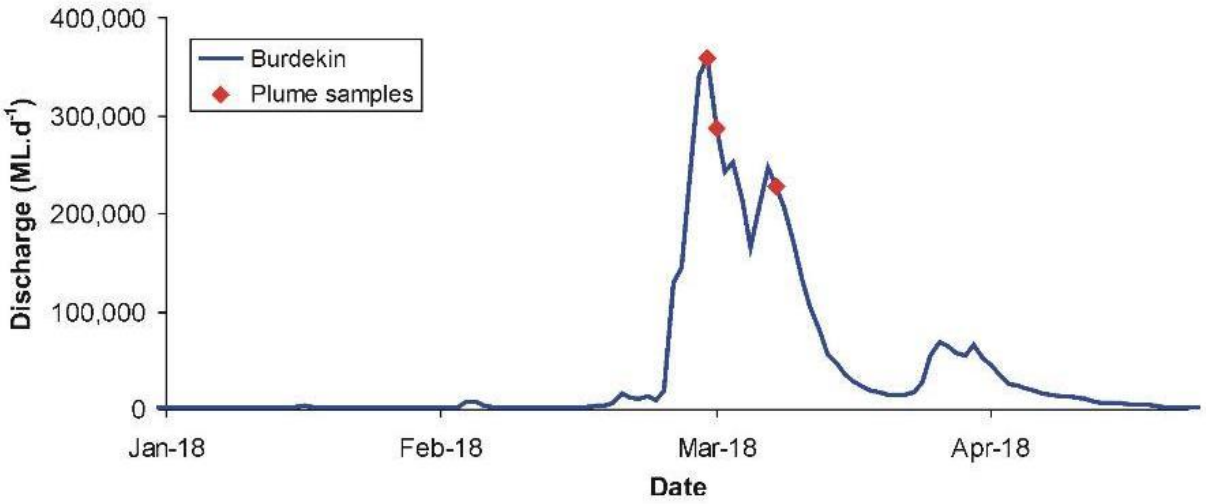

Figure 3.11. River discharge (in ML per day) from January 1 to April 30 2018 for the Burdekin River (Clare gauge). Red diamonds show when plume sampling occurred offshore from the Burdekin River mouth.

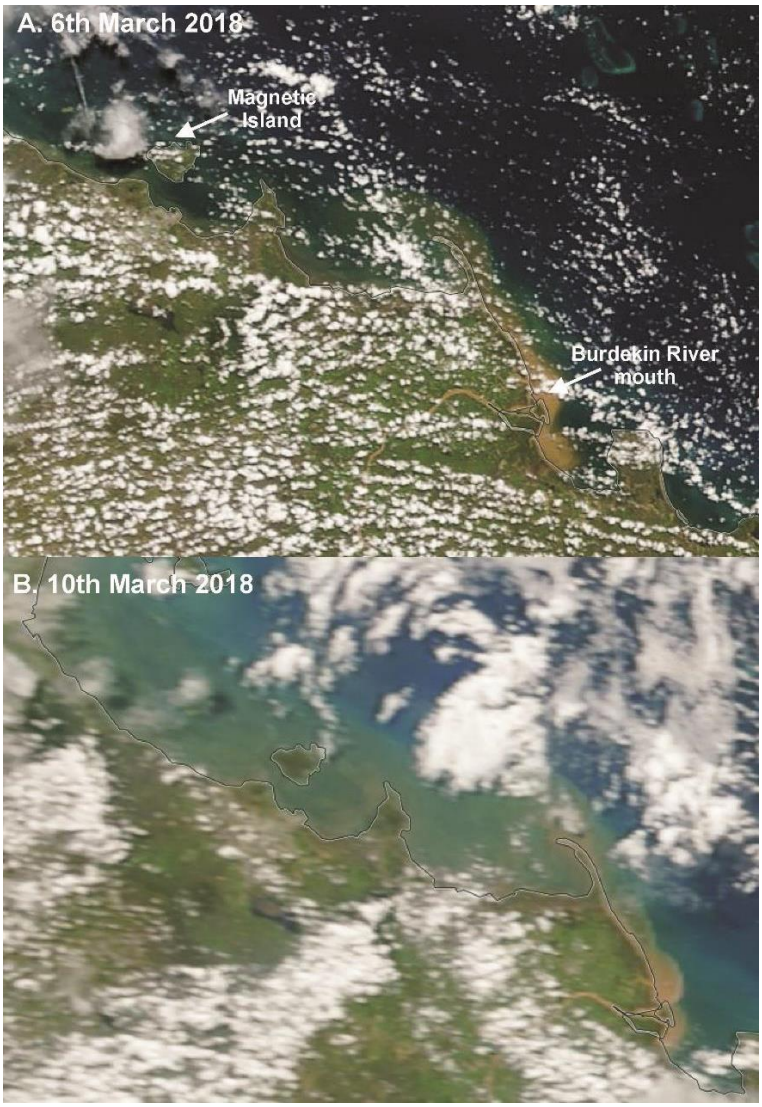

Figure 3.12. Satellite images of the flood plume from the Burdekin River on the 6th (A) and 10th (B) March 2018.

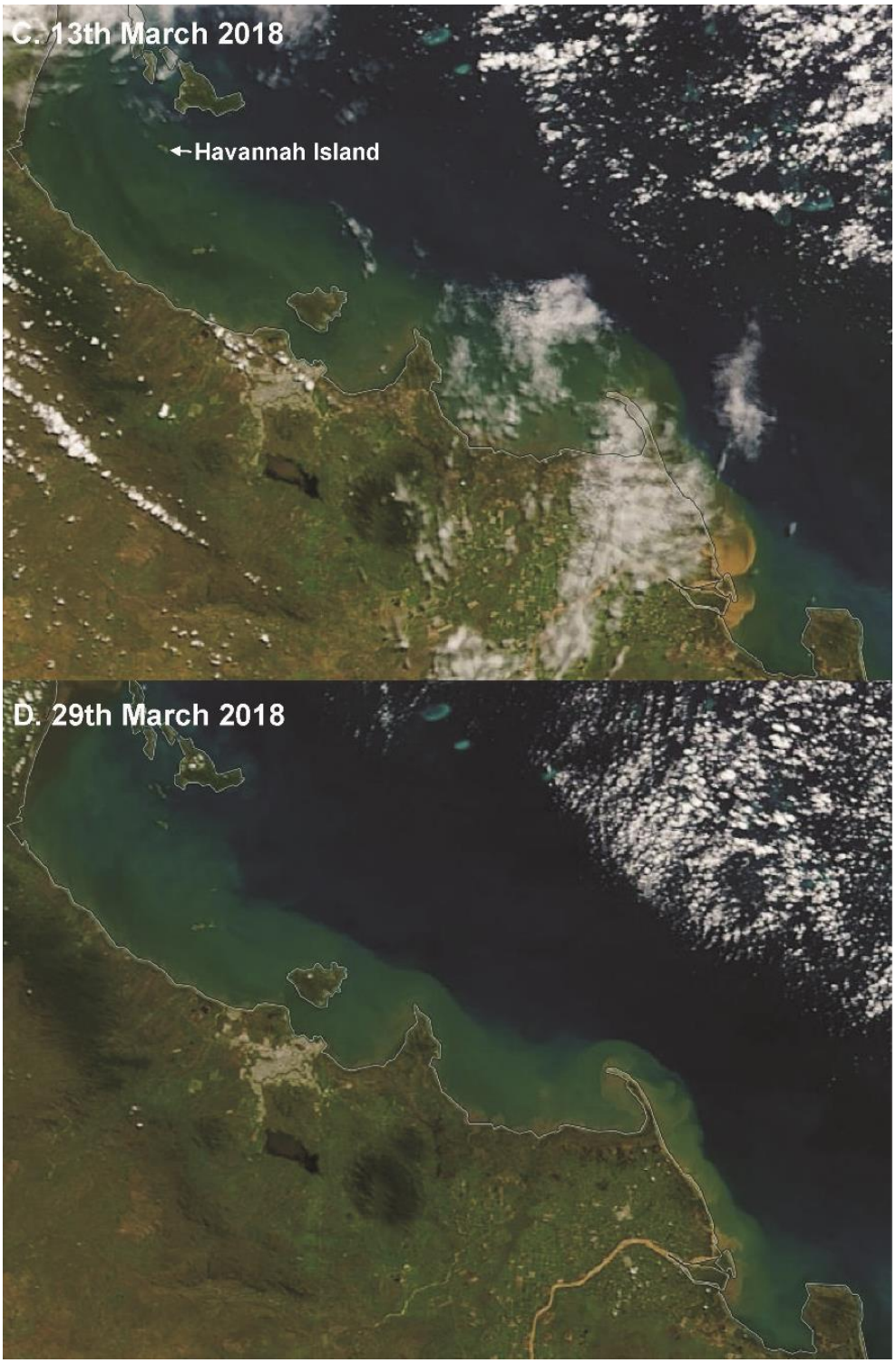

Figure 3.12. (continued). Satellite images of the flood plume from the Burdekin River on the 13th (C) and 29th (D) March 2018.

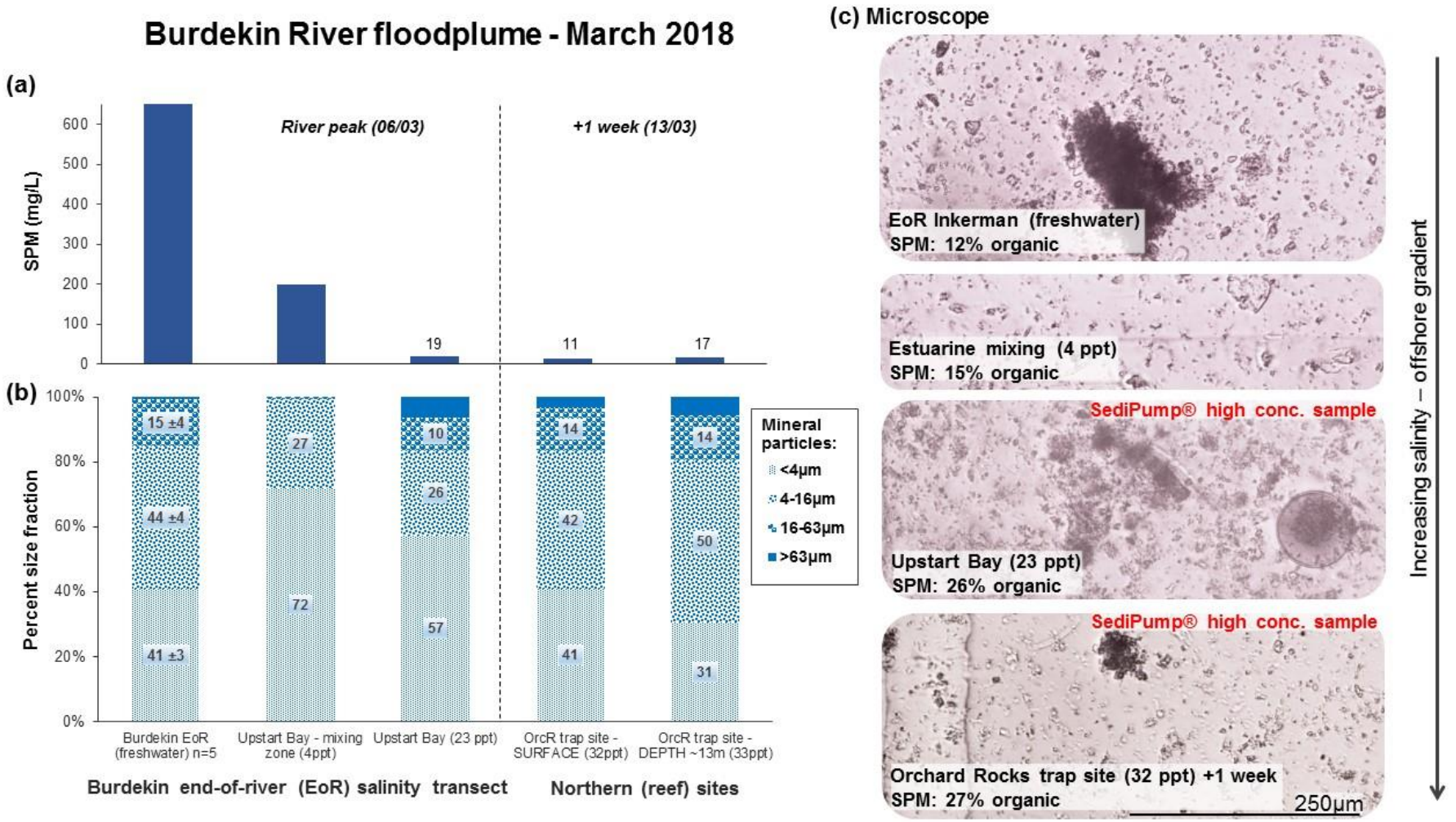

Figure 3.13. Suspended particulate matter, mineral particle size and floc microscope images for the 2018 Burdekin River estuarine mixing zone (Upstart Bay) on March 6, 2018 and northern (reef) site on March 13, 2018.

Figure 3.14. A. Photos showing changes in suspended particulate matter over the Burdekin estuarine mixing zone within Upstart Bay following peak river discharge on March 6, 2018. B. Suspended particulate matter collected in the plume (surface) at the Orchard Rocks trap site (13th March); as concentrated sediment collected by the SediPump® over 2 hours of plume water pumping (~10,000L, left), and the lower concentration grab sample collected at this site (right). In this SediPump® sample image, the plume sediment being carried as far as this northern Orchard Rocks site is shown to be similar in colour to that at the river mouth in A.

Suspended particulate matter characterisation

The collection of SPM samples throughout the estuarine mixing zones of the Burdekin and Tully Rivers using the SediPump® allows enough material for a thorough characterisation to be performed. Here, we examine changes in particle size, microscopy, organic content and sediment colour. The particle size of the samples across the estuarine mixing zone become finer following the initial deposition of sediment at the river mouth (Figure 3.15). Experimental work carried out by team members highlights the importance of a sample pre-treatment (using hydrogen peroxide) to remove the organic materials that bind the sediment flocs. In particular, the samples taken in the higher salinity zones (>20 salinity) from the Burdekin plume show the greatest variation in particle size between the salt removed (i.e. very little pre-treatment) and the organics-removal treatment, although large differences were also observed in the samples from the end-of-river sites for the Tully and Johnstone Rivers (Figure 3.15D-E). In those cases (i.e. Burdekin plume salinities >20 and Tully and Johnstone end-of-river), sediment flocs can be observed in the microscope images (Figure 3.15C-E). The organics-removal (hydrogen peroxide) treatment of the sample breaks apart the flocs and the particle size distribution shifts towards a finer size fraction (Figure 3.15). Indeed, the <20 µm fraction increases by 14-35% for those samples from the Burdekin, Tully and Johnstone (Tables 3.2 and 3.3). We are conducting further trials to examine whether an additional treatment to remove carbonate material (i.e. plankton casings in the plume and shell material in the traps) is required. This may be particularly important for the sediment trap samples as well as the plume samples from the higher salinity zone where preliminary results suggest that the particle size distribution may shift to an even finer fraction with the treatment to remove carbonate (i.e. currently shown as “coarse” mineral sediment in Figure 3.13B).

Organic content measured in the 2017 and 2018 Burdekin flood plume events increased from ~11% at end-of-river (freshwater) to ~25% in the higher salinity offshore plume waters (Table 3.1, Figures 3.10C and 3.13C). Bainbridge et al. (2012) measured higher organic content in offshore plume waters in previous, larger Burdekin discharge events. In comparison, Tully end-of-river (freshwater) organic content was higher (~18-20%) in both 2017 and 2018 events, before increasing to 25-33% in the higher salinity offshore plume waters (Table 3.2, Figures 3.3C and 3.7C). Sediment colour only displays minor changes in the sediment collected over the estuarine mixing zone for the 2018 Burdekin flood plume (Figure 3.16). We note clay mineralogy and geochemistry results are not yet available from the laboratory following extensive preparation in our laboratory for the removal of salts and recovery of the <10 µm fraction. These data are expected to improve our understanding of these changes in sediment character over the estuarine mixing zone, as well as provide critical tracing fingerprints for catchment source discrimination.

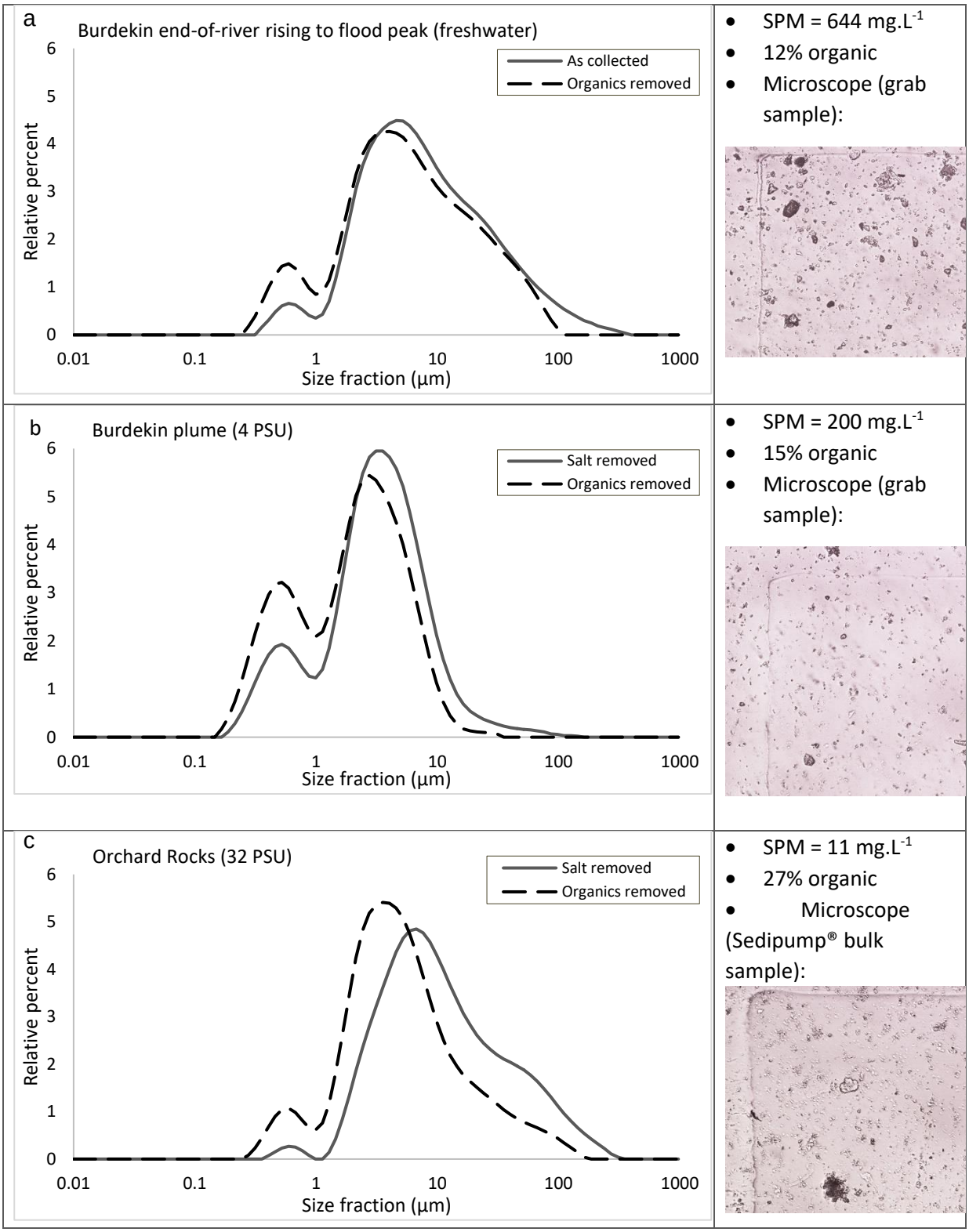

Figure 3.15. Suspended particulate matter characteristics of Burdekin River and flood plume samples collected at (a) end-of-river, (b) low salinity (Upstart Bay) and (c) high salinity on the inner shelf (Orchard Rocks, Magnetic Island), including sample particle size before and after removal of the organic component (left panel) and SPM, organic content and microscope imagery of each sample (right panel).

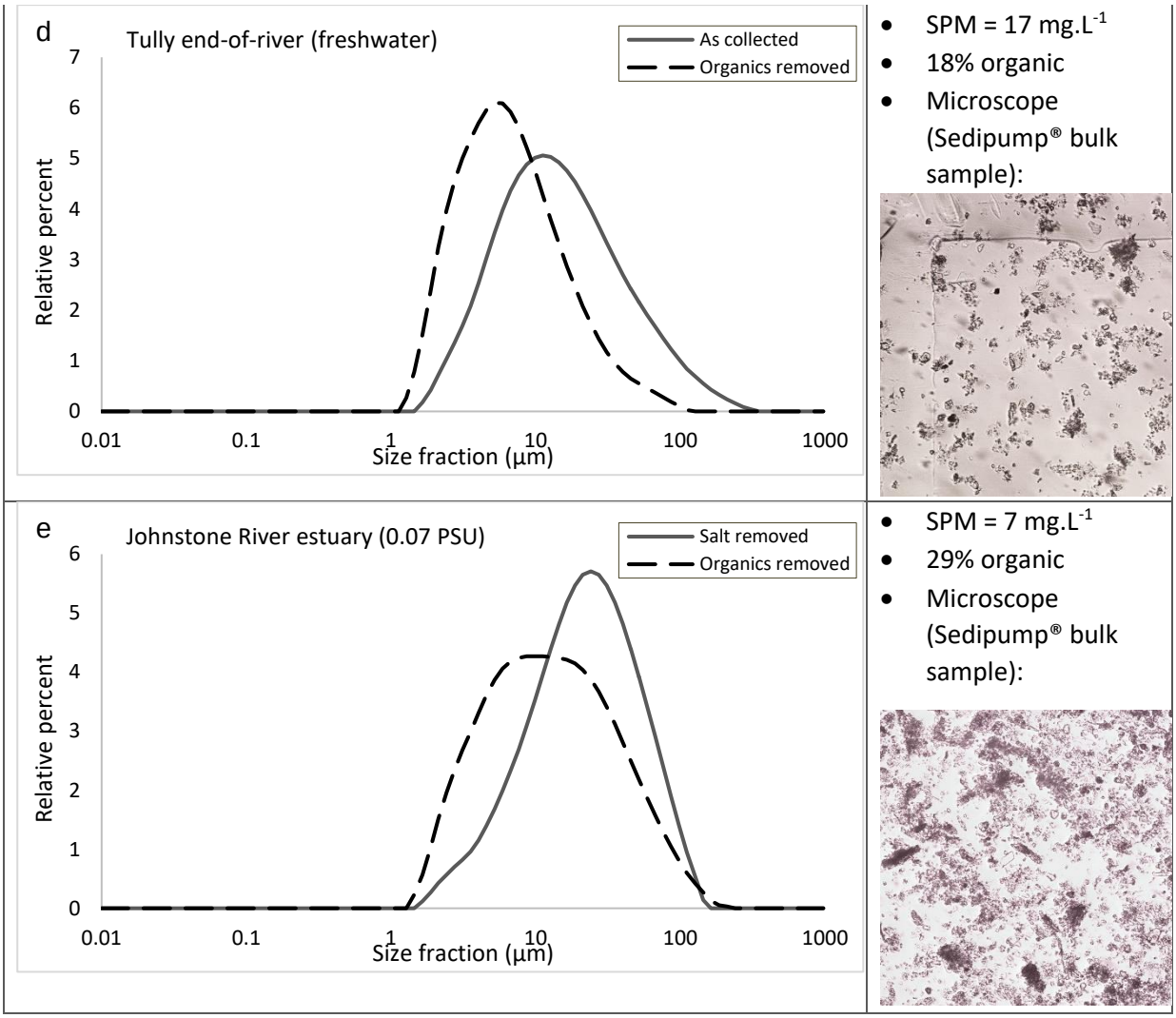

Figure 3.15. (cont). Suspended particulate matter characteristics of (d) Tully River (end-of-river) and (e) Johnstone River estuary (Flying Fish Point), including sample particle size before and after removal of the organic component (left panel) and SPM, organic content and microscope imagery of each sample (right panel).

Table 3.1. Summary table of the March 2018 Burdekin River flood event. Table includes suspended particulate matter, proportion organic, particulate organic matter, particle size fraction and colour (Munsell colour chart).

Burdekin River transect	Date	Salinity (PSU)	SPM (mg. L^{-1})	% Organic	~ POM (mg. L^{-1})	Particle size fraction		
						Proportion <20 µm (%)	Proportion <20 µm following organic removal (%)	Colour
End-of-river - Inkerman (event range)	03-08/03	0.050	434-998	12-13	5.3-15.3	76-93	82-93	-
River mouth/estuary (Upstart Bay)	06/03	4	200	15	1.7	97	100	10YR (4/4) dark yellowish brown
Inner plume (Upstart Bay)	06/03	23	19	26	0.5	80	85	10YR (4/4) dark yellowish brown
Geoffrey Bay - trap site (Mag. Is.; inner-shelf)	13/03	31	11	27	0.7	-	-	-
Orchard Rocks - trap site (Mag. Is.; inner-shelf)	13/03	32	12	27	0.3	70	87	2.5Y (4/3) olive brown
Orchard Rocks - trap site (12-14m depth)	13/03	33	17	24	0.2	70	84	2.5Y (4/2) dark grayish brown

Table 3.2. Summary table of the February 2018 Tully River to Dunk Island transect during Tully and Herbert River flooding. Table includes suspended particulate matter, proportion organic, particulate organic matter content, particle size fraction and colour (Munsell colour chart).

Burdekin River transect	Date	Salinity (PSU)	SPM (mg. L^{-1})	% Organic	~ POM (mg. L^{-1})	Particle size fraction		Colour
						Proportion <20 µm (%)	Proportion <20 µm following organic removal (%)	
South Johnstone R	08/02	0.05	35	23	1.4	25	60	10YR (3/3, 3/4) dark brown-dark yellowish brown
Johnstone R estuary (Flying Fish Point)	08/02	0.07	7	29	0	43	64	10YR (3/3) dark brown
Tully River mouth/estuary	09/02	0.05	17	18	1.9	62	88	10YR (4/4) dark yellowish brown
Tully River mouth/estuary	09/02	5	20	20	0.3	49	71	2.5Y(4/3 or 4/4) olive brown
Inner plume – midway to Dunk Island	09/02	22	9	33	0.3	61	91	2.5Y(4/3 or 4/4) olive brown
Depth sample (9m)	09/02	31	16	19	0.7	-	-	-
Dunk Island - trap site (inner-shelf)	09/02	33	8	33	0	70	84	2.5Y(4/2) dark grayish brown
Depth sample (7-9m)	09/02	34	9	22	0	-	-	-
Dunk Island - trap site (inner-shelf)	14/02	33	5	40	0	63	95	5Y(4/3) olive
Depth sample (7m)	14/02	34	4	25	0.2	-	-	-
Ellison Reef (mid-shelf)	14/02	33	8	29	0.1	41	79	5Y(5/3) olive
Depth sample (15m)	14/02	33	3	33	0.2	-	-	-

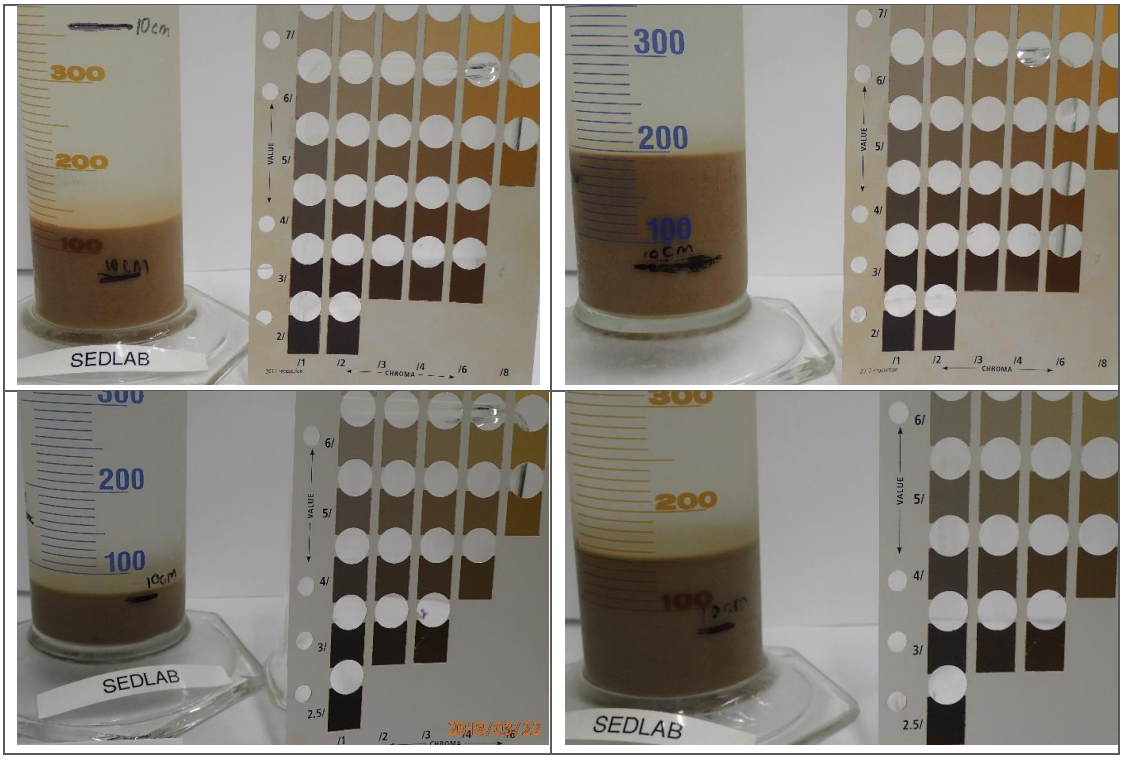

Figure 3.16. Burdekin River flood plume sediment collected within the Upstart Bay inner plume at the river mouth/estuary (salinity = 4; top left) and higher salinity (salinity = 23; top right) on 6th March 2018, and samples collected above the Orchard Rocks resuspension trap site on 13th March 2018, as collected at surface (bottom left) and depth (bottom right).

4.0 FLOOD PLUME PART 2: DISSOLVED INORGANIC NITROGEN GENERATION IN RIVERINE SEDIMENT PLUMES OF THE GBR (DES COMPONENT)

Recent research has indicated that particulate nutrients associated with fine sediment are bioavailable to marine phytoplankton of the Great Barrier Reef (GBR) (Franklin et al., 2018; Garzon-Garcia et al., 2018). The magnitude of this bioavailability depends not only on the sediment load, but on sediment characteristics associated with its parent soil. These characteristics vary with soil type, land use and erosion process (e.g., surface versus subsurface erosion). The bioavailability of particulate nutrients to phytoplankton is mediated by microorganisms (e.g., bacteria and fungi) which mineralise organic nutrients into inorganic forms that are directly available and preferentially used by phytoplankton [e.g., dissolved inorganic nitrogen (DIN)]. DIN is of particular importance because nitrogen is considered to be the limiting nutrient for phytoplankton growth in the GBR (Furnas et al., 2005). The magnitude of the contribution to marine DIN from riverine sediment plumes has not been studied to date. Understanding this contribution will enhance risk assessment of anthropogenic sediment and associated particulate nutrients to the Reef. It also improves our understanding of the complex dynamics of large floc formation (muddy marine snow) in riverine sediment plumes (Bainbridge et al., 2012).

Research questions

This component of the research (Garzon-Garcia et al., *In preparation*) was carried out at the Department of Environment and Science (DES) by the Catchment and Riverine Processes group – Landscape Sciences, to answer the following research questions:

- What is the magnitude of DIN generated in river sediment plumes?
- Do DIN generation rates and dynamics change with position in the plume?

Methods

Intact water samples collected from three sediment plumes were incubated in the laboratory to quantify DIN generation rates and understand the dynamics of various nutrient fractions. Incubation experiments were carried out for two plumes from the Burdekin River [cyclone Debbie plume Mar-Apr 2017 (a plume sourced from the Bowen, Bogie and Broken (BBB) sub-catchments of the Burdekin River catchment) and an Upper Burdekin River sourced plume March 2018 (Upper B)] and one plume in the Tully River (February 2018) (for detailed description of the sampled plume events see Section 3).

Samples for incubation were obtained using grab-sampling at end-of-catchment sites and various positions along a salinity gradient from sediment plumes. Samples were chilled immediately, kept in the dark and sent overnight to the Chemistry Centre at DES. A water sample for each position in the plume was incubated in a shaker incubator for 7 days at 25°C in the dark and destructive sampling at 0, 1, 3 and 7 days was carried out to analyse for all particulate and dissolved carbon, nitrogen and phosphorus fractions.

Additionally, a strong salt ammonium-N extraction (either using 2M KCl or 0.5 M K_2SO_4)[1] was carried out for each plume sample to quantify the adsorbed ammonium present in the sediment [particulate inorganic N (PIN)] at different positions in the BBB plume. The BBB plume results indicated that most of the adsorbed ammonium is desorbed between 0 PSU and 6 PSU. Consequently, ammonium-N extractions were only carried out for end-of-catchment and ~0 PSU samples for the Upper B plume and a Johnstone River plume that coincided with the Tully River plume event.

Potential net nitrogen mineralisation rates (potential DIN generation rates) were obtained for each position in the plume by fitting a linear first order model (best fit).
The Burdekin River plumes were divided in four sectors according to estimated sediment travel times and total suspended solids concentration (Figure 4.1):

1. a freshwater sector (Burdekin River at Inkerman to 0.1 PSU), with an estimated travel time of 1 hr;
2. a turbid sector (0.1 PSU to 11.7 PSU), with an estimated travel time of 4-7 hours;
3. a clearer sector (11.7 PSU to Orchard Rocks), with an estimated travel time of 3-5 days and;
4. a clearer sector (11.7 PSU to Palm Island), with an estimated travel time of 4-8 days.

DIN generated loads for each plume sector were calculated using the fitted equations, the plume travel time for each sector and the event sediment load estimated to remain in suspension for each sector. The load remaining in suspension for each sector was calculated using changes in sediment concentrations for different positions in the plume. The average plume travel times were obtained from the eReefs model by calculating the time between the fastest rates of conservative tracer increase across the different positions in the plumes. Estimated plume travel times were verified by comparing them with times between the event peak at end-of-catchment and observed peaks in the turbidity logger at Orchard Rocks and Havannah Island.

Results and Discussion

The potential DIN generation associated with particulates in the marine environment was significant in the two plumes sourced from different areas of the Burdekin River catchment (BBB, Upper B). It was not significant in the Tully River plume. The total potential load of DIN estimated to be generated in the Burdekin plumes was 105 and 86 tonnes, which is equivalent to 38% and 12% of the whole of catchment DIN loads of 278 and 685 tonnes of DIN contributed at the end of river for the BBB and Upper B events, respectively (Figure 4.1). These loads were generated in 4 to 8 days of average sediment travel time during the whole duration of the plume event. The estimated cumulative DIN load generated in each of the plume sectors can be observed in Figure 4.1.

[1] The method was changed from 2M KCl to 0.5M K_2SO_4 for the second year of sampling, considering the latter method allows for direct quantification of the soluble organic fractions on extracts of recovered sediment samples. This makes it a more practical method when working on both sediment suspensions and sediment samples. Results from both methods are not significantly different as per a comparison carried out for 58 soils (Adjusted R^2 = 0.98, $p<0.0001$) and 44 sediments (<10 um) (Adjusted R^2 =0.98, $p<0.0001$) from the Johnstone and Bowen River catchments.

Particulate inorganic nitrogen (PIN) conversion to DIN (i.e. ammonium desorption) was an important process accounting for between 23% and 60% of the generated DIN load. All PIN was converted to DIN at salinities below 11.7 PSU. This occurs because of the higher ionic strength in the water as salinity increases, which allows for the replacement of the NH_4-N^+ by other cations (Mackin and Aller, 1984). The remaining 40 to 77% was contributed by microbial mineralisation of the organic nitrogen (PON+DON). There is a trend for DON concentrations to decline along the plume (Figure 4.2) as well as during incubation experiments for all plume samples. This suggests that there is a large contribution of terrestrial sources to DON in plume water and some production along the plume. The decrease in DON may be partly explained by mineralisation of DON to generate DIN as well as by dilution with marine water.

Potential mineralisation rates had the tendency to increase along the plumes with faster mineralisation rates at higher salinities. The BBB plume had significantly larger potential mineralisation rates (Figure 4.3). Importantly, mineralisation was still increasing linearly at the end of the incubation experiments (Figure 4.4). This indicates that the sediment and associated particulate nitrogen have the potential to continue to generate DIN once deposited on the marine floor and/or resuspended. Previous research in the GBR has demonstrated that 74 to 92 % of deposited PN is mineralised to DIN and an average of 50% of deposited PN is lost through denitrification (Alongi et al., 2007). For the Upper B plume, mineralisation rates, drastically decreased 1 week after the event (Figure 4.3). This indicates that the bioavailability of the organic matter for microbial mineralisation was reduced. Mineralisation rates are those measured in laboratory conditions so may not necessarily be the same as in situ, however the incubation experiments enable the removal of the effect of algae, allowing the quantification of gross DIN generation. The value of this type of experiment is that it provides additional information on the cycling rates of N in the plume (Figure 4.1) which cannot be obtained from direct DIN measurements of the plume water (Figure 4.2).

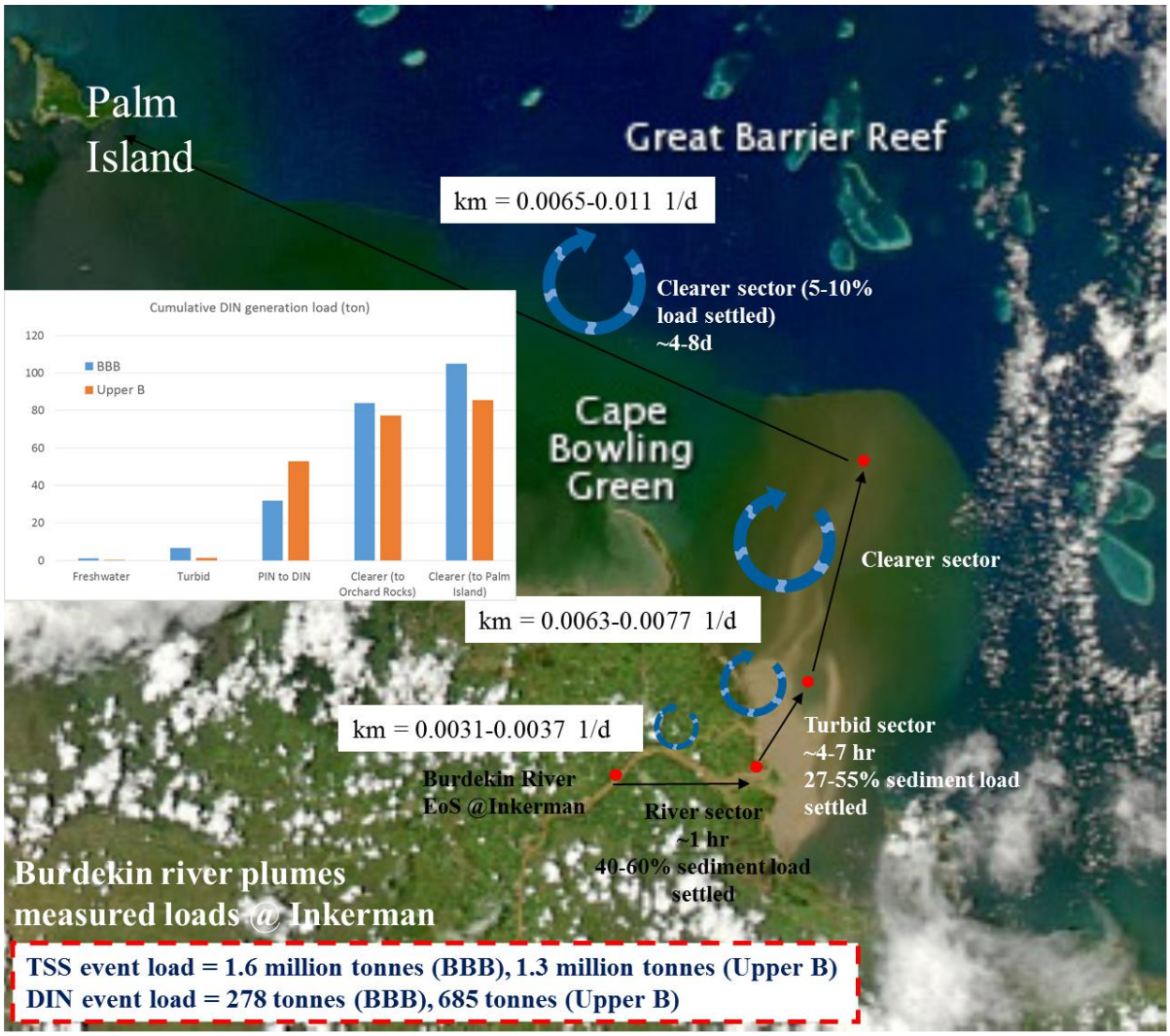

Figure 4.1. Estimated cumulative DIN generation loads associated with particulates and corresponding organic N mineralisation rates from the BBB plume and the Upper B plume at the river sector (Inkerman EoS – 0.1 PSU), turbid sector (0.1 PSU – 11.7 PSU), clearer sector to Orchard Rocks (3-5 days of travel time) (>11.7 PSU) and clearer sector to Palm Island (4-8 days of travel time). The total estimated event loads at Inkerman end-of-catchment are 1.6 and 1.3 million tonnes of TSS and 278 and 685 tonnes of DIN, for the BBB and Upper B events, respectively (Garzon-Garcia et al., In preparation).

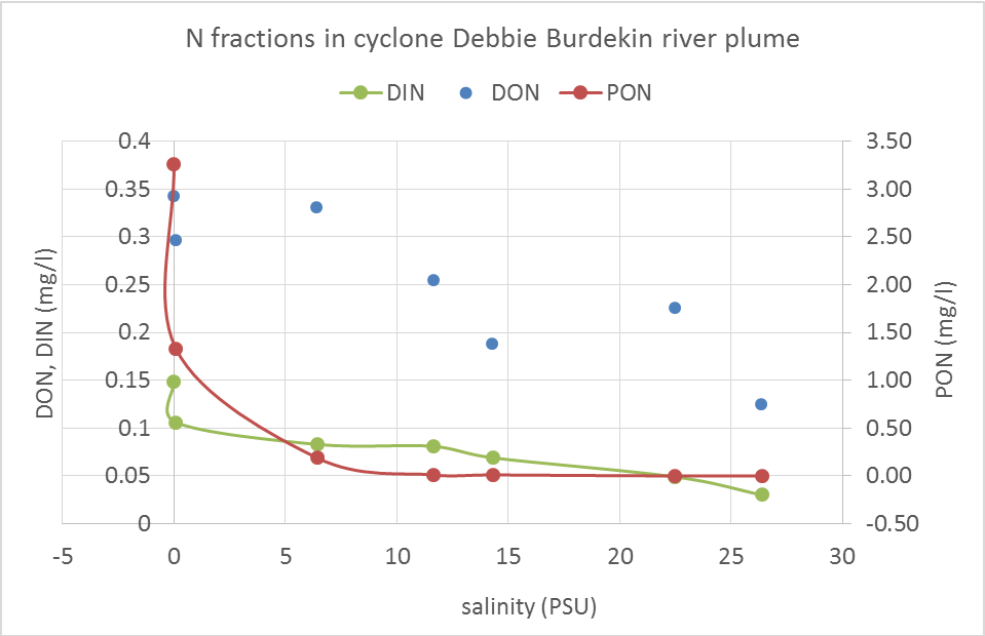

Figure 4.2. DON, DIN and PON in Cyclone Debbie Burdekin plume water along a salinity gradient going from 0 PSU at Inkerman EoS to 26 PSU (Source: Lewis, Bainbridge et al., in prep.)

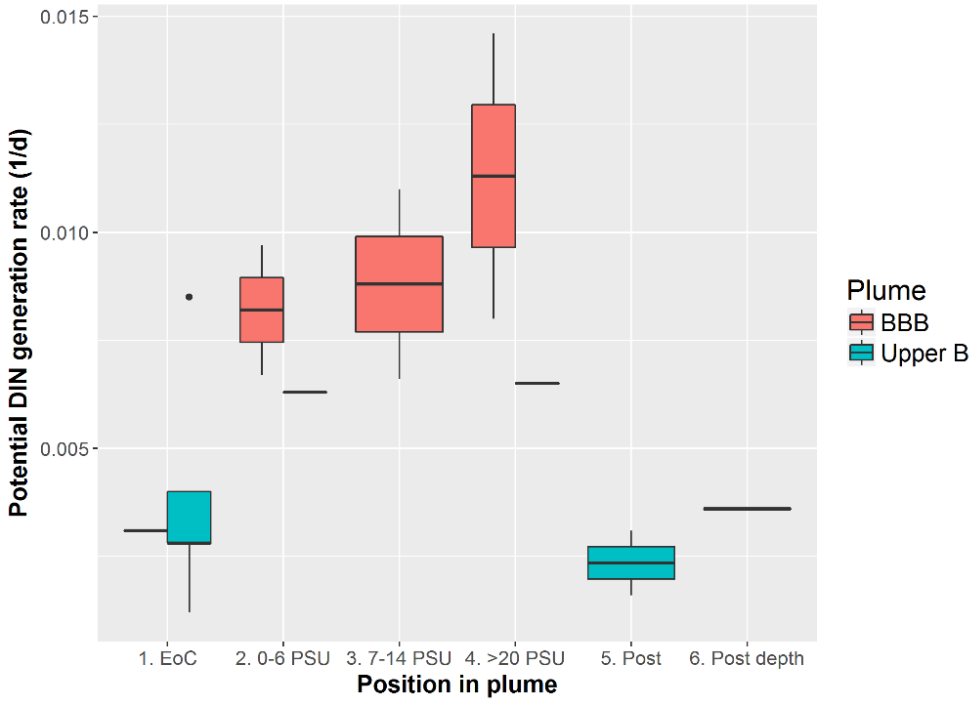

Figure 4.3. Potential DIN generation rates from mineralisation for different positions in the BBB and Upper B, Burdekin plumes. Sampled positions include end-of catchment (EoC), 0-6 PSU, 7-14 PSU, >20 PSU, approximately 1 week post-event at surface (Post) and at depth (~4 m) (Post depth).

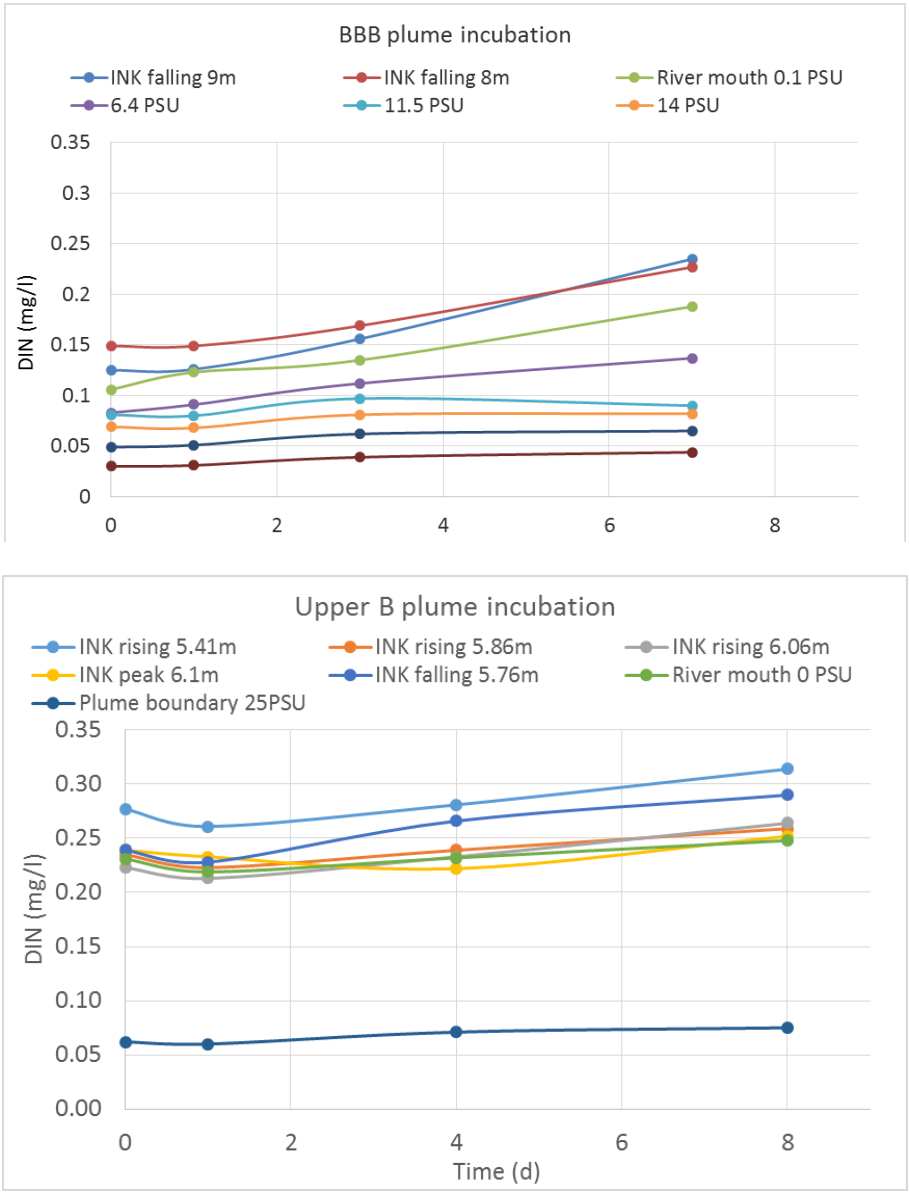

Figure 4.4. DIN concentration during incubation experiments for BBB plume samples (a) and upper B plume samples (b) (net potential mineralisation rates can be seen Figure 4.1) (Garzon-Garcia et al, in prep).

Extension work

The proposed extension of NESP TWQ Hub Project 2.1.5 will continue to characterise the nutrient bioavailability of the environmentally detrimental sediment to the Reef by sampling additional sediment flood plumes and resuspension events. The extension will specifically focus on the Burdekin River, aiming at sampling and analysing a larger event than that previously sampled. Additionally, more limited sampling and analysis of a Johnstone River sediment plume will be undertaken. This work together with a sensitivity analysis of the parameters used in the model and additional experiments to include the role of plume dilution on DIN generation rates will increase our confidence on how much DIN is generated from particulate sources in plumes [including the desorption of ammonium and mineralisation of organic matter (incubation experiments)]. These results will then be combined with sediment and organic matter tracing results to determine the dominant source of sediment producing DIN in the marine environment.

5.0 FLOOD PLUME PART 3: ORGANIC TRACING AND CHARACTERISATION (GRIFFITH UNIVERSITY COMPONENT)

Tracing the source of sediments and nutrients to the Great Barrier Reef (GBR) – exploring the use of organic fingerprint methods to differentiate sediments and particulate nitrogen from different land uses (Griffith University Component)

SUMMARY

This study aimed to develop a novel biogeochemical fingerprint technique to differentiate between the main land use sources of plume and river-bed sediments and associated particulate nutrients (e.g., nitrogen). New approaches [isotopic ($\delta^{15}N$, $\delta^{13}C$) signature, ^{13}C NMR spectroscopy] were also explored to identify the chemical and biological nature and dynamics of organic nutrients associated with sediments moving to the GBR lagoon. The key results included:

a) The combined use of isotopic and geochemical signatures enables the SIAR model to provide an accurate estimation of source apportionment from different land uses and can be used as a valuable new sediment and particulate nutrient tracing tool. The mean modelling results indicated that forest was the largest source of river bed sediments at the Johnstone River mouth with a mean sediment contribution of 33.1% (SD=14.5) followed by grazing land use (beef and dairy combined) with a mean sediment contribution of 25.1% (SD=13.9). Mean proportional contributions of sugarcane and bananas were 21.4% (SD=13.5) and 20.4% (SD=13.2), respectively. The contributions from native forest and sugarcane to the suspended sediments delivered to the river estuary were similar to the river bed sediments, and native forest with 33.1% was still the dominant source of plume sediment in the 2018 flood event. The contribution of bananas (26.7%, SD=15.2) to the suspended sediments was higher compared to the river bed sediments.These preliminary results are consistent with Hunter and Walton (2008) reporting forest as the main source of sediments in the Johnstone catchment. However, as only one snapshot sampling was carried out in this preliminary study, multiple samples from the Johnstone River catchment and plume over another season is recommended in the extension component of this project to further improve reliability of the model prediction.

The trend in the contribution of different land uses to the PN bound to suspended sediments was almost similar to that of particulate nutrients bound to river bed sediment. Forest was the main source of PN attached to suspended (53.5%, SD=7.3) and river bed sediment (52.6%, SD=11.4). Sugarcane with 8.6% (SD=1.9) and 8.5% (SD=0.9) had the lowest contribution to PN discharged to the marine environment as bound to suspended and river bed sediments, respectively. Although the contribution of forest to both bed and suspended sediment and PN delivered to the Johnstone River's estuary was high, these contributions were disproportionately small, since rainforest covered 52% of the catchment land area. Table 5.2 shows that rainforest had the lowest proportional enrichment (PE) (% contribution to the river estuary/% land use area) towards the bed and suspended sediments delivered to the Johnstone River estuary. In comparison, banana and sugarcane had the highest PE to the both bed and suspended sediments delivered to the coast, respectively.

b) Soils, riverbed sediments, plume samples and marine sediments showed distinct patterns of ^{13}C NMR spectra. The PCA on ^{13}C NMR spectra data showed that soil samples from different land uses in the Johnstone River catchment were totally different from the sediments collected from the marine environment. Plume samples from all three rivers (the Johnstone, Tully and Burdekin) shared a similar pattern to the soil samples from the Johnstone catchment in terms of ^{13}C NMR signature, indicating that the organic composition of the sediment were likely of terrestrial origin.

c) The ^{13}C NMR spectroscopy showed that the soluble component of organic matter is predominantly labile organic fractions (carbohydrates, di-O-alkyl and methoxy groups). The ^{13}C NMR spectra of foam samples collected from the upper catchment of the Johnstone River also showed that about 50% of organic matter in the foam sample was labile organic C (carbohydrates, di-O-alkyl and methoxy groups). Grass species and sugarcane had greater proportions of labile organic fractions (di-O-alkyl, carbohydrates and methoxy groups) in their leaf samples than other species, indicating that grass and sugarcane leaf litter would be more easily decomposed compared with other species.

d) There were different patterns in C functional groups among the three rivers (Johnstone, Tully and Burdekin) as revealed by ^{13}C NMR spectroscopy. The plume from the Johnstone River had the highest proportion (46%) of labile organic fraction (carbohydrate, di-O-alkyl and methoxyl), followed by Tully River (40%) and the Burdekin River had the lowest proportion (35%). The plume samples from the Burdekin River had a higher proportion of recalcitrant C fractions (e.g., aliphatic, aryl C) than those from Johnstone and Tully Rivers. In addition, the A/O-A ratio was much greater for the plume samples collected from the Burdekin River (0.79) than those from Johnstone and Tully Rivers (0.46-0.55), indicating the organic matter in the Burdekin plume samples had been decomposed to a greater extent, compared with those from the Johnstone and Tully Rivers.

e) Preliminary results showed that the plume samples from the Johnstone, Tully and Burdekin Rivers had a different bacterial community pattern compared to the riverbed sediment samples from the Johnstone catchment, with Proteobacteria being predominant and followed by Bacteroidetes in the plume samples, while Proteobacteria, Actinobacteria and Acidobacteria were predominant in the riverbed sediment samples. The fungal community composition also showed distinct patterns between the riverbed sediments and plume samples. Basidiomycota was dominant, followed by Rozellomycota in the plume sample, while Rozellomycota, Chytridiomycota and Mortierellomycota were predominant in riverbed sediment samples. These different patterns may be related to the source of organic matter in sediments and different environmental factors (pH, salinity, hydrology etc.). The determination of the bacterial and fungal communities in soils and riverbed sediments in the Burdekin catchment is planned in the extension component to ascertain if these are similar to the Johnstone and hence confirm if changes occur in the estuarine mixing zone (i.e. flood plumes).

Introduction

The research on nutrient export from the Great Barrier Reef (GBR) catchment to reef has largely focussed on inorganic nutrients such as NH_4^+-N, NO_x-N and PO_4^{3-}. While the loads and source of the particulate nitrogen (N) (PN) have also been examined, its liability is less understood (see Waterhouse et al., 2018); this is important as PN constitutes a major proportion of the N exported from the river catchments (Hunter and Walton 2008; Brodie et al., 2015). In order to develop sound strategies to manage PN discharge and understand its potential detrimental impacts on the GBR lagoon, it is necessary to identify the main sources of sediments and associated N delivered from the GBR catchment (Bahadori et al. 2018). In addition, the chemical and biological nature of the organic component of the sediments (riverbed, suspended and marine) in the GBR area is largely unknown and is critical for understanding their influence on reef health.

Sediment fingerprinting techniques utilise a combination of field sampling, biogeochemical analyses in the laboratory and statistical modelling to allocate the contribution of each source of sediments and nutrients delivered to and/or exported from the rivers (Haddadchi et al. 2013). In this technique, a number of biogeochemical properties are measured in both soil samples of potential sources within the upstream catchment and sediment mixtures collected at the river outlets. A stepwise discriminant statistical analysis is used to select a suite of elements which distinguishes between the sources, and then a mixing model is employed to determine the specific contributions from the discrete sources (Collins et al. 2017). Sediment fingerprinting techniques rely upon identifying significant differences in the chemical properties from different sediment sources. Properties that can be used to discriminate sources are: a) Major and minor element geochemistry, which is related to geological substrate but also modified by soil formation processes and weathering and hence has potential to discriminate land use (Collins and Walling 2002; Collins et al. 2010; Haddadchi, Olley, and Laceby 2014); and b) Biochemical properties, which have been used in recent studies to discriminate between potential sediment sources with different land uses, vegetation species, management systems and microbial communities. In this technique, some natural characteristics of source such as stable isotopes in organic compounds (e.g., $\delta^{15}N$, $\delta^{13}C$), biomarkers (e.g., Phospholipids, fatty acids) and DNA based techniques are employed as biochemical fingerprints (Glendell et al. 2018; Alewell et al. 2016). The accuracy and robustness of mixing model outputs highly depends on the discriminative power of selected tracers and the type of model used in fingerprinting techniques.

Aims of this study were to:

- **a)** develop a novel technique of combined geochemical and isotopic fingerprints to differentiate between the main land use sources of plume and river-bed sediments and associated PN that were exported to the coast through the Johnstone River, and to quantitatively allocate these non-point pollutants (sediments and N) to the four major land uses in that catchment.
- **b)** explore new approaches [isotopic ($\delta^{15}N$, $\delta^{13}C$) signature, ^{13}C NMR spectroscopy and DNA fingerprints] to identify the chemical and biological nature and dynamics of organic nutrients associated with sediments moving to the GBR lagoon.

Methodology

Soil and sediment sampling and preparation

In this study, soil samples were collected from land use sources that may potentially contribute sediments and particulate N into the river during rainfall events and transport them downstream. Four potential land use sources were identified and sampled in July 2016 including grazing (beef and dairy have been combined), sugarcane, forest and banana. These sources were selected after an extensive literature review and field investigations. Considering the unequal distribution of land-uses along the Johnstone River, the whole river catchment was divided into two geographical sections including the upper and lower Johnstone in order to select sampling sites. Grazing of beef cattle occurred throughout the catchment, while dairy farming was restricted to the upper, more elevated areas, while sugarcane (except a few small farms in upper catchment) and bananas were grown only in the lower catchment. For representative soil sampling, 20 sampling points were selected throughout the catchment. Grazing and forest soil samples were exclusively collected from the upper catchment, while banana soil samples were collected from the lower catchment. Sugarcane soil samples were collected from both sections including two samples from the lower and three samples from the upper Johnstone catchment. Sampling locations for different sources were selected using maps prepared by ArcGIS (10.0) (Bahadori et al. 2018). The river bed sediment sampling from the river mouth was also carried out at the same time as soil sampling in July 2016. The river bed sediment samples were collected from the top 10 cm using a trowel.

In order to ensure the consistency and to facilitate the direct comparison of soil and river bed sediments, all the collected samples were air dried, gently crushed using a pestle and mortar and then passed through 63 µm sieve. Before that, the collected samples were once passed through 4 mm and then 2 mm sieves and all physically visible fragments such as root and plant litter were removed from samples (Collins, Walling, and Leeks 1997). Plume samples were centrifuged upon their arrival at the laboratory to recover as much sediment as possible from the buckets, and then were freeze dried prior to chemical analyses. There was no need for passing suspended sediments through a sieve as they were already less than 63 µm in size.

Stable isotopes and geochemical analysis

In accordance with the procedure for measuring the stable isotope $\delta^{15}N$, all soil and sediment samples were pelletized in tin capsules. For $\delta^{13}C$, first inorganic carbonates were removed by shaking the small aliquot (2–5 g of each sample) with 2 ml of 10% hydrochloric acid (HCl) and allowing the suspension to stand overnight. More HCl was added to the samples until no further effervescence occurred. The sample was finely ground in a mortar and pestle after being dried at 60°C for 48 h. Then the samples were pelletized in silver capsules and weighed for analysis with a Sercon Hydra 20-22 Europa EA-GSL isotope-ratio mass spectrometer. Stable isotope ratios are reported in standard delta (δ) notation per mil (‰) as:

$$\delta X = [(R_{sample}/R_{standard})-1]\times 1000$$

where X is ^{13}C or ^{15}N and $R=^{13}C/^{12}C$ or $^{15}N/^{14}N$, respectively. In this study, in order to determine the useful geochemical signatures, a total of 21 chemical elements (Na, K, Mg, Ca, Mn, Zn, Al, Cu, Sn, Ni,, Co, Cr, Pt, Pb, As, Hg, Fe, Ag, S, P and Au) were analysed in soils, using ICP-OES; Perkin Elmer; Optima 8300, after direct digestion with nitric and perchloric acid (Bahadori et al. 2018).

Hydrofluoric acid pre-treatment of soil samples and carbon-13 solid state NMR spectroscopy

Pre-treatment of soil and sediment samples with HF before solid-state ^{13}C CPMAS NMR analysis removes substantial amounts of Fe^{2+} and Mn^{2+} in soil and concentrates the organic matter content of the whole sample, improving the signal/noise ratio. In this study, all soil and sediment samples for NMR analysis were pre-treated with 5% HF. Solid-state ^{13}C CPMAS NMR spectra of the HF treated soils were obtained at a frequency of 100.6 MHz on a 300 MHz Varian VNMRS spectrometer (Varian Inc., CA). Samples were packed in a silicon nitride rotor (optical density=7mm) and spun at 5 kHz at the magic angle. Single contact times of 2 ms were applied, with an acquisition time of 14 ms, and a recycle delay of 1.5 s. Approximately 20000 transients were collected for all samples and a Lorentzian line broadening function of 150 Hz was applied to all spectra. Chemical shift values were referenced externally to hexamethylbenzene at 132.1 ppm, which is equivalent to tetramethylsilance at 0 ppm. The solid-state ^{13}C CPMAS NMR spectra were divided into the seven common chemical shift regions: aliphatic C (0-45 ppm), methoxyl C (45-60 ppm), carbohydrate C (60-90 ppm), di-o-alkyl (90-110 ppm), aryl C (110-145 ppm), O aryl C (145-160 ppm) and carboxyl C (160-180 ppm) and the relative intensity for each region was determined by integration using Varian NMR 3.1A software package (Chen, Xu, and Mathers 2004).

Table 5.1. Number of laboratory analyses completed on the samples in this study.

Sample\analyses	DIN (NH_4, NOx)	Stable Isotopes	NMR	DNA sequencing	Amino acids	Particle size	Elemental analysis (ICP)
Plant material	66	100	44	-	-	-	90
Soil	56	108	40	12	28	30	104
Sediment	150	260	92	23	12	10	130
Water	150	-	-	-	-	-	33
Total	**422**	**468**	**176**	**35**	**40**	**40**	**357**

Statistical analysis and modelling

The most discriminative group of geochemical elements (acid extractable Zn, Pt and S) was selected after a stepwise discriminant statistical analysis, and the discriminative power of isotopic signatures ($\delta^{13}C$, $\delta^{15}N$) was assessed using paired t-tests for the comparisons of data with equal means and variance. Principal component analysis (PCA) was used to separate the different land uses using geochemical or isotopic signatures alone or combined signatures. Then, for the first time a combination of isotopic and selected geochemical properties ($\delta^{13}C$, $\delta^{15}N$, Zn, Pt and S) were modelled with SIAR V4 to estimate the contribution of different land uses of the Johnstone River catchment to both riverbed and suspended sediments. SIAR has recently been widely used in sediment fingerprinting using a Bayesian mixing approach and model fitting with Markov Chain Monte Carlo (MCMC) simulations of plausible values consistent with the data (n = 30,000). The PCA was also used to show the main origin of

organic nutrients in the suspended sediments that are most likely to reach the GBR through the flood event (Bahadori et al. 2018).

Soil DNA isolation and pyrosequencing

The total genomic DNA was extracted from 0.3-0.5 g of frozen soil using MoBio Powersoil DNA isolation kit following the manufacture`s instruction. 10-fold dilution of DNA template was used for downstream PCR analysis to reduce PCR inhibitors such as humic acid. PCR products for pyrosequencing were amplified with the bar-coded primers F515 (5'-GTGCCAGCMGCCGCGGTAA-3') and R806 (5'-GGACTACVSGGGTATCTAAT-3'), targeting the V4 region of the bacterial and archaeal 16S rRNA genes. The forward primer consisted of the 454 adapter A, 10-based MID barcodes, 4-bp linker sequence (TCAG), along with the primer F515. The reverse primer consisted of the 454 adapter B, 4-bp linker sequence (TCAG) along with the primer R806. PCR amplifications were performed in triplicate in 30 µl reaction containing 1× PCR buffer, 3.0 mM $MgCl_2$, 400 µM each dNTP, 2.5 U Ex Taq™ DNA polymerase (TaKaRa, Shiga, Japan), 0.5 µM of each bar-coded primer. We used the following PCR thermal profile: 94° C for 5 min, 34 cycles consisting of 95 °C for 30 s, 53 °C for 45 s, 72 °C for 60 s, and final extension at 72 °C for 60 s. Pooled PCR products for each soil sample were purified using a Wizard SV Gel and PCR Clean-Up System (Promega, Madison, WI). The purity and concentration were checked using a NanoDrop 1000 spectrophotometer (Thermo Scientific, Wilmington, DE) and Qubit fluorometer with Quant-iT dsDNA HS Assay Kits (Invitrogen, Eugene, OR), respectively. Equimolar amounts of PCR products with different barcodes were combined into one sample and sent to Macrogen (Seoul, Korea) for pyrosequencing using Roche/454 GS FLX Titanium platform.

Results and discussion

a) Developing a novel approach of combining isotopic and geochemical signatures to differentiate the sources of sediments and particulate nutrients from different land uses

The PCA results presented in Figure 5.1 show that a combination of both geochemical and isotopic signatures is able to differentiate between all potential land use sources of sediments in the Johnstone River catchment. The PCA has revealed two principal components with a cumulative variance of 77.3 %. PC1 was responsible for 46.7 % variance and is best represented by Pt, Zn and $\delta^{15}N$. These properties can be used to separate grazing (beef and dairy combined) and sugarcane as well as to discriminate between banana and forest land uses. PC2 is best represented by $\delta^{13}C$ and S, accounting for 30.6% of total variance. These specific properties also play a notable role in differentiating between land uses covered with tree species (banana and forest) and grasses (sugarcane and grazing) in this catchment (Figure 5.1) (Bahadori et al. 2018).

The $\delta^{13}C$'s ability to discriminate between sources is based on the fact that different photosynthetic pathways result in distinct $\delta^{13}C$ fractionations. The majority of tree species follow the Calvin-Benson cycle (C_3) photosynthetic pathway with a mean $\delta^{13}C$ of −28‰. Some cropping plants and dominant grass species in warmer climates, on the other hand, mainly follow the Hatch-Slack cycle (C_4) pathway with a mean $\delta^{13}C$ of −13‰ (Coleman 2012). Therefore, $\delta^{13}C$ can be considered as a signature to discriminate between the sources of organic matter derived from C_3 and C_4 plants in tropical and subtropical environments.

Generally, $\delta^{15}N$ fractionation is much more complex than $\delta^{13}C$ due to multiple N sources and different potential internal transformations which can affect N isotopic ratios in derived organic matter from different plant materials. The atmospheric N (N_2) is the major form of N in the biosphere with $\delta^{15}N$ of 0‰. The majority of N in the rest of the biosphere also has $\delta^{15}N$ values between −10‰ and +10‰ (Peterson and Fry 1987). Several studies have used isotopic signatures to differentiate between subsoil and topsoil as the potential sources of sediments and particulate nutrients to the rivers (Laceby et al. 2016; Blake et al. 2012). However, these signatures are not able to differentiate the land uses covered with the vegetation that follows the same photosynthetic pathways (Bahadori et al. 2018).

The potential of geochemical signatures in separating sources is based on the theory that rock types can influence the geochemical properties of soils during the process of soil formation and development. Therefore, soils lying over different geological structures usually reflect a distinct group of geochemical fingerprints which is highly dependent on their source lithology. As a result, the origin of discharged and transported sediments in a water way can be traced back using these distinct geochemical fingerprints, if they retain the distinguishable signatures of their original rock parents. Despite the popularity of geochemical fingerprinting, this technique is usually used to differentiate sources with different geological properties, and is not able to distinguish between different land uses on the same geological structures. Therefore, it is necessary to have a combination of several diagnostic soil and sediment properties through which we can have a more discriminative approach in identifying the origin of sediments and associated nutrients, specifically when a great number of sources needs to be investigated, and if the objective of the study is to determine contributions from different land uses (Figure 5.1) (Bahadori et al. 2018; Collins et al. 2017).

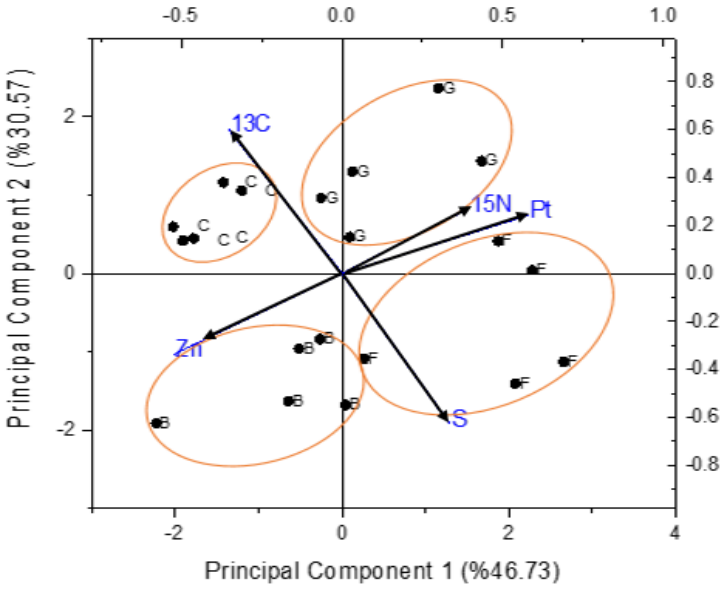

Figure 5.1. Principal Components Analysis (PCA) plot of combined isotopic and geochemical signatures for four land use sources of sediments (G: grazing (beef and dairy combined), C: sugarcane, F: forest, B: banana) in the Johnstone River catchment.

The SIAR modelled results showed that forest was the largest source of river bed sediments at the Johnstone River mouth with a mean sediment contribution of 33.1% (SD=14.5) followed

by grazing land use (beef and dairy combined) with a mean sediment contribution of 25.1% (SD=13.9) (Figure 5.2A). Mean proportional contributions of sugarcane and banana were 21.4% (SD=13.5) and 20.4% (SD=13.2), respectively. The contribution of different land uses to the suspended sediments collected in January 2018 was also modelled in the SIAR mixing model. The contributions from native forest and sugarcane to the suspended sediments delivered to the river estuary were similar to the river bed sediments, and native forest with 33.1% was still the dominant source of suspended sediment in 2018 flood event. The contribution of bananas (26.7%, SD=15.2) to the suspended sediments was higher compared to the river bed sediments (Figure 5.2A). These preliminary results are consistent with Hunter and Walton (2008) reporting forest as the main source of sediments in the Johnstone catchment. However, as only one snapshot sampling was carried out in this preliminary study, multiple samples from the Johnstone River catchment and plume over season is recommended in the extension component of this project to further improve reliability of the model prediction.

The trend in the contribution of different land uses to the PN bound to suspended sediments was almost similar to that of particulate nutrients bound to river bed sediment. Forest was the main source of PN attached to suspended (53.5%, SD=7.3) and river bed sediment (52.6%, SD=11.4). Sugarcane with with 8.6% (SD=1.9) and 8.5% (SD=0.9) had the lowest contribution to PN discharged to the marine environment as bound to suspended and river bed sediments, respectively (Figures 5.2B).

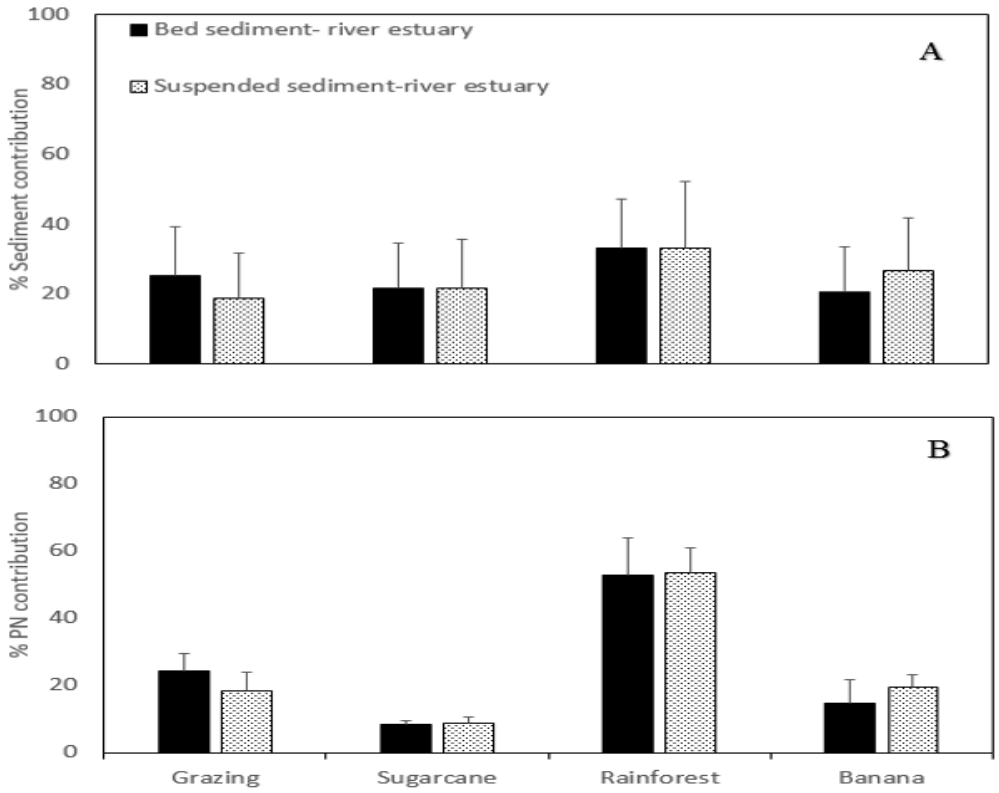

Figure 5.2. Contributions of different sources (grazing, sugarcane, rainforest and banana) to exported bed sediments (A), suspended sediments (A) and particulate nitrogen (PN) associated with river bed sediment (B) and plume sediment (B) to the Johnstone River estuary.

Although the contribution of forest to both bed and suspended sediment and PN delivered to the Johnstone River's estuary was high, these contributions were disproportionately small, since rainforest covered 52% of the catchment area. Table 5.2 below shows that rainforest had the lowest proportional enrichment (PE) (%contribution to the river estuary/%land use area) towards the bed and suspended sediments delivered to the Johnstone River estuary which is a natural contribution and reflects that there is a lot of relatively undisturbed forest in the Johnstone catchment. Banana and sugarcane had the highest PE to the both bed and suspended sediments delivered to the coast, respectively which shows that these land uses are likely much greater contributors by area than forest and contributors that can be managed.

Table 5.2: The proportion enrichment (PE) for different land uses contribution to sediments and particulate nitrogen (PN) discharged to the Johnstone River's estuary

Land use	Land area (% total)	Proportion enrichment (PE) (%contribution to the river estuary / %land use area)			
		Suspended sediment	PN (associated with suspended sediment)	Bed sediment	PN (associated with bed sediment)
Grazing	20.9	1.2	1.2	0.9	0.9
Sugarcane	14.0	1.5	0.6	1.5	0.6
Forest	52.0	0.6	1.0	0.6	1.0
Banana	4.3	4.7	3.4	6.2	4.5

b) Use of ^{13}C NMR spectroscopy to understand the chemical nature of organic matter of soil, leaf, sediment and foam samples

Understanding the chemical nature of organic matter in soil, leaf, sediment and foam is critical for predicting the release of nutrients (e.g., N) from mineralisation of organic matter during transportation of sediments. The soluble component of organic matter is predominantly labile organic fractions (carbohydrates, di-O-alkyl and methoxy groups) (Figure 5.3A). This indicates that this proportion of organic C would firstly move with water from land to water and provide energy for microbial activity and degradation of organic matter, facilitating the release of available nutrients. The ^{13}C NMR spectra of foam samples collected from forest land use on the upper catchment of the Johnstone River also showed that about 50% of organic matter is labile organic C (carbohydrates, di-O-alkyl and methoxy groups) (Figure 5.3B) and hence fast turnover of the organic matter associated with foams is expected.

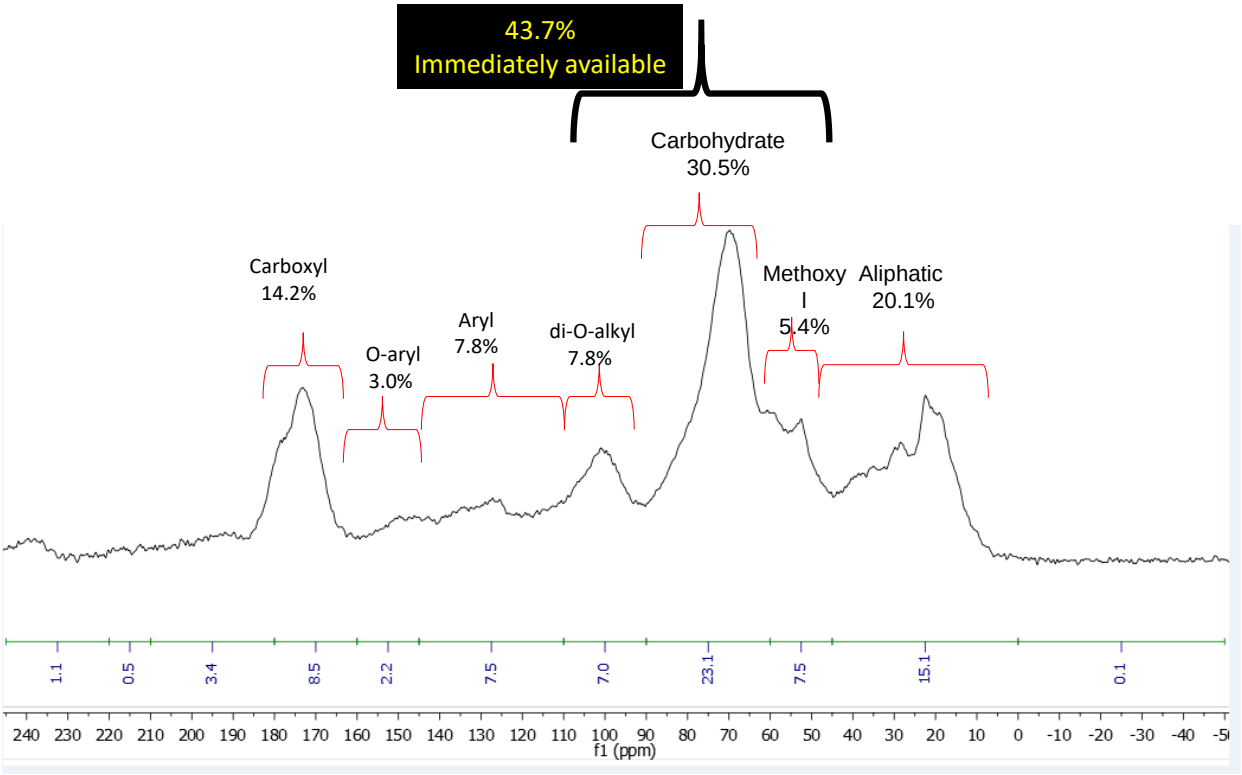

Figure 5.3A. Chemical nature of <u>dissolved organic matter</u> extracted from forest litter materials as revealed by ^{13}C NMR CP MASS.

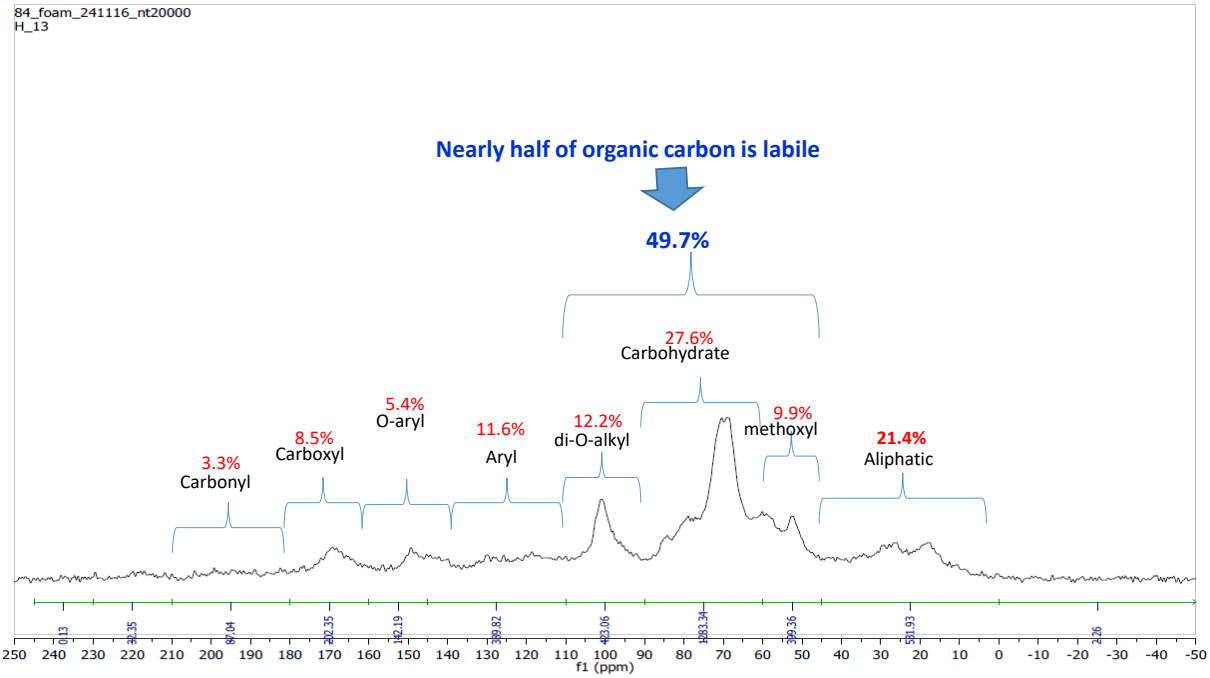

Figure 5.3B. Chemical composition of organic matter (using ^{13}C NMR CP MASS) <u>in foam sample collected</u> in pristine waters, upper catchment of the Johnstone River.

Table 5.3. Proportion (%) of different carbon functional groups in leaf organic matter of different vegetation types (grass, sugarcane, forest and banana) as revealed by ^{13}C NMR CP MASS.

Vegetation type	carbonyl C	Carboxyl C	O-aryl C	aryl C	di-O-alkyl C	carbohyd C	methoxyl C	aliphatic C
Sugarcane	1.49	6.51	2.44	7.40	14.17	48.08	9.18	10.73
Forest	1.85	7.50	3.92	8.53	13.21	40.07	8.96	15.05
Banana	2.11	11.36	2.52	7.63	11.47	37.73	9.16	18.01
Grazing	1.61	7.89	2.46	6.86	13.44	46.37	9.03	12.33

The nutrient input from the decomposition of leaf organic matter from different land uses is a major part of particulate nutrient export from land to water. Sugarcane had a higher proportion (48% carbohydrates) in their leaf than other plants (Table 5.2), followed by grass species (46% carbohydrates) and then forest and banana (40-38% carbohydrates) land uses (Figure 5.3C). On the other hand, grass leaves had less aryl C group (less labile, 7% aryl C) compared with forest and banana (9-8%) (Figure 5.3C). These results showed that grass and sugarcane leaf litter would be more easily decomposed compared with other species. Moreover, grass and sugarcane soils have a greater carbohydrate fraction compared with other species (Figure 5.3D), which is consistent to the trend in C NMR spectra for leaf samples among different species (Figures 5.3, C and D).

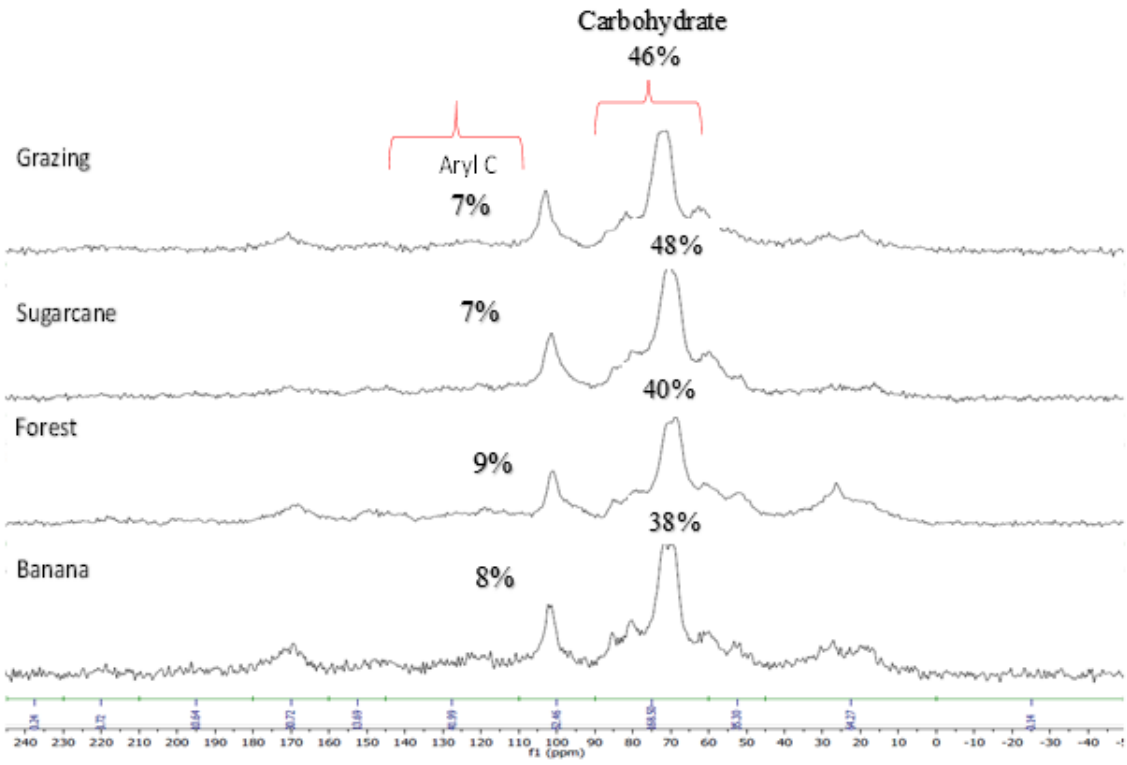

Figure 5.3C. Chemical composition of leaf organic matter of different vegetation types (grass, sugarcane, forest and banana) as revealed by ^{13}C NMR CP MASS.

The ^{13}C NMR spectral pattern for riverbed and marine sediment trap sediments (Figures 5.3E, 5.4A, 5.4B) varied with the locations where they were collected, particularly in key recalcitrant organic fractions (e.g., aliphatic, aryl C fractions), which can be used as potential ^{13}C NMR

fingerprints to differentiate the sources of sediments and particulate nutrients (Golding, Smernik, and Birch 2004).

	carboxyl	Oaryl	aryl	di-O-alkyl	carbohyd	methoxyl	aliphatic
Chemical shift (ppm)	180 .. 160	160 .. 145	145 .. 110	110 .. 90	90 .. 60	60 .. 45	45 .. 0
Sugarcane	9.9	4.8	24.4	10.1	26.0	6.9	17.9
grazing	9.6	3.6	17.6	9.8	27.9	8.8	22.7
forest	9.6	4.6	21.6	10.3	24.5	7.5	21.8
banana	9.4	4.8	22.7	10.4	24.8	7.6	20.3

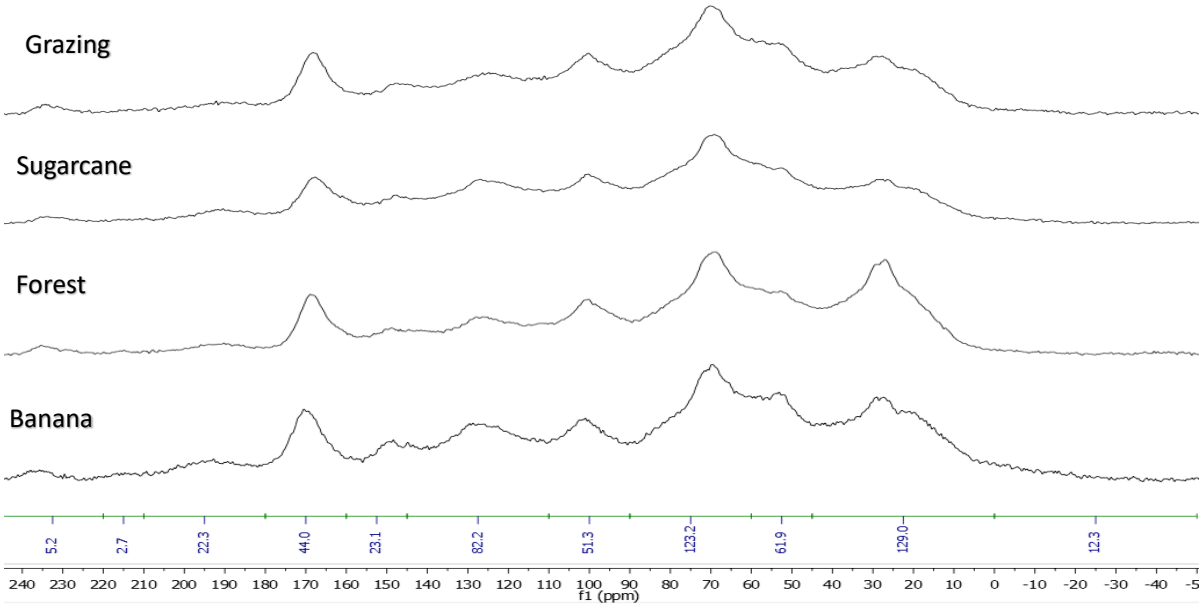

Figure 5.3D. Chemical composition of organic matter in soils under different land uses (grass, sugarcane, forest and banana) as revealed by ^{13}C NMR CP MASS.

	carboxyl	Oaryl	aryl	di-O-alkyl	carbohyd	methoxyl	aliphatic
Chemical shifts	180 .. 160	160 .. 145	145 .. 110	110 .. 90	90 .. 60	60 .. 45	45 .. 0
Upper catchment	8.3	4.5	19.9	10.1	26.0	7.0	24.2
Lower catchment	9.9	4.5	22.7	9.1	24.9	7.1	21.7
River mouth-sea water	6.4	5.2	27.3	8.0	20.8	6.6	25.7

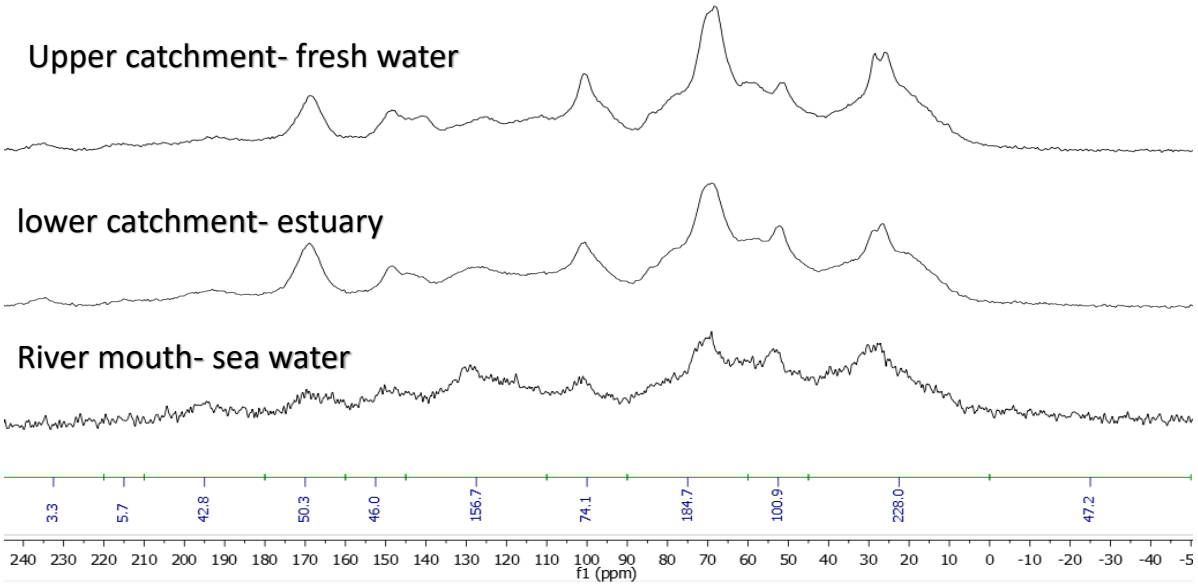

Figure 5.3E. Chemical composition of organic matter in the Johnstone river bed sediments as revealed by ^{13}C NMR CP MASS.

	carboxyl	Oaryl	aryl	di-O-alkyl	carbohyd	methoxyl	aliphatic
Chemical shift	180 .. 160	160 .. 145	145 .. 110	110 .. 90	90 .. 60	60 .. 45	45 .. 0
Dunc Island	11.1	4.7	27.7	5.6	19.0	5.0	26.8
pelorus	12.7	5.1	31.0	5.0	18.7	3.2	24.4
Orpheus Island	7.2	5.0	28.5	8.1	20.0	5.9	25.3
Havanna Island	9.8	3.7	15.6	7.0	21.6	10.5	31.8

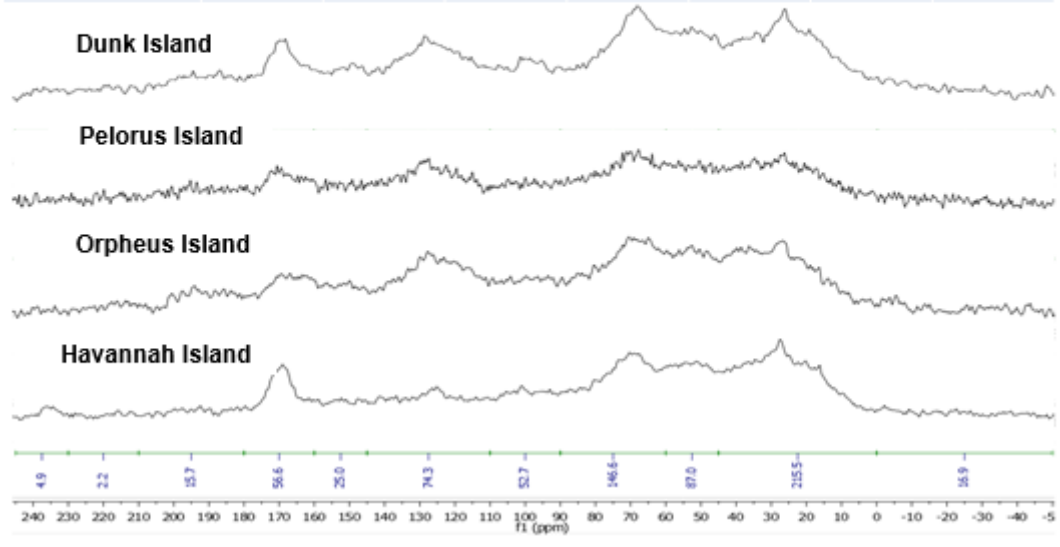

Figure 5.4A. Chemical composition of organic matter in marine sediments collected from sediment traps (Dunk Island, Pelorus Island, Orpheus Island, Havannah Island) as revealed by ^{13}C NMR CP MASS.

	Carboxyl	O-aryl	Aryl	di-O-alkyl	Carbohydrate	Methoxyl	Aliphatic
Chemical shift (ppm)	180 .. 160	160 .. 145	145 .. 110	110 .. 90	90 .. 60	60 .. 45	45 .. 0
Cleveland	9.9	3.5	19.0	6.1	19.0	8.6	33.9
Geoffrey bay	11.7	3.6	18.4	5.6	21.0	7.6	32.1
Magnetic Island- orchid rock	10.2	3.9	26.2	6.0	18.1	5.9	29.7
Middle reef	11.5	2.8	16.1	7.1	24.4	9.0	29.0

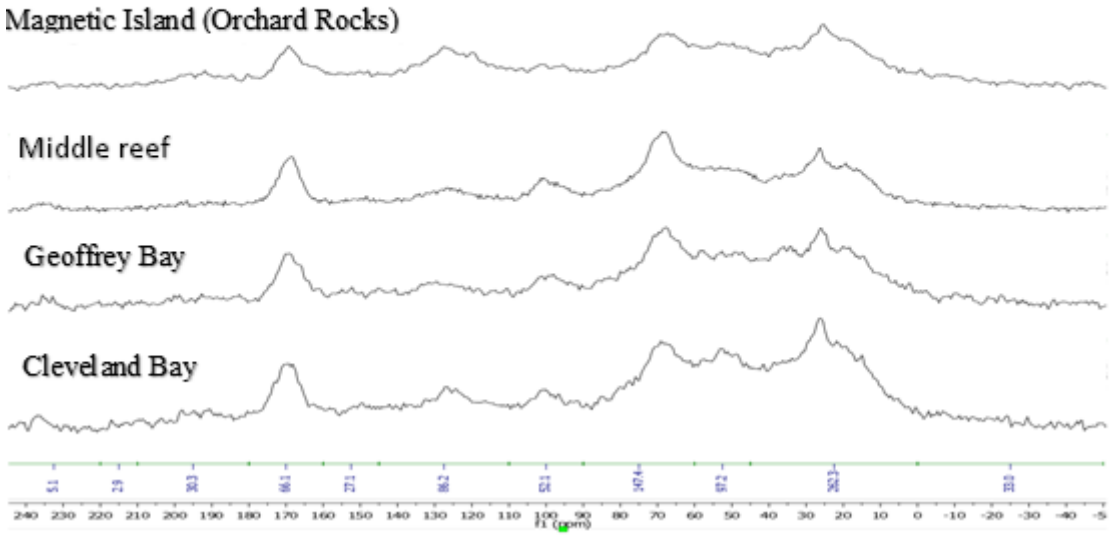

Figure 5.4B. Chemical composition of organic matter in marine sediments collected from different sediment traps (Magnetic Island, Middle reef, Geoffrey Bay, Cleveland Bay) as revealed by ^{13}C NMR CP MASS.

c) Exploring ^{13}C NMR spectra fingerprint method to differentiate sources of suspended sediments and marine sediments.

The ^{13}C NMR results for soil, plume suspended sediment and marine sediment (sediment trap) samples are presented in Figures 5A and B. The PCA was used to demonstrate the distribution of NMR signals between broad chemical shift regions in the different samples. The samples taken from the Wet Tropics region (Tully and Johnstone plume suspended sediments) are different from the Burdekin River plume suspended sediments. Burdekin plume suspended sediments were more enriched in aliphatic, O-aryl and aryl organic compounds, while Johnstone plume suspended sediment samples were mainly composed of di-O-alkyl and carbohydrate. Carboxyl was the dominant organic compound in the plume sediments collected from the Tully River mouth (Figure 5.5A). The PCA also showed that soil samples collected from different land uses in the Johnstone catchment are totally different from the sediments collected from the marine environment (Figure 5.5B). The terrestrial soil samples in the Johnstone catchment mainly contain aryl, O-aryl, carbohydrate and di-O-alkyl while the marine sediments collected from sediment traps mainly are composed of aliphatic and carboxyl compounds (Figure 5.5B) (Golding, Smernik, and Birch 2004).

The PCA results using ^{13}C NMR spectra show that plume suspended sediment samples from the Wet Tropics region (Johnstone and Tully) and Burdekin are more similar to the soil samples collected from the Johnstone catchment rather than marine sediments (Figure 5.5B). Thus, taken together, the data indicate that plume sediments carry the signature of terrestrial plant-derived source material (Figure 5.5B). Of these three main rivers, the Johnstone had the highest carbohydrate and di-O-alkyl content. There are clear differences between soil samples from the Johnstone catchment and the marine sediment trap samples. Sediment traps contain more aliphatic and recalcitrant compounds compared to soil samples (Figure 5.5B) (Golding, Smernik, and Birch 2004). Indeed the analysis of soil samples from the Burdekin catchment is required to directly compare with the sediment trap samples.

The stable isotope ($\delta^{13}C$, $\delta^{15}N$) results for soil, plume suspended sediment and marine sediment (sediment trap) samples are presented in Figures 5C and 5D. The PCA was used to demonstrate the distribution of different samples as a function of their stable isotope signatures. The samples taken from the Wet Tropics region (Tully and Johnstone plume suspended sediments) are different to the Burdekin River plume suspended sediments. Burdekin suspended plume sediments were more enriched in ^{13}C, while Johnstone and Tully plume samples were characterised by higher ^{15}N (Figure 5.5C). The PCA results also show that soil samples from different land uses in the Johnstone catchment are totally different from sediments collected from the marine environment in the sediment traps (Figure 5.5D). Plume samples from the Wet Tropics region including the Johnstone and Tully Rivers are more similar to soil samples from the Johnstone catchment rather than the marine sediment trap sediments. However, Burdekin plume suspended sediments have a similar isotopic signature to marine sediments from the sediment traps (Figure 5.5D). In that regard, most of the sediment traps are deployed in the region (with the exception of Dunk Island) that is most influenced by the Burdekin River flood plume and hence this result is not completely unexpected.

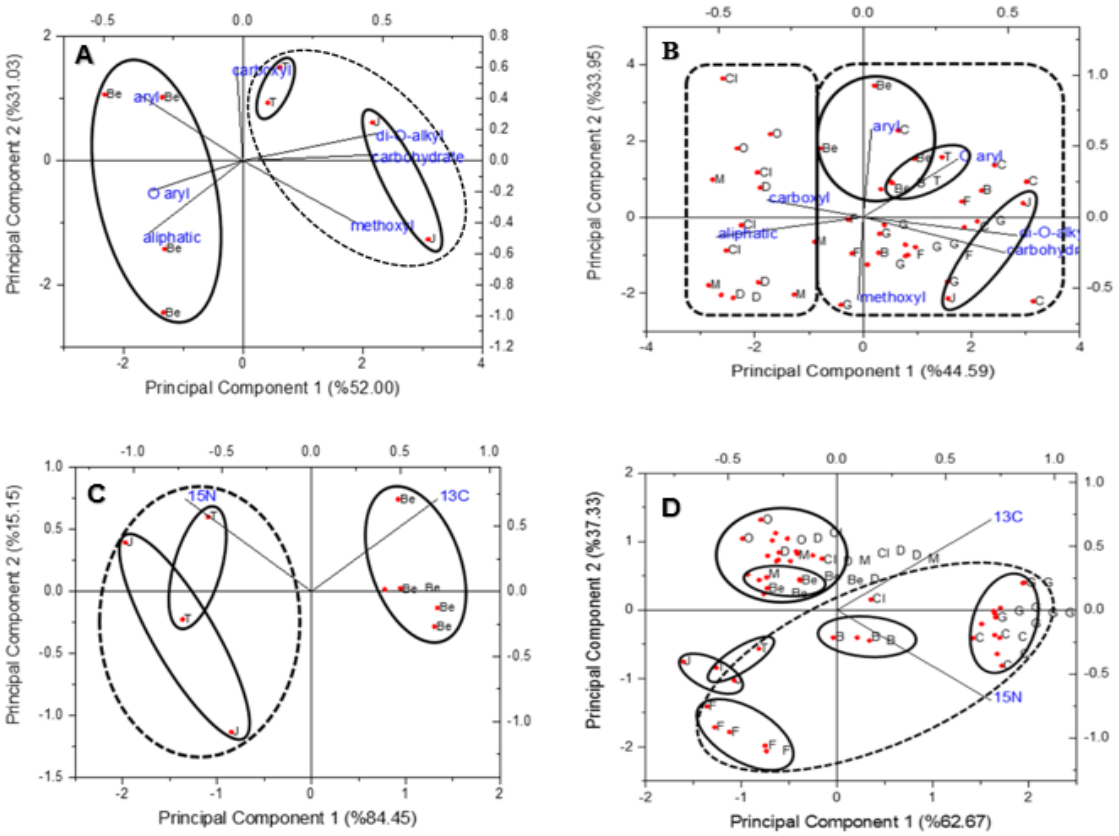

Figure 5.5. NMR and isotopic signatures for soil, plume and trap sediments (G: soil under grazing (beef and dairy); C: soil under sugarcane; F: soil under forest; B: soil under banana; J: Johnstone plume sediment; T: Tully plume sediment; Be: Burdekin plume sediment; D: Dunk island sediment trap; O: Orchard Rocks sediment trap; Cl: Cleveland Bay sediment trap; M: Middle reef sediment trap).

d) Chemical composition of flocs (plume samples) and associated bacterial and fungal community in the GBR area

The ^{13}C NMR spectra of the plume suspended sediment samples collected from the three rivers (Johnstone, Tully, Burdekin) are shown in Figure 5.6 and Table 5.4. Results showed there are different patterns in C functional groups among the three rivers. The plume from the Johnstone River had the highest proportion (46%) of labile organic fraction (carbohydrate, di-O-alkyl and methoxyl), followed by the Tully River (40%) and with lowest proportion for Burdekin River (35%) (Table 5.2, Figure 5.6). The plume suspended sediment samples from the Burdekin River had a higher proportion of recalcitrant C fractions (e.g., aliphatic, aryl C) than those from the Johnstone and Tully Rivers. Therefore, the A/O-A ratio was much greater for the plume samples collected from the Burdekin River (0.79) than those from the Johnstone and Tully Rivers (0.46-0.55), indicating the organic matter in the Burdekin plume samples were decomposed to a greater extent (i.e. with a higher proportion of the recalcitrant organic fraction remaining) compared with those from the Johnstone and Tully rivers (Chen, Xu, and Mathers 2004) (Table 5.4). Different patterns of ^{13}C NMR spectra among the plume samples collected from different rivers provide an excellent opportunity of serving as a fingerprint (^{13}C NMR) to differentiate the sources of the sediments (Golding, Smernik, and Birch 2004). This has been discussed in the last section (Part c – Results and Discussion)

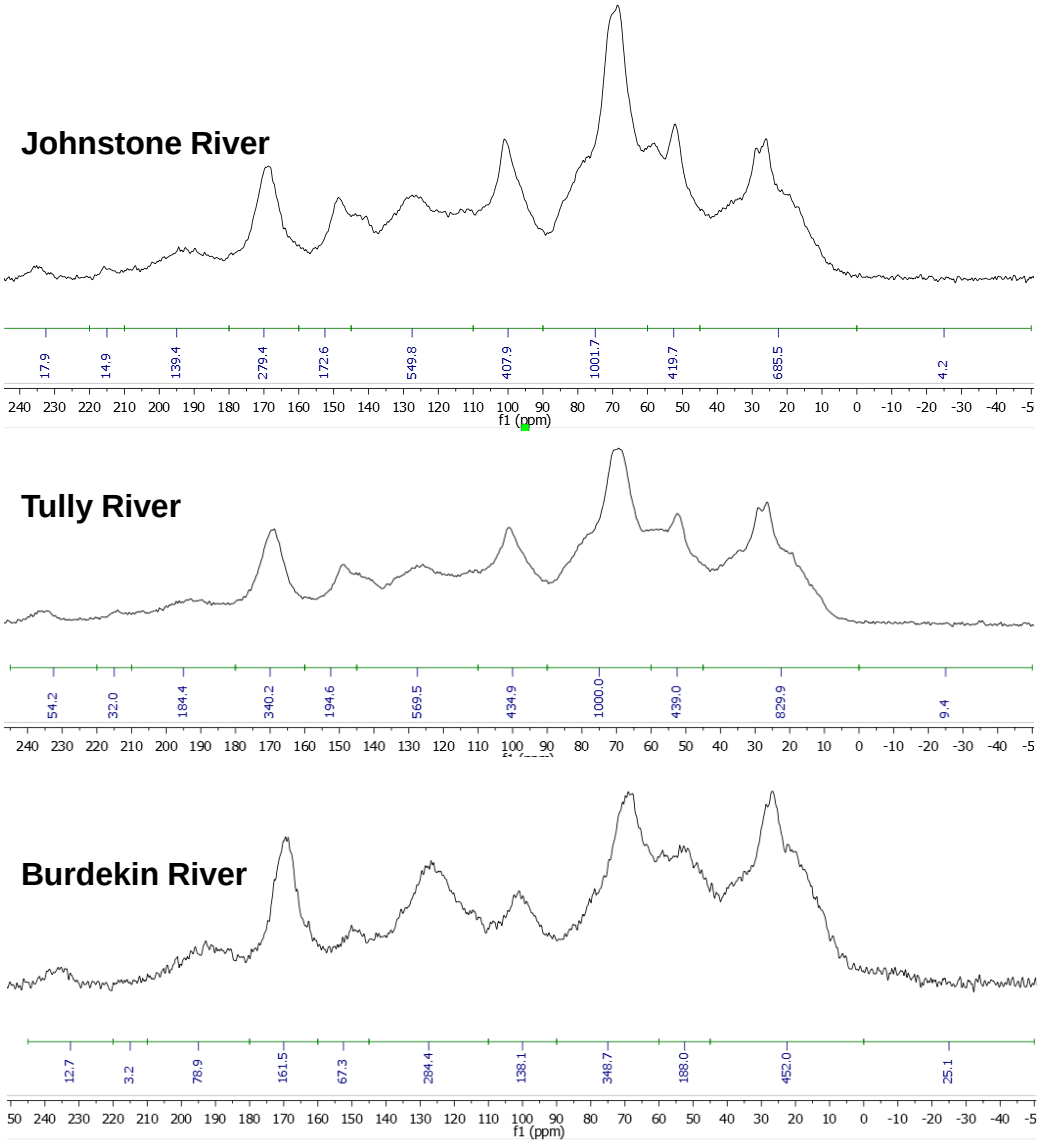

Figure 5.6. ^{13}C CPMAS NMR spectra of plume samples collected from the river month of three rivers (Johnstone, Tully, Burdekin) in the GBR area.

Table 5.4. Composition of C functional groups (%) in plume samples collected from the river month of three rivers (Johnstone, Tully, Burdekin) in the GBR area as characterized by ^{13}C cross-polarization magic-angle-spinning nuclear magnetic resonance (CP MAS NMR) spectroscopy.

	Carboxyl	O-aryl	Aryl	di-O-alkyl	Carbohydrate	Methoxyl	Aliphatic	Labile fractions	A/O-A ratio	*n*
Johnstone	8.67±0.26	4.3±0.56	19.86±3.81	10.35±0.37	26.71±0.78	8.84±1.72	21.17±3.55	45.91±0.56	0.46±0.07	2
Tully	11.21±0.18	4.62±0.27	22.79±0.55	9.06±0.49	23.90±1.15	6.76±0.66	21.65±1.62	39.72±0.98	0.55±0.05	2
Burdekin	9.04±2.13	5.22±0.89	23.69±2.22	6.89±0.45	21.34±0.84	6.47±1.21	27.35±2.51	34.70±1.55	0.79±0.04	4

Labile fractions = sum of carbohydrate, di-O-alkyl and methoxyl C; n = number of samples; A/-A ratio = the ratio of alkyl C region intensity (0–45 ppm) to O-alkyl C region intensity (45 –110 ppm) as an index of the extent of decomposition.

The preliminary results on community composition of dominant bacterial and fungal phyla for the plume and riverbed sediments samples are presented in Figures 5.7 and 5.8, respectively. For the bacterial community, the plume sample showed a very different pattern compared to the riverbed sediment samples from the Johnstone River (Figure 5.7), with Proteobacteria being predominant and followed by Bacteroidetes in the plume sample, while Proteobacteria, Actinobacteria and Acidobacteria were predominant in the riverbed sediment samples. Regarding the fungal community composition, there were distinct patterns between the riverbed sediment samples and the plume sample from the Johnstone River (Figure 5.8). Basidiomycota was dominant, followed by Rozellomycota in the plume sample, while Rozellomycota and Chytridiomycota in SG1 and Rozellomycota, Mortierellomycota and Chytridiomycota in SG1 (Figure 5.8). These different patterns may be related to the source of organic matter in sediments and different environmental factors (pH, salinity, hydrology etc.) (Angly et al. 2016).

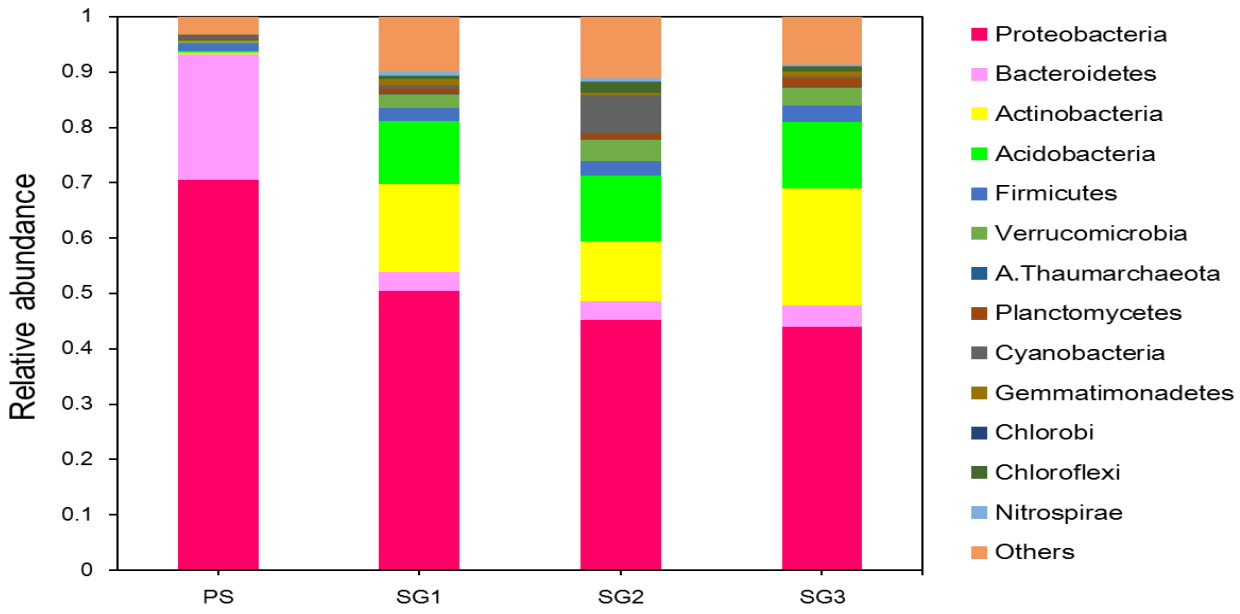

Figure 5.7. Percent community composition of numerically dominant bacterial phyla across riverbed sediments (SG1, SG2, SG3) along salinity gradient (increasing) and plume sample (PS) in the Johnstone River.

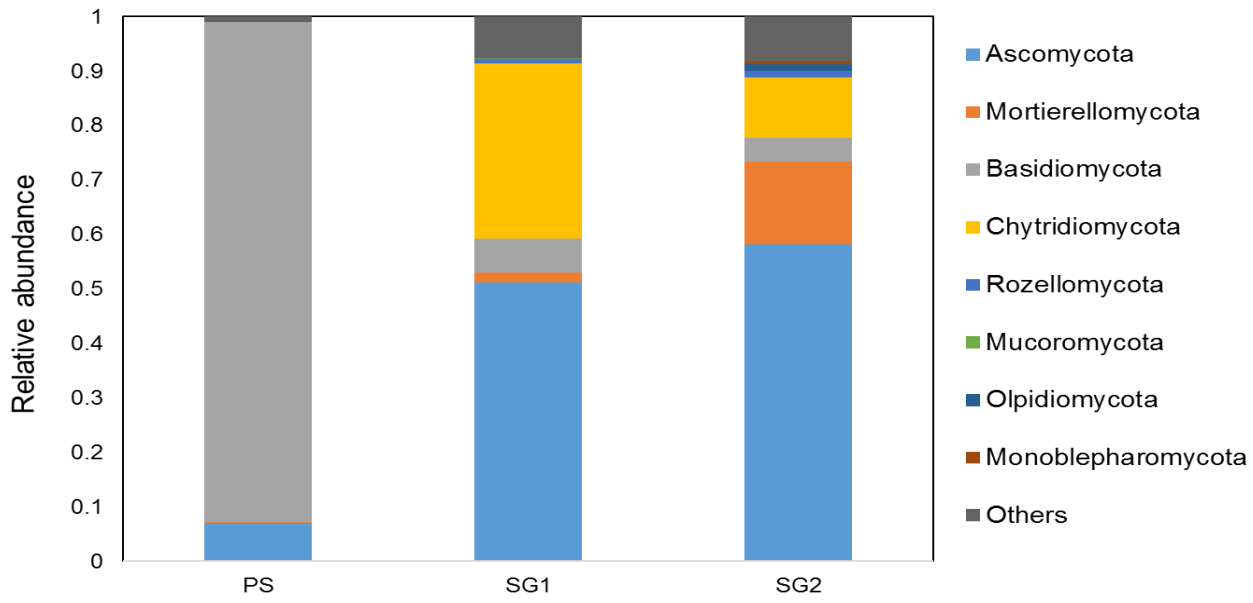

Figure 5.8. Percent community composition of numerically dominant fungal phyla across riverbed sediments (SG1, SG2) and plume sample (PS) in the Johnstone River.

6.0 MARINE SEDIMENT TRAP AND LOGGER DATA

The sediment trap, nephelometer (i.e. measure of turbidity, wave pressure, light etc at 10 min intervals) and current meter configuration (Figure 6.1) have now been deployed for 2 ½ years (and counting) at our sampling sites and provide key insights on sediment dynamics in the inshore GBR region. We note that due to a lack of a moderate to major flood event from the Burdekin River to influence our sites over the 2016-2018 period our interpretations can only be based on what we have observed thus far and may be subject to change in the coming seasons. In any case, the plots highlight some of our early key findings and provide insight on how the wealth of data collected in the project can be presented effectively. Our preliminary findings suggest that the sediment dynamics at marine sites in the inshore GBR region likely fall into three separate categories including 1. Sites where the input of new terrigenous sediments have by far the greatest influence on sediment exposure and subsequent resuspension (e.g. Dunk Island, Orpheus Island, Havannah Island, Cleveland Bay?); 2. Sites where the input of new terrigenous sediments are at least equivalent to resuspension events which likely increases upon larger river discharge events (e.g. Cleveland Bay?, Orchard Rocks) and; 3. Sites where the input of new terrigenous sediments are less than or equal to common resuspension events (e.g. Middle Reef, Geoffrey Bay). Hence because of these differences in sediment dynamics, the study reveals which sites are most influenced by newly delivered riverine sediment and hence where management in the catchment for sediment erosion would improve water quality and likely ecosystem health at those coral reef and seagrass meadow sites.

The time series from Dunk Island clearly highlights the influence of 'new sediment' delivered from the Tully (and possibly Murray and Herbert) River where the sediment accumulation in our traps markedly increase in the deployment periods where large floods have occurred (Figure 6.2). The amount of sediment in the traps from the 22nd November 2016 to 12th February 2017 deployment period constitute an accumulation rate of 1.81 g.d^{-1}, over 20-fold higher than the previous deployment period (0.08 g.d^{-1}). While the accumulation rate in the traps over the flooding events in 2018 were not as high (0.49 and 0.47 g.d^{-1}, respectively), they were still over 5 times the accumulation rate measured under dry season conditions coinciding with low flow in the Tully River during the 20th July 2017 to 28th September 2017 deployment (0.08 g.d^{-1}) (Figure 6.2). Moreover, the accumulation rates in the traps for the two deployments (lasting February to July 2017) following the large Tully River flow event in January 2017 were also elevated compared to the late dry season values (0.33 and 0.36 g.d^{-1}, respectively compared to 0.08 g.d^{-1}). Indeed, the SSC peaks in resuspension events were much higher in the February to July 2017 period of the record compared to the June to December 2016 period despite similar wave pressure events. This finding supports Fabricius et al.'s (2016) assertion that the new sediment delivered is more easily resuspendable and that water clarity is reduced for several months following a large river flow event. Interestingly, despite the change in sediment mass in the traps over the deployments, the sediment particle size did not show large variability over the different deployment periods (Figure 6.3).

The time series from the Havannah Island trap set up highlights the influence of the 2018 Burdekin River discharge event on the turbidity and sediment trap data (Figure 6.4). However, sediment accumulation rates increased in the traps for the deployment period prior to the Burdekin flood in March 2018 (14th December to 16th February) and result trends were different

across the trap locations set up for this site. For example, at the location with the nephelometer (~ 5 m water depth), sediment accumulation rates for the December 2017 to February 2018 period were 0.27 $g.d^{-1}$ compared to 0.20 $g.d^{-1}$ in the period coinciding with the Burdekin flood while the deeper site (12 m water depth) ~ 50 m offshore from the nephelometer site had higher accumulation rates coinciding with the Burdekin flood (0.34 $g.d^{-1}$) compared to the previous deployment (0.26 $g.d^{-1}$) (HAV1-toe in Figure 18). The accumulation rates in the sediment traps on the other side of the island were comparable over the two periods (0.12 and 0.13 $g.d^{-1}$, respectively: HAV2 in Figure 6.4). It is possible there was a localised runoff event in the December 2017 to February 2018 period that accounts for the increased sediment accumulation. In any case, accumulation rates in the traps were generally > 2 fold higher in this period compared to rates measured in previous deployments (~ 0.08 $g.d^{-1}$) (Figure 6.4). Overall the data indicate that sediment resuspension events around Havannah Island seem to occur less frequently compared to the Dunk Island and Geoffrey Bay sites.

Similarly to the Havannah Island time series, the Orpheus Island data (Figure 6.5) show a clear influence of the 2018 Burdekin River (and possibly Herbert) flood on both suspended sediment concentration and sediment trap accumulation of this site. The accumulation rates in the sediment trap deployed at this site from this period (February to June 2018: 0.29 $g.d^{-1}$) was 2.6 fold or greater than the previous and subsequent deployments. Interestingly, the sediment trap site at Pelorus Island (PEL) did not show the same influence in terms of mass accumulated in the traps from the 2018 flood event. Overall, the Orpheus Island site displays one of the lower sediment influenced sites (i.e. amongst the lowest suspended sediment concentrations), although river discharge events (likely Burdekin) influence sediment dynamics at this site.

While the 2018 flood plume from the Burdekin River is clearly evident in the suspended sediment concentration data from Geoffrey Bay, the accumulation in the sediment traps was comparable to previous deployment periods and the SSC data during this flood event was equal or much lower than resuspension events occurring before the flood (Figure 6.6). This result is somewhat unexpected, but given that Cleveland Bay is generally muddier compared to Halifax (i.e. where Havannah Island and Orpheus Island sites are located) and Rockingham Bays (i.e. Dunk Island), the sediment dynamics in Geoffrey Bay may only be influenced by much larger Burdekin flood events. Alternatively, the composition of the sediment in the traps may be different following the flood event, although further data processing and additional analysis (e.g. geochemistry, clay mineralogy) are required to consider all potential possibilities. Nevertheless, the sediment trap accumulation data from Geoffrey Bay appear to show a seasonal variation in the amount of sediment trapped (Figure 6.6).

Unfortunately logger issues at the Orchard Rocks site precluded reliable suspended sediment concentration data being recorded for the Burdekin discharge event in 2018 (Figure 6.7). However, the light values during this period were greatly suppressed and suspended sediment concentrations were recorded by the logger during the 2017 discharge event from the Burdekin River which were similar to previous and subsequent resuspension events. Similarly to Geoffrey Bay, the sediment accumulation rates in the SediSampler® were higher prior to the flood event, although a seasonal pattern was apparent in the dataset. This site is much deeper (~ 16 m) than most of our other sites (~ 5 m) and hence light levels are generally much lower and also strongly influenced by flood and resuspension events.

The logger data from Middle Reef showed that resuspension events outside of the discharge events from the Burdekin River (and other local rivers) dominated suspended sediment concentrations, although there was still some influence of elevated river discharge at this site (Figure 6.8). Hence the data show that Middle Reef is influenced by local sediment resuspension regimes (possibly including dredging) and that management in the catchment to reduce erosion is unlikely to greatly influence sediment regimes at this site.

In comparison to Middle Reef, the Cleveland Bay site was strongly influenced by the 2018 Burdekin River flood event where suspended sediment concentrations were the highest recorded in our time series (Figure 6.9). We note that this dataset was restricted due to regular site disturbance and the disappearance of sediment traps and, on two occasions, the nephelometer. The dataset is also quite 'spikey' and needed extensive data cleaning to ascertain 'real' versus 'not possible' trends. In any case, while the data show regular resuspension events at this shallow site (in the order of 2 to 6 m depth), the suspended sediment concentrations during the 2018 Burdekin River flood and resuspension events following suppressed light conditions for a longer period than the previous resuspension events without the influence of the flood. This finding needs to be confirmed with subsequent events, however, at this stage our current dataset appears to support the previous assertion that the Burdekin River greatly influences the light regime in this section of Cleveland Bay which hosts the vast majority of the seagrass meadows (Petus et al., 2014).

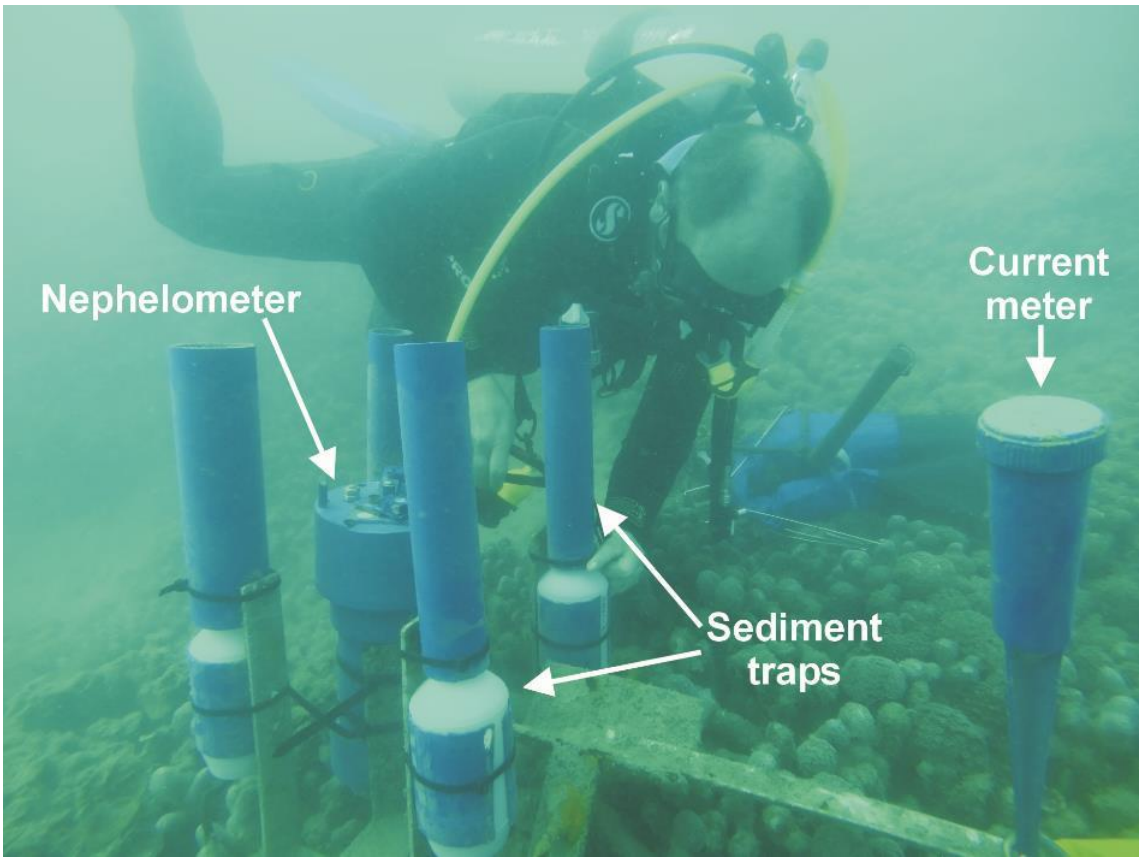

Figure 6.1. The SediSampler® (Sediment traps), surrounded by the nephelometer and current meter (Image: Ian McLeod).

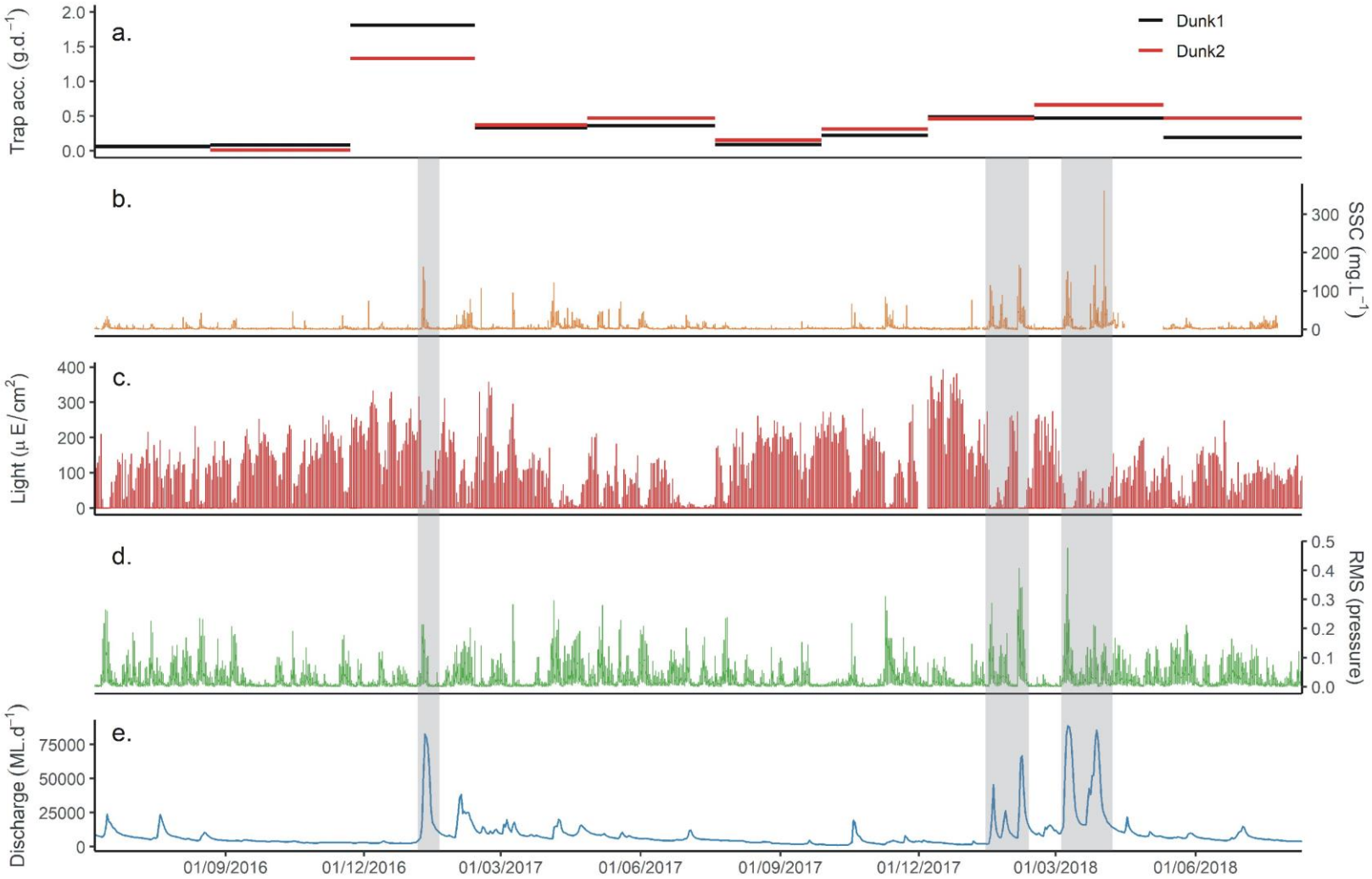

Figure 6.2. Time series of sediment trap and logger data for the Dunk Island site including (a) average sediment trap accumulation (g.d^{-1}) over the deployment periods, (b) continuous 10 min suspended sediment concentration (SSC) data based on calibrations from normalised NTU readings in section 2, (c) continuous 10 min light readings, (d) continuous 10 min wave pressure data and (e) daily discharge from the Tully River at the Euramo gauge.

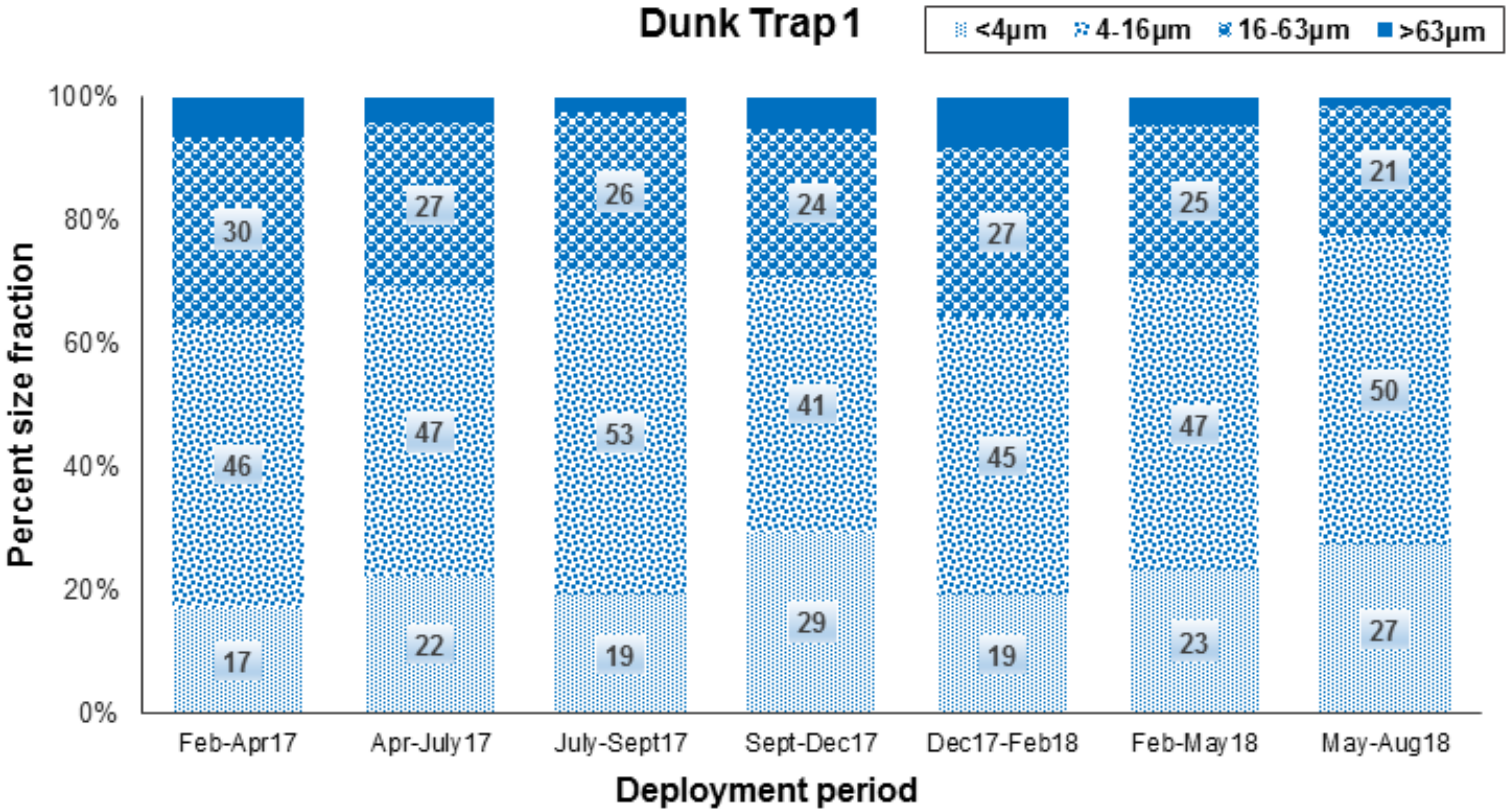

Figure 6.3. Sediment particle size (organic removed) variability in the sediment traps deployed at Dunk Island.

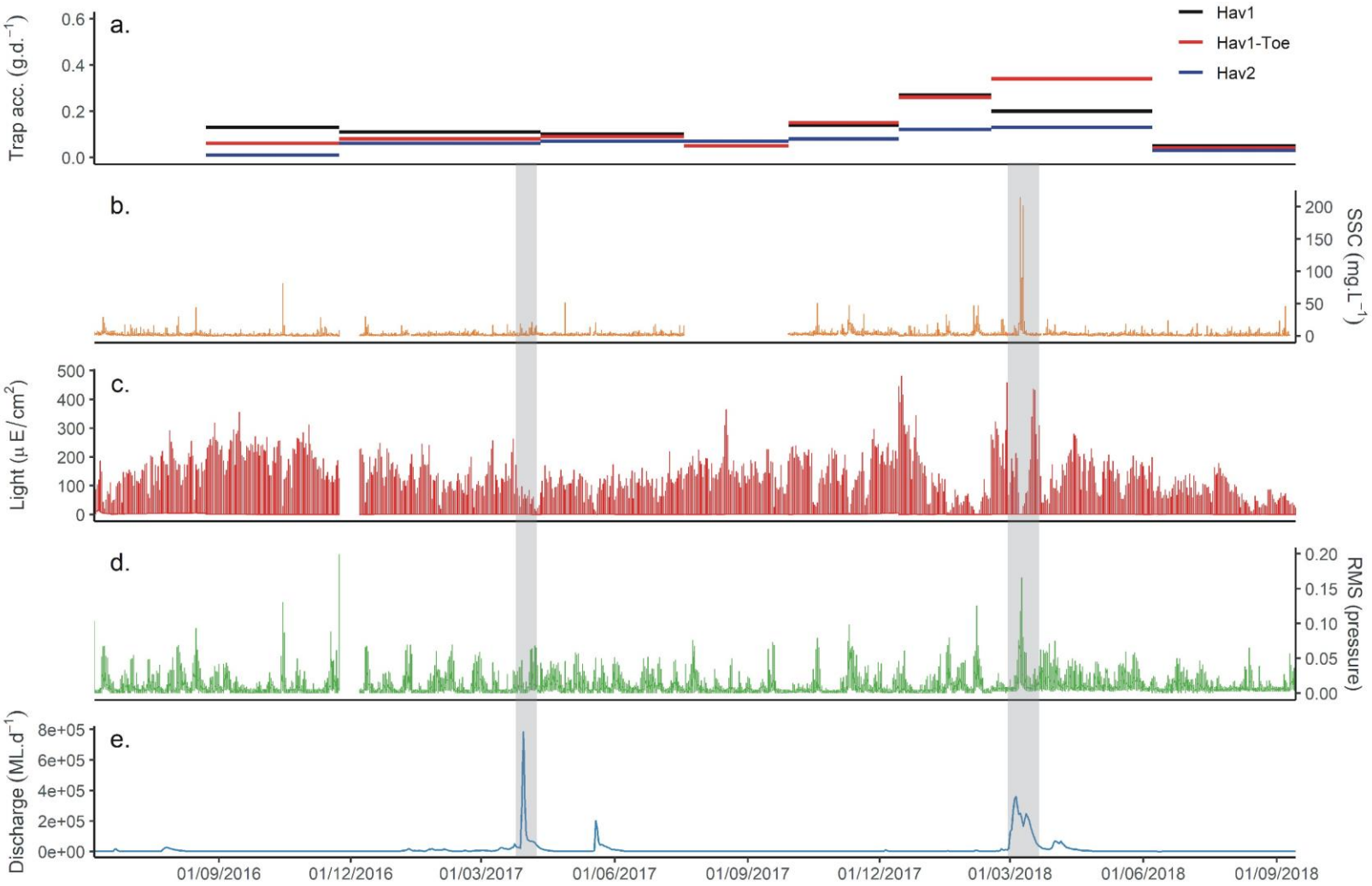

Figure 6.4. Time series of sediment trap and logger data for the Havannah Island site including (a) average sediment trap accumulation (g.d^{-1}) over the deployment periods, (b) continuous 10 min suspended sediment concentration (SSC) data based on calibrations from normalised NTU readings in section 2, (c) continuous 10 min light readings, (d) continuous 10 min wave pressure data and (e) daily discharge from the Burdekin River at the Clare gauge.

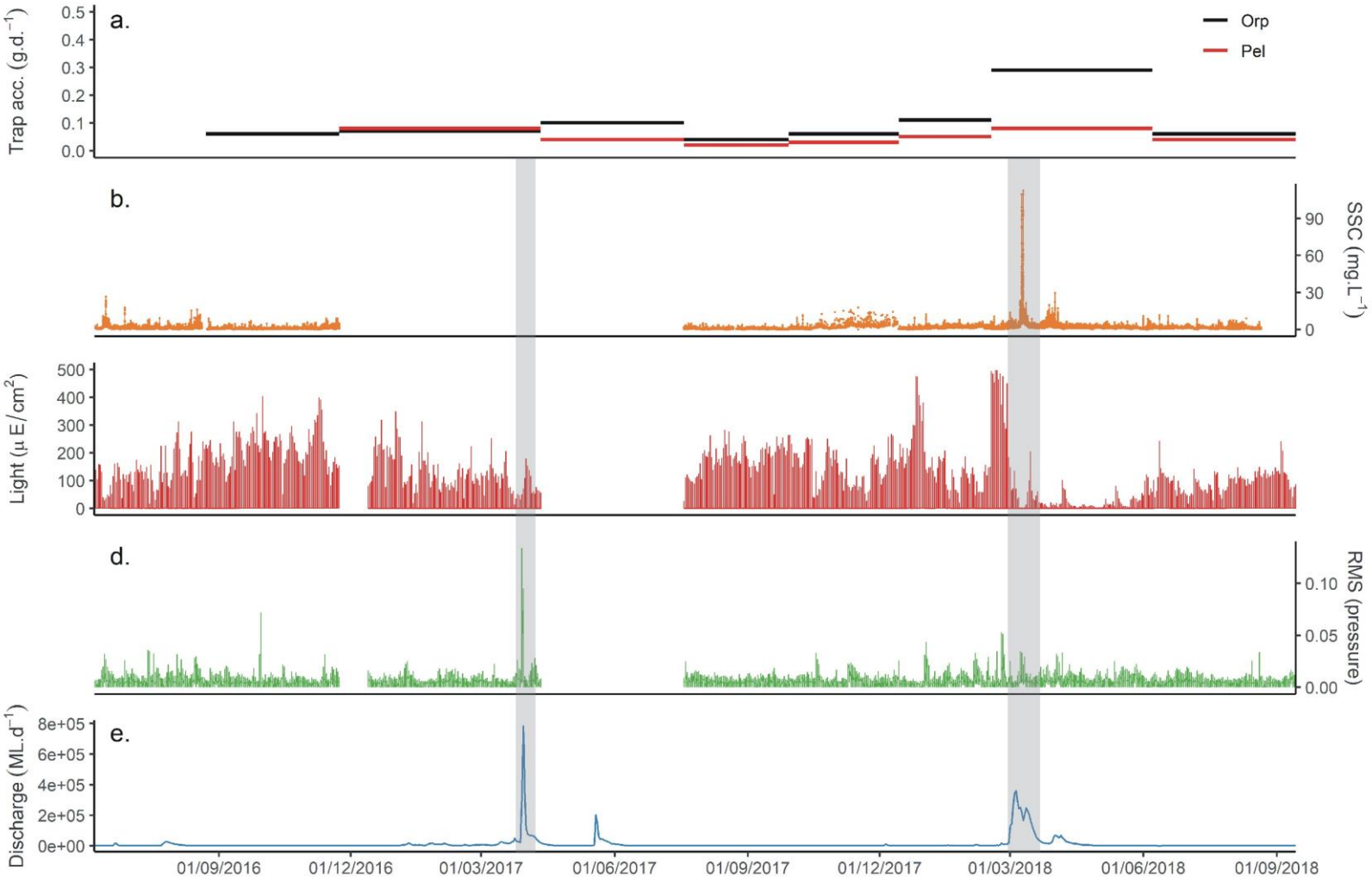

Figure 6.5. Time series of sediment trap and logger data for the Orpheus Island site including (a) average sediment trap accumulation (g.d^{-1}) over the deployment periods, (b) continuous 10 min suspended sediment concentration (SSC) data based on calibrations from normalised NTU readings in section 2, (c) continuous 10 min light readings, (d) continuous 10 min wave pressure data and (e) daily discharge from the Burdekin River at the Clare gauge.

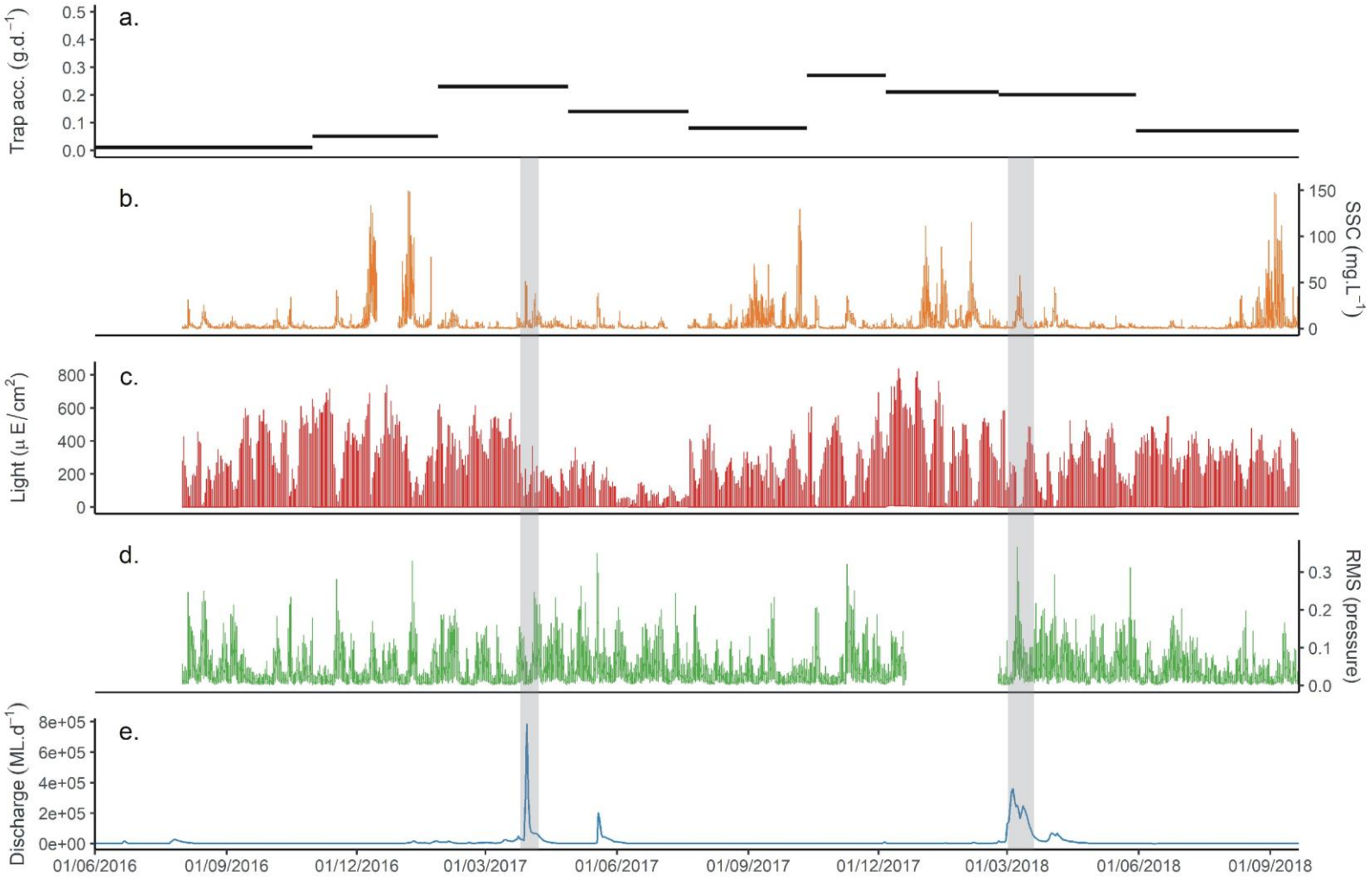

Figure 6.6. Time series of sediment trap and logger data for the Geoffrey Bay, Magnetic Island site including (a) average sediment trap accumulation (g.d^{-1}) over the deployment periods, (b) continuous 10 min suspended sediment concentration (SSC) data based on calibrations from normalised NTU readings in section 2, (c) continuous 10 min light readings, (d) continuous 10 min wave pressure data and (e) daily discharge from the Burdekin River at the Clare gauge.

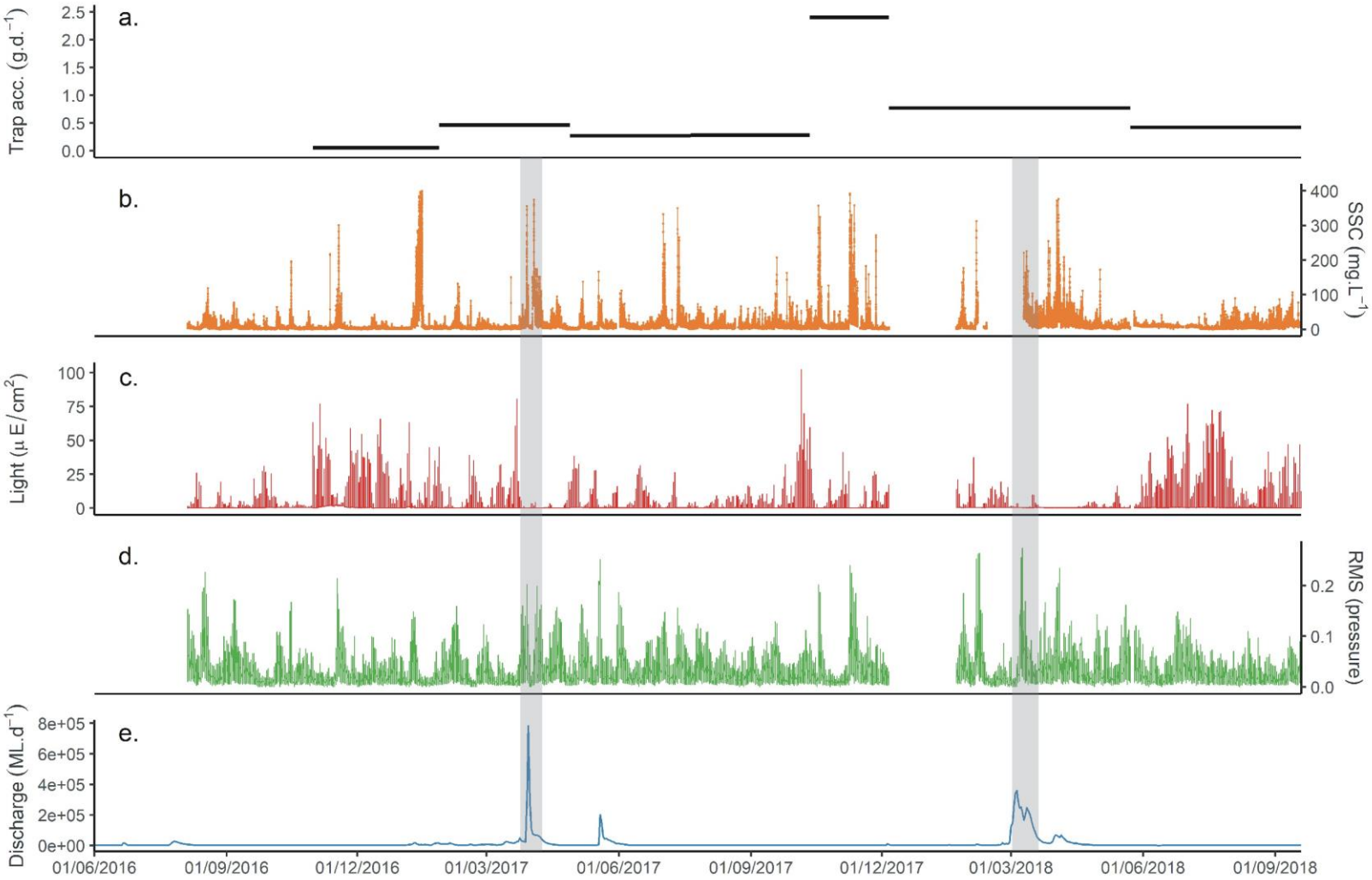

Figure 6.7. Time series of sediment trap and logger data for the Orchard Rocks including (a) average sediment trap accumulation (g.d^{-1}) over the deployment periods, (b) continuous 10 min suspended sediment concentration (SSC) data based on calibrations from normalised NTU readings in section 2, (c) continuous 10 min light readings, (d) continuous 10 min wave pressure data and (e) daily discharge from the Burdekin River at the Clare gauge.

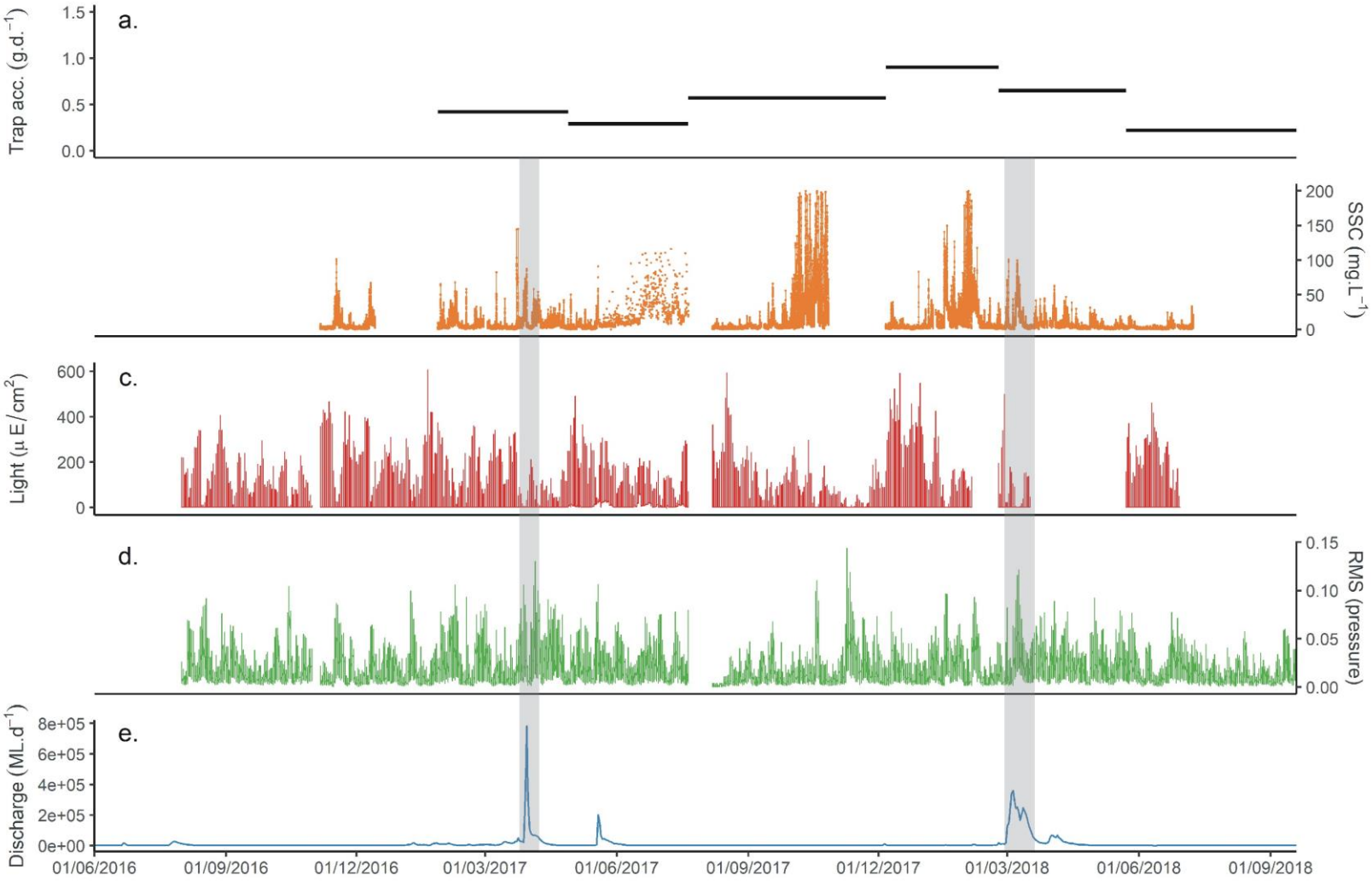

Figure 6.8. Time series of sediment trap and logger data for the Middle Reef including (a) average sediment trap accumulation (g.d^{-1}) over the deployment periods, (b) continuous 10 min suspended sediment concentration (SSC) data based on calibrations from normalised NTU readings in section 2, (c) continuous 10 min light readings, (d) continuous 10 min wave pressure data and (e) daily discharge from the Burdekin River at the Clare gauge.

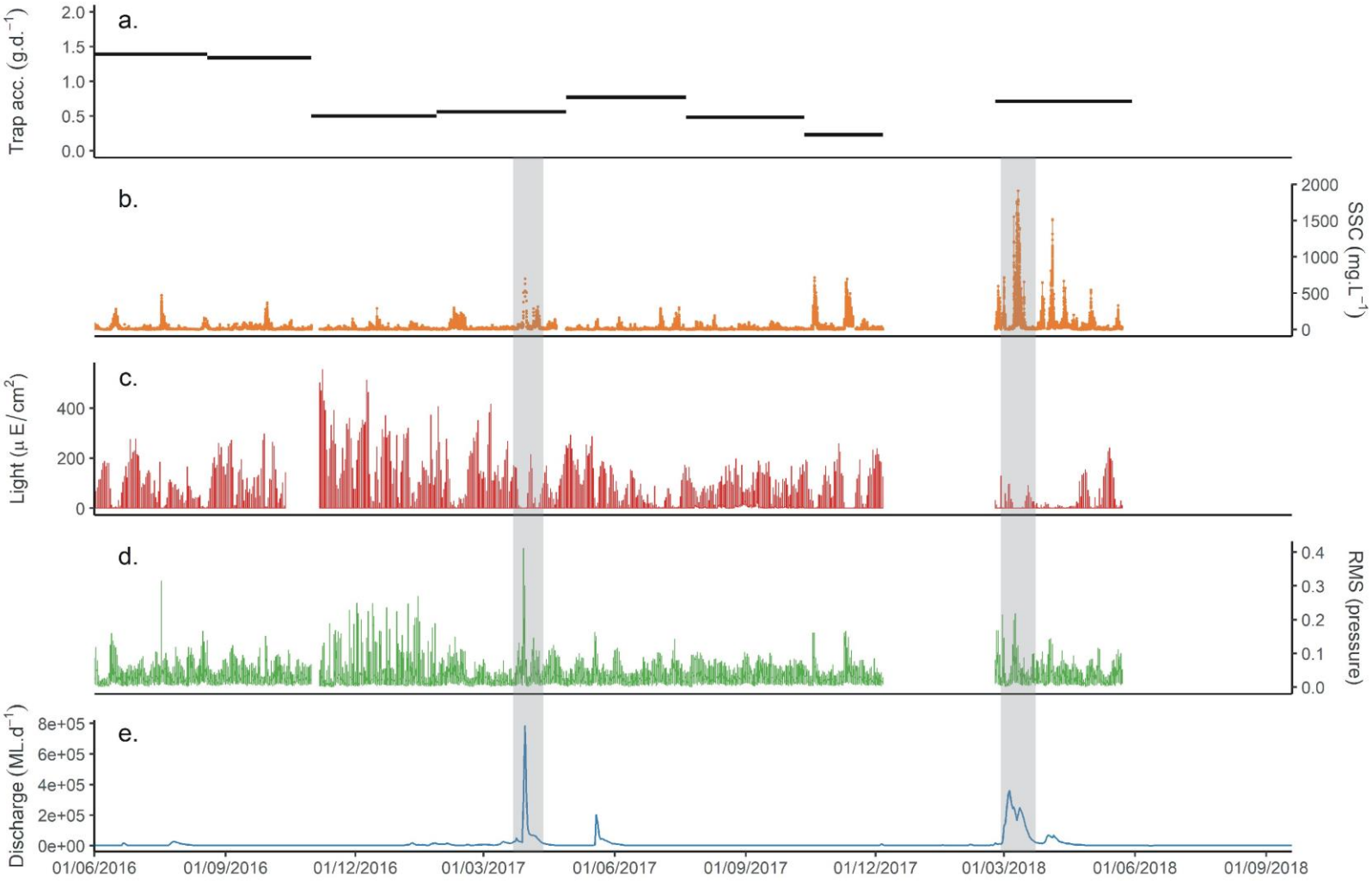

Figure 6.9. Time series of sediment trap and logger data for the Cleveland Bay including (a) average sediment trap accumulation (g.d^{-1}) over the deployment periods, (b) continuous 10 min suspended sediment concentration (SSC) data based on calibrations from normalised NTU readings in section 2, (c) continuous 10 min light readings, (d) continuous 10 min wave pressure data and (e) daily discharge from the Burdekin River at the Clare gauge.

7.0 CONCLUSIONS

This NESP TWQ Hub program has developed new techniques for measuring and tracing suspended particle matter across the catchment to reef continuum. Some of the key findings of the program include:

- *In situ* continuous turbidity and light loggers and sediment trap accumulation dataset. Newly delivered sediment from the Tully River influenced turbidity regimes surrounding Dunk Island for ~5 months following flood events in 2017 and 2018.
- Developed novel sampling techniques to characterise and trace the origin(s) and fate of environmentally detrimental sediment within the GBR delivered from the Burdekin, Tully and Johnstone Basins. A novel method of combining organic tracing with trace element data to trace land use sources of the particulate nutrients exported from river basins.
- Considerable contribution of dissolved inorganic nitrogen in the Burdekin flood plume that has desorbed from sediment (ammonium ions) and the mineralization of particulate organic matter.
- Mineral Particles <20 µm associated with terrestrial organic matter travel furthest in the marine environment.
- Considerable effort into knowledge transfer and extension of the preliminary project findings/conceptual understanding to a wide range of stakeholders has occurred.

REFERENCES

Alewell, Christine, Axel Birkholz, Katrin Meusburger, Yael Schindler Wildhaber, and Lionel Mabit. 2016. 'Quantitative sediment source attribution with compound-specific isotope analysis in a C3 plant-dominated catchment (central Switzerland)', Biogeosciences, 13: 1587-96.

Alongi DM, Trott LA, Pfitzner J. 2007. Deposition, mineralization, and storage of carbon and nitrogen in sediments of the far northern and northern Great Barrier Reef shelf. *Continental Shelf Research* 27, 2595-2622.

American Public Health Association 2005. Standard Methods for the Examination of Water and Wastewaters, 21st ed., Am. Water Works Assoc. and Water Environ. Fed., Wash.

Angly, Florent E, Candice Heath, Thomas C Morgan, Hemerson Tonin, Virginia Rich, Britta Schaffelke, David G Bourne, and Gene W Tyson. 2016. 'Marine microbial communities of the Great Barrier Reef lagoon are influenced by riverine floodwaters and seasonal weather events', PeerJ, 4: e1511.

Bahadori, Mohammad, Chengrong Chen, Stephen Lewis, Mehran Rezaei Rashti, Freeman Cook, Andrew Parnell, Maryam Esfandbod, and Sue Boyd. 2018. 'A novel approach of combining isotopic and geochemical signatures to differentiate the sources of sediments and particulate nutrients from different land uses', Science of The Total Environment.

Bainbridge, Z.T. Wolanski, E. Álvarez-Romero, J.G. Lewis, S.E. Brodie, J.E. 2012. Fine sediment and nutrient dynamics related to particle size and floc formation in a Burdekin River flood plume, Australia. *Marine Pollution Bulletin* 65, 236-248.

Bainbridge, Z.T. Lewis, S.E. Smithers, S.G. Kuhnert, P.M. Henderson, B.L. Brodie, J.E. 2014. Fine-suspended sediment and water budgets for a large, seasonally dry tropical catchment: Burdekin River catchment, Queensland, Australia. *Water Resources Research* 50, 9067–9087.

Bainbridge, Z. Lewis, S. Bartley, R. Fabricius, K. Collier, C. Waterhouse, J. Garzon-Garcia, A. Robson, B. Burton, J. Wenger, A. Brodie, J. in review. Fine sediment and particulate organic matter: a review and case study on ridge-to-reef transport, fates, and impacts on marine ecosystems. *Marine Pollution Bulletin*.

Bartley, R. Bainbridge, Z.T. Lewis, S.E. Kroon, F.J. Brodie, J.E. Wilkinson, S.N. Silburn, M.D. 2014. Relating sediment impacts on coral reefs to watershed sources, processes and management: A review. *Science of the Total Environment* 468-469, 1138-1153.

Blake, William H, Katherine J Ficken, Philip Taylor, Mark A Russell, and Desmond E Walling. 2012. 'Tracing crop-specific sediment sources in agricultural catchments', Geomorphology, 139: 322-29.

Brodie, J., Burford, M., Davis, A., da Silva, E., Devlin, M., Furnas, M., Kroon, F., Lewis, S., Lønborg, C., O'Brien, D., Schaffelke, B., Bainbridge, Z. 2015. The relative risks to water quality from particulate nitrogen discharged from rivers to the Great Barrier Reef in comparison to other forms of nitrogen. TropWATER Report 14/31, Centre for Tropical Water & Aquatic Ecosystem Research, James Cook University, Townsville, 93 pp.

Chen, CR, ZH Xu, and NJ Mathers. 2004. 'Soil carbon pools in adjacent natural and plantation forests of subtropical Australia', Soil Science Society of America Journal, 68: 282-91.

Chiswell S. and Nodder S. 2015. Tilt-induced biases in sediment trap functioning. J. Geophys. Res. Oceans 120, 8381-8391.

Coleman, David C. 2012. Carbon isotope techniques (Academic Press).

Collins, AL, S Pulley, Ian DL Foster, Allen Gellis, P Porto, and AJ Horowitz. 2017. 'Sediment source fingerprinting as an aid to catchment management: a review of the current state of knowledge and a methodological decision-tree for end-users', Journal of Environmental Management, 194: 86-108.

Collins, AL, and DE Walling. 2002. 'Selecting fingerprint properties for discriminating potential suspended sediment sources in river basins', Journal of Hydrology, 261: 218-44.

Collins, AL, DE Walling, and GJL Leeks. 1997. 'Sediment sources in the Upper Severn catchment: a fingerprinting approach', Hydrology and Earth System Sciences Discussions, 1: 509-21.

Collins, AL, DE Walling, L Webb, and P King. 2010. 'Apportioning catchment scale sediment sources using a modified composite fingerprinting technique incorporating property weightings and prior information', Geoderma, 155: 249-61.

Cooper, M. Lewis, S.E. Smithers, S.G. 2017. Spatial and temporal dynamics of suspended sediment causing persistent turbidity in a large reservoir: Lake Dalrymple, Queensland, Australia. *Marine and Freshwater Research* 68, 1377-1390.

Devlin, M.J. Brodie, J. 2005. Terrestrial discharge into the Great Barrier Reef Lagoon: nutrient behaviour in coastal waters. *Marine Pollution Bulletin* 51, 9-22.

Fabricius, K.E., Logan, M., Weeks, S., Brodie, J., 2014. The effects of river run-off on water clarity across the central Great Barrier Reef. *Marine Pollution Bulletin* 84, 191-200.

Fabricius, K.E. Logan, M. Weeks, S.J. Lewis, S.E. Brodie, J. 2016. Changes in water clarity in response to river discharges on the Great Barrier Reef continental shelf: 2002-2013. *Estuarine, Coastal and Shelf Science* 173, A1-A15.

Franklin HM, Garzon-Garcia A, Joanne. B, Moody PW, De Hayr RW, Burford MA. 2018. A novel bioassay to assess phytoplankton responses to soil-derived particulate nutrients. *Science of the Total Environment* 636, 1470-1479.

Furnas M, Mitchell A, Skuza M, Brodie J. 2005. In the other 90%: phytoplankton responses to enhanced nutrient availability in the Great Barrier Reef Lagoon. *Marine Pollution Bulletin* 51, 253-265.

Gardner W. 1980. Sediment trap dynamics and calibration: a laboratory evaluation. *Journal of Marine Research* 38(1):17-39.

Gardner W. 1985. The effect of tilt on sediment trap efficiency. Deep-sea Research. Vol 32, No 3 pp 349-361.

Garzon-Garcia A, Burton J, Lewis S, Bainbridge Z, Ellis R, Askildsen M, et al. In preparation. The bioavailability of particulate nitrogen in sediment: ridge to reef sources and processes [December 2018].

Garzon-Garcia A, Burton J, Franklin HM, Moody PW, De Hayr RW, Burford MA. 2018. Indicators of phytoplankton response to particulate nutrient bioavailability in fresh and marine waters of the Great Barrier Reef. *Science of the Total Environment* 636, 1416-1427.

Gray, J. R., Glysson, G. D. Turcios, L. M. Schwarz G. E. 2000). Comparability of suspended-sediment concentration and total suspended solids data, U.S Geol. Surv. Water Resour. Invest. Rep. 00–4191, 14 pp.

Glendell, M, R Jones, JAJ Dungait, K Meusburger, AC Schwendel, R Barclay, S Barker, S Haley, TA Quine, and Jeroen Meersmans. 2018. 'Tracing of particulate organic C sources across the terrestrial-aquatic continuum, a case study at the catchment scale (Carminowe Creek, southwest England)', Science of The Total Environment, 616: 1077-88.

Golding, CJ, RJ Smernik, and GF Birch. 2004. 'Characterisation of sedimentary organic matter from three south-eastern Australian estuaries using solid-state 13C-NMR techniques', Marine and Freshwater Research, 55: 285-93.

Haddadchi, Arman, Jon Olley, and Patrick Laceby. 2014. 'Accuracy of mixing models in predicting sediment source contributions', Science of The Total Environment, 497: 139-52.

Haddadchi, Arman, Darren S Ryder, Olivier Evrard, and Jon Olley. 2013. 'Sediment fingerprinting in fluvial systems: review of tracers, sediment sources and mixing models', International Journal of Sediment Research, 28: 560-78.

Hunter, Heather M, and Richard S Walton. 2008. 'Land-use effects on fluxes of suspended sediment, nitrogen and phosphorus from a river catchment of the Great Barrier Reef, Australia', Journal of Hydrology, 356: 131-46.

Kroon, F.J., Kuhnert, P.M., Henderson, B.L., Wilkinson, S.N., Kinsey-Henderson, A., Brodie J.E., Turner R.D.R., 2012. River loads of suspended solids, nitrogen, phosphorus and herbicides delivered to the Great Barrier Reef lagoon. *Marine Pollution Bulletin* 65, 167-181.

Laceby, J Patrick, Sylvain Huon, Yuichi Onda, Veronique Vaury, and Olivier Evrard. 2016. 'Do forests represent a long-term source of contaminated particulate matter in the Fukushima Prefecture?', Journal of Environmental Management, 183: 742-53.

Lewis, S.E. Olley, J. Furuichi, T. Sharma, A. Burton, J. 2014. Complex sediment deposition history on a wide continental shelf: implications for the calculation of accumulation rates on the Great Barrier Reef. *Earth and Planetary Science Letters* 393, 146-158.

Lewis S., Bartley R., Bainbridge Z., Wilkinson, S., Burton J., Bui, E. 2015. Burdekin sediment story. Report No. 15/50 for the NQ Dry Tropics NRM, Centre for Tropical Water & Aquatic Ecosystem Research (TropWATER) Publication, James Cook University, Townsville, 44 pp.

Mackin JE, Aller RC. Ammonium adsorption in marine-sediments. Limnology and Oceanography 1984; 29: 250-257.

Noder S and Bridget A. 1999. The effects of multiple trap spacing, baffles and brine volume on sediment trap collection efficiency. Journal of Marine Research Vol 57 No.3 537-559.

Neukermans, G. Ruddick, K. Loisel, H. Roose, P. 2012. Optimization and quality control of suspended particulate matter concentration measurement using turbidity measurements. Limnology and Oceanography: Methods 10, 1011-1023.

Peterson, Bruce J, and Brian Fry. 1987. 'Stable isotopes in ecosystem studies', Annual Review of Ecology and Systematics, 18: 293-320.

Petus, C., Collier, C., Devlin, M., Rasheed, M., McKenna, S., 2014. Using MODIS data for understanding changes in seagrass meadow health: A case study in the Great Barrier Reef (Australia). Marine Environmental Research 98, 68-85.

Stevens, T. 2013. Suspended sediment sampler. Australian Patent AU 2013206318.

Stevens, T. 2018. Improved sampler system and method. Australian Provisional Patent Application No. 2018904949.

Wallace, R. Huggins, R. King, O. Gardiner, R. Thomson, B. Orr, D. N. Ferguson, B. Taylor, C. Severino, Z. Smith, R. A. Warne, M. St. J. Turner, R. D. R. Mann, R. M. 2016. Total suspended solids, nutrient and pesticide loads (2014–2015) for rivers that discharge to the Great Barrier Reef – Great Barrier Reef Catchment Loads Monitoring Program. Department of Science, Information Technology and Innovation. Brisbane.

Waterhouse, J., Burton, J., Garzon-Garcia, A., Lewis, S., Brodie, J., Bainbridge, Z., Robson, B., Burford, M., Gruber, R., Dougall, C. (2018). *Synthesis of knowledge and concepts - Bioavailable Nutrients: Sources, delivery and impacts in the Great Barrier Reef, July 2018. Supporting Concept Paper for the Bioavailable Nutrients Workshop, 15 March 2018.* Supported by the Office of the Great Barrier Reef's Queensland Reef Water Quality Program, and the Australian Government National Environmental Science Program Tropical Water Quality Hub (84pp.).

Reef & Rainforest
RESEARCH CENTRE

www.nesptropical.edu.au